A DISSERTATION FOR THE DEGREE OF DOCTOR OF PHILOSOPHY

Growth Estimation of Hydroponically-grown Bell Pepper (*Capsicum annuum* L.) using Recurrent Neural Network through Nondestructive Measurement of Leaf Area Index and Fresh Weight

엽면적지수와 생체중 연속 측정을 통한 순환 신경회로망 기반 수경재배 파프리카의 생육 추정

BY

JOON WOO LEE

AUGUST, 2019

MAJOR IN HORTICULTURAL SCIENCE AND BIOTECHNOLOGY

DEPARTMENT OF PLANT SCIENCE

THE GRADUATE SCHOOL OF SEOUL NATIONAL UNIVERSITY

Growth Estimation of Hydroponically-grown Bell Pepper (*Capsicum annuum* L.) using Recurrent Neural Network through Nondestructive Measurement of Leaf Area Index and Fresh Weight

Joon Woo Lee

Department of Plant Science

The Graduate School of Seoul National University

ABSTRACT

Smart farms are emerging as ICT technologies have recently been applied to existing agricultural technologies. Completion of smart farms requires quantitative analysis of complex, diverse, and unpredictable relationships between crops and the environment. This calls for the development of new algorithms to interpret agricultural big data and systems that can continuously, automatically, and non-destructively monitor the response of crops to the environment. In this study, an algorithm was developed to estimate the growth of hydroponically grown bell pepper crops in response to environmental factors. The development of measuring methods that could automatically and continuously collect the growth characteristics was preceded. The leaf area index (LAI) of the bell

pepper crops was estimated using light interception profile of crop canopy, including quantitative relationship between external weather, and time factors. Ray-tracing simulation and machine learning were used to analyze these factors quantitatively. The actual LAI was estimated with high accuracy for the developed method. The fresh weight measurement system of was designed to measure the weight of the total cultivation system considering the physiological and cultural characteristics of bell pepper crops. In addition, changes of water content in the substrate were corrected to calculate only the fresh weight of the crop. Developed fresh weight measurement systems were able to estimate the actual fresh weight with high accuracy. With crop growth characteristics collected using the developed measurement methods, and the environment factors collected using sensors, the crop growth estimation algorithm was machine learned. As crop growth affected by cumulative changes of the environmental factors, the RNN algorithm, specialized in chronologically data, was selected. Using the training test accuracy, major environmental factors were selected and the optimal algorithm was developed. Additional data were collected from the experimental conditions independently of the algorithm training conditions, to validate the developed algorithm. The accuracy of the process-based growth model (PBM) was compared to evaluate that of the developed algorithm. In validation, the accuracy of the developed algorithm showed a similar to or higher than that of the PBM. Therefore it was conformed that the growth characteristics of crops could be collected as big data and the crop growth could be efficiently analyzed by using the systems and methodologies developed in this study.

Additional keywords: Automatic measurement, Crop growth model, Leaf area index, Machine learning; Ray-tracing

Student Number : 2014-30378

CONTENTS

LIST OF TABLES

LIST OF FIGURES

LIST OF ABBREVIATIONS

ANN	Artificial neural network
CIE	International Commission on Illumination
DAT	Days after transplanting
DW	Dry weight
FDR	Frequency domain reflectometry
FFW	Fresh weight of fruit
FW	Fresh weight
GRU	Gated recurrent unit
LAI	Leaf area index
LF	Length of fruit
LSTM	Long short-term memory
MC	Moisture content
MSE	Mean square error
PBM	Process based model
RMSE	Root mean square error
RNN	Recurrent neural network
RWC	Relative water content
SW	System weight
TW	Fully turgid weight
WF	Width of fruit

GENERAL INTRODUCTION

Bell pepper is an economically important vegetable worldwide, and generally grown hydroponically in precisely-controlled greenhouses because of its high sensitivity to environmental conditions (Jang et al., 2018; Ngouajio et al., 2008; Sezen et al., 2006). In these cultivation conditions, the crop growth responds to the controlling environment conditions in greenhouses. For quantitatively analyze the growth response of the crop to the environment conditions, to continuously collect crop growth characteristics and environmental factors is important.

Leaf area index (LAI), the leaf area per unit cultivation area, is one of the important growth characteristics. Crop leaves absorb light, produce biochemical energy, and exchange carbon (Cope et al., 2012; Sala et al., 2015). LAI quantitatively correlates with crop canopy photosynthesis and transpiration (Suguiyama et al., 2014; Yamori et al., 2016). LAI is important for estimating crop growth and yield (Bertin and Heuvelink, 1993; Jones et al., 1991). The weight of crops is also a key parameter used in most of crop growth models (Heuvelink, 1999; Jones et al., 1991; Martínez-Ruiz et al., 2019; Shamshiri et al., 2016). In the growth models, the weight of crops is used as dry matter, however it is important to measure the fresh weight of the crop because most horticultural crops are sold in fresh weights (Marcelis et al., 1998). Data of leaf area and crop weight are usually collected through destructive means, which inherently limits the potential for continuous measurement of crop growth changes and affects crop growth and development due to changes in light interception by adjacent crops (Peksen, 2007).

The crop growth has been quantitatively analyzed using process based models (PBM) using environmental factors. PBM consists of modules that various physiological processes of crops such as photosynthesis, respiration, biomass assimilation, biomass distribution, and stress response. Using PBM, the growth and development of crops can be simulated through various process modules according to input variables. Since PBM aims to include all biochemical functions of plants, various modules are subjected to complicated calculations for even a single variable, and many indices are to be calibrated. Big data have been collected in greenhouses, but PBM has limitations in processing such big data. Machine learning-based algorithms have recently been used to process big data. Therefore, the relationships of crop growth with environmental factors could be analyzed by using such machine learning algorithms. Among the machine learning algorithms, recurrent neural network (RNN) is optimized for analyzing accumulated time series data. Since the growth responses of crops are determined by cumulative environmental factors, RNN could be useful for analyzing the relationship between environment and crop growth.

The objectives of this study were to develop methodologies for continuous, automatic, and non-destructive collection of LAI and fresh weight of hydroponically-grown bell pepper crops, to develop an algorithm to estimate the growth with RNN, to validate the developed algorithm under various greenhouse conditions, and to evaluate the accuracy of the algorithm compared to PBM.

LITERATURE REVIEW

Non-destructive measurements of leaf area index

Simulation techniques can be applied for estimating LAI of crop (Liet al., 2006; Rodríguez et al., 2015; Wang et al. 2017). However, there are limitations in estimating dynamic changes in LAI, because occurrences caused by various factors during cultivation. Regression equation with leaf area and leaf width measurements is generally used for measuring the LAI non-destructively in many crops (apples, Sala et al., 2015; blue berries, NeSmith, 1991; cucumbers, Blanco and Folegatti, 2003; eggplants, Rivera et al., 2007; grapes, Montero et al., 2000; roses, Rouphael et al., 2010; tomatoes, Schwarz and Klaring, 2001; and zucchini plants, Rouphael et al., 2006). Regression equation methods are time and labor-consuming by measuring leaf length and leaf width for all leaves of individual plants. Therefore, to measure the dynamic changes or large amount, automatic, non-destructive, and continuous measurements of LAIs are needed (Spitters, 1990). For automated continuous measurements of LAI, phenotypes of crop shape and form have recently been produced by 3D laser scanning, RGB camera, and thermal cameras (Dhondt et al., 2013; Fiorani and Schurr, 2013; Llop et al., 2016; Nguyen et al., 2015; Sun et al., 2018; Rose et al., 2014). However, this image processing methodology requires high cost for the measurements and analyzations of crop shape and form (El-Omari and Moselhi, 2011; Paulus et al., 2013; Vos et al., 2010), with high demands on platform to build low-cost crop's shapes (Paulus et al., 2014; Yang et al., 2013), having difficulties for applications in industrial greenhouses.

Non-destructive measurements of crop fresh weight

Chen et al. (2016) calculated the fresh weight of hydroponically-grown lettuce crops using compressive force load cells installed between a disk on which the crop was fixed and another disk fixed to the planting bed. This method is suitable for the deep water culture that the moisture in the sponge block fixing the crop is always saturated. However, this methodology is not suitable for the substrate hydroponic cultivation condition, because irrigation, drainage, and water uptake of crops continuously change the water content in the substrate. Baas and Slooweg (2004) developed a system for measuring the fresh weight of gerbera planted on a rockwool substrate using a compressive force load cell and frequency domain reflectometry (FDR) sensor. The system calculates the fresh weight of crops excluding the weight of water in the substrate with FDR sensor. However, since the FDR sensor measures the volume of water, calibration is required to convert it to weight. In addition, since this system can measure only the gravitational weight of the crop, it is difficult to be applied to bell pepper cultivation where the crop is supported by the string trellis. CropAssist is a commercial product developed to measure fresh weights of trellised crops (Helmer et al., 2005). CropAssist measures the change of crop weight by tensile load cell (upper load cell) installing between the greenhouse frame and the aluminum bar, which supported the string trellis. In addition, a compressive force load cell (lower load cell) is installed under the substrate of the crop to estimate the change in the amount of water in the substrate. In various previous studies, crop growth and transpiration were estimated using CropAssist

(Ahmad et al., 2013; Battista et al., 2015; Ehret et al., 2011; Story and Kacira, 2015). However, these studies are limited to tomato and cucumber that weight the crops entirely on the string trellis. Suitable methods for bell pepper where the weight of the crop is divided into upward (training wire supporting weight) and downward (gravitational weight) are needed to be developed.

Crop growth models

Crop growth models have become essential to support scientific research, crop management, and agricultural policy analysis, with mathematical and quantitative expressions of plant growth processes affecting interactions among genes, environments, and crop management (Fischer et al. 2000; Hammer et al., 2002; Hansen, 2002). Crop growth models generally include simulations of plant growth, development, biomass distribution (leaves, stems, roots, and reproductive structures), and yield. Crop growth models can simulate changes of crop growth index variables (e.g., LAI and biomass), biomass partitioning to each organ, and yields prediction in response to cultivar characteristics, environmental factors (e.g., solar radiation, temperature and CO_2), and management practices (Huang et al, 2013; Yang et al., 2004). Ideally, such model-simulated responses can be used to infer responses by real systems. Virtual experiments (simulations) using the models can thus complement real experiments, but model responses relative to real system responses are needed to be evaluated for a range of conditions to establish confidence in the model, and to provide a measure of uncertainty. Little has been done to establish uncertainty of agricultural systems models until recently

(Asseng et al., 2013, Rosenzweig et al., 2013a, b). Advanced computer technology allows simulations close to actual crop growth, which is regulated by the complex interaction of many factors (Oteng-Darko et al., 2012). Crop growth models require many input data (e.g., management practices, cultivar parameters, soil properties, and weather data) to predict crop growth and yield (Basso et al., 2013; Machwitz et al., 2014).

Application of artificial neural network to agricultural research

Artificial neural network (ANN) provides a way of analyzing complex nonlinear and multi-dimensional data sets arising from data collection (Wang, 2005). ANN could be used for high levels of abstraction from raw data (LeCun et al., 2015). ANN has widely been used in agricultural research for the purpose of analyzing the biochemical and physiological characteristics of various crop cultivations (Arab et al., 2010; Eftekhari et al., 2018; Ehret et al., 2011; Kucukonder et al., 2016). Among ANN algorithms, recurrent neural network (RNN) is useful for analyzing chronological data and this algorithm shows better accuracy than previous algorithms (Adavanne et al., 2017; Ororbia et al., 2017). RNN has an advantage of inputting big data of relatively long period and the length of output values is also unlimited theoretically (Hochreiter and Schmidhuber, 1997). The crop growth responses to the environment are determined by accumulated time series data from environmental factors. In order to accurately predict the growth of crops in various climatic conditions, the cultivation of the crops must be performed on the basis of previous environmental factors.

LITERATURE CITED

Abadi, M., Barham, P., Chen, J., Chen, Z., Davis, A., Dean, J., and Kudlur, M. (2016). Tensorflow: A system for large-scale machine learning. In 12th {USENIX} Symposium on Operating Systems Design and Implementation 16, 265-283.

Ahmad, U., Subrata, D.M., and Arif, C. (2013). Speaking plant approach for automatic fertigation system in greenhouse. arXiv preprint arXiv:1303.1869.

Ahmadi, H. and Golian, A. (2010). The integration of broiler chicken threonine responses data into neural network models. Poultry Science 89, 2535-2541.

Arab, M.M., Yadollahi, A., Shojaeiyan, A., and Ahmadi, H. (2016). Artificial neural network genetic algorithm as powerful tool to predict and optimize in vitro proliferation mineral medium for g × n15 rootstock. Frontiers in Plant Science 7, 1526.

Asseng, S., Ewert, F., Rosenzweig, C., Jones, J.W., Hatfield, J.L., Ruane, A.C., and Brisson, N. (2013). Uncertainty in simulating wheat yields under climate change. Nature Climate Change 3, 827.

Atzberger, C. (2013). Advances in remote sensing of agriculture: Context description, existing operational monitoring systems and major information needs. Remote Sensing 5, 949-981.

Avotins, A., Potapovs, A., Apse-Apsitis, P., and Gruduls, J. (2018). Crop weight measurement sensor for IoT based industrial greenhouse systems. Agronomy Research 16, 952-957.

Baas, R. and Slootweg, C. (2004). On-line acquisition of plant related and environmental parameters (plant monitoring) in gerbera: Determining plant responses. Acta Horticulturae 654, 139-146.

Baas, R., Straver, N.A., Shmulevich, I., Galili, I., Seginer, J., Bailey, B., and Gieling, T. (2001). In situ monitoring water content and electrical conductivity in soilless media using a frequency-domain sensor. In Proceedings of the 3rd International Symposium on Sensors in Horticulture, 295-303.

Bailey, B.N. (2018). A reverse ray-tracing method for modelling the net radiative flux in leaf-resolving plant canopy simulations. Ecological Modelling 368, 233-245.

Baoyun, W. (2009). Review on internet of things. Journal of Electronic Measurement and Instrument 12, 1-7.

Bertin, N. and Heuvelink, E. (1993). Dry-matter production in a tomato crop: comparison of two simulation models. Journal of Horticultural Science 68, 995-1011.

Besharat, F., Dehghan, A.A., and Faghih, A.R. (2013). Empirical models for estimating global solar radiation: A review and case study. Renewable and Sustainable Energy Reviews 21, 798-821.

Boote, K.J., Jones, J.W., Hoogenboom, G., and Pickering, N.B. (1998). Simulation of crop growth: CROPGRO model. Agricultural Systems Modeling and Simulation 18, 651-692.

Boote, K.J., Jones, J.W., Batchelor, W.D., Nafziger, E.D., and Myers, O. (2003). Genetic coefficients in the CROPGRO–soybean model. Agronomy Journal 95, 32-51.

Boote, K.J., Rybak, M.R., Scholberg, J.M., and Jones, J.W. (2012). Improving the CROPGRO-tomato model for predicting growth and yield response to temperature. HortScience 47, 1038-1049.

Buck-Sorlin, G., de Visser, P.H., Henke, M., Sarlikioti, V., Van Der Heijden, G.W., Marcelis, L.F., and Vos, J. (2011). Towards a functional-structural plant model of cut-rose: simulation of light environment, light absorption, photosynthesis, and interference with the plant structure. Annals of Botany 108, 1121-1134.

Castro, S.M., Saraiva, J.A., Lopes-da-Silva, J.A., Delgadillo, I., van Loey, A., Smout, C., and Hendrickx, M. (2008). Effect of thermal blanching and of high pressure treatments on sweet green and red bell pepper fruits (*Capsicum annuum* L.). Food Chemistry 107, 1436-1449.

Chen, T.W., Henke, M., de Visser, P.H., Buck-Sorlin, G., Wiechers, D., Kahlen, K., and Stützel, H. (2014). What is the most prominent factor limiting photosynthesis in different layers of a greenhouse cucumber canopy? Annals of Botany 114, 677-688.

Chen, W.T., Yeh, Y.H.F., Liu, T.Y., and Lin, T.T. (2016). An automated and continuous plant weight measurement system for plant factory. Frontiers in Plant Science 7, 392.

Chi, M., Plaza, A., Benediktsson, J.A., Sun, Z., Shen, J., and Zhu, Y. (2016). Big data for remote sensing: Challenges and opportunities. Proceedings of the Institute of Electrical and Electronics Engineers 104, 2207-2219.

Cho, Y.Y., Oh, S., Oh, M.M., and Son, J.E. (2007). Estimation of individual leaf area, fresh weight, and dry weight of hydroponically grown cucumbers (*Cucumis sativus* L.) using leaf length, width, and SPAD value. Scientia Horticulturae 111, 330-334.

Cope, J.S., Corney, D., Clark, J.Y., Remagnino, P., and Wilkin, P. (2012). Plant species identification using digital morphometrics: A review. Expert Systems with Applications 39, 7562-7573.

Ćosić, M., Stričević, R., Djurović, N., Moravčević, D., Pavlović, M., and Todorović, M. (2017). Predicting biomass and yield of sweet pepper grown with and without plastic film mulching under different water supply and weather conditions. Agricultural Water Management 188, 91-100.

Csizinszky, A.A. (1999). Yield and nutrient uptake of capistrano 'bell peppers in Compost-amended sandy soil. In Proceeding-Florida State Horticultural Society 112, 333-336.

Da Silva, I.N., Spatti, D.H., Flauzino, R.A., Liboni, L.H.B., and dos Reis Alves, S.F. (2017). Artificial neural networks. Cham: Springer International Publishing.

Darula, S. and Kittler, R. (2002). CIE general sky standard defining luminance distributions. Proceedings eSim, 11-13.

Dayan, E., Van Keulen, H., Jones, J.W., Zipori, I., Shmuel, D., and Challa, H. (1993). Development, calibration and validation of a greenhouse tomato growth model: I. Description of the model. Agricultural Systems 43, 145-163.

De Gelder, A., Dieleman, J.A., Bot, G.P.A., and Marcelis, L.F.M. (2012). An overview of climate and crop yield in closed greenhouses. Journal of Horticultural Science and Biotechnology 87, 193-202.

De Visser, P.H.B., van der Heijden, G., and Buck-Sorlin, G. (2014). Optimizing illumination in the greenhouse using a 3D model of tomato and a ray tracer. Frontiers in Plant Science 5, 48.

Eftekhari, M., Yadollahi, A., Ahmadi, H., Shojaeiyan, A., and Ayyari, M. (2018). Development of an artificial neural network as a tool for predicting the targeted phenolic profile of grapevine (*Vitis vinifera*) foliar wastes. Frontiers in Plant Science 9, 837.

Ehret, D.L., Hill, B.D., Helmer, T., and Edwards, D.R. (2011). Neural network modeling of greenhouse tomato yield, growth and water use from automated crop monitoring data. Computers and Electronics in Agriculture 79, 82-89.

El-Omari, S. and Moselhi, O. (2011). Integrating automated data acquisition technologies for progress reporting of construction projects. Automation in Construction 20, 699-705.

Fang, H., Li, W., Wei, S., and Jiang, C. (2014). Seasonal variation of leaf area index (LAI) over paddy rice fields in NE China: Intercomparison of destructive sampling, LAI-2200, digital hemispherical photography (DHP), and AccuPAR methods. Agricultural and Forest Meteorology 198, 126-141.

Flexas, J., Ribas-Carbó, M., Bota, J., Galmés, J., Henkle, M., Martínez-Cañellas, S., and Medrano, H. (2006). Decreased Rubisco activity during water stress is not induced by decreased relative water content but related to conditions of low stomatal conductance and chloroplast CO_2 concentration. New Phytologist 172, 73-82.

Fonseca, S.C., Oliveira, F.A., and Brecht, J. K. (2002). Modelling respiration rate of fresh fruits and vegetables for modified atmosphere packages: a Review. Journal of Food Engineering 52, 99-119.

Frans, M., Moerkens, R., Van Gool, S., Sauviller, C., Van Laethem, S., Luca, S., ... and Ceusters, J. (2018). Modelling greenhouse climate factors to constrain internal fruit rot (*Fusarium* spp.) in bell pepper. Journal of Plant Diseases and Protection 125, 452-432.

Gijzen, H., Heuvelink, E., Challa, H., Marcelis, L.F.M., Dayan, E., Cohen, S., and Fuchs, M. (1997). HORTISIM: a model for greenhouse crops and greenhouse climate. Acta Horticulturae 456, 441-450.

Glenn, D.M., Bassett, C.B., Tworkoski, T., Scorza, R., and Miller, S.S. (2015). Tree architecture of pillar and standard peach affect canopy transpiration and water use efficiency. Scientia Horticulturae 187, 30-34.

Gupta, D.K., Kumar, P., Mishra, V.N., Prasad, R., Dikshit, P.K.S., Dwivedi, S.B., ... and Srivastava, V. (2015). Bistatic measurements for the estimation of rice crop variables using artificial neural network. Advances in Space Research 55, 1613-1623.

Gupta, R., Tiwari, G. N., Kumar, A., and Gupta, Y. (2012). Calculation of total solar fraction for different orientation of greenhouse using 3D-shadow analysis in Auto-CAD. Energy and Buildings 47, 27-34.

Hsiao, T.C., Heng, L., Steduto, P., Rojas-Lara, B., Raes, D., and Fereres, E. (2009). AquaCrop—the FAO crop model to simulate yield response to water: III. Parameterization and testing for maize. Agronomy Journal 101, 448-459.

Hashem, I.A.T., Yaqoob, I., Anuar, N.B., Mokhtar, S., Gani, A., and Khan, S.U. (2015). The rise of “big data” on cloud computing: Review and open research issues. Information Systems 47, 98-115.

Helmer, T., Ehret, D. L., and Bittman, S. (2005). CropAssist, an automated system for direct measurement of greenhouse tomato growth and water use. Computers and Electronics in Agriculture 48, 198-215.

Hemming, S., Dueck, T., Janse, J., and van Noort, F. (2007). The effect of diffuse light on crops. In International Symposium on High Technology for Greenhouse System Management: Greensys2007, 801, 1293-1300.

Henke, M. and Buck-Sorlin, G. H. (2018). Using a full spectral raytracer for calculating light microclimate in functional-structural plant modelling. Computing and Informatics 36, 1492-1522.

Heuvelink, E. (1999). Evaluation of a dynamic simulation model for tomato crop growth and development. Annals of Botany 83, 413-422.

Hilker, T., Coops, N.C., Schwalm, C.R., Jassal, R.P.S., Black, T.A., and Krishnan, P. (2008). Effects of mutual shading of tree crowns on prediction of photosynthetic light-use efficiency in a coastal Douglas-fir forest. Tree Physiology 28, 825-834.

Hitz, T., Henke, M., Graeff-Hoenninger, S., and Munz, S. (2019). Three-dimensional simulation of light spectrum and intensity within an LED growth chamber. Computers and Electronics in Agriculture 156, 540-548.

Himeno, S., Azuma, W., Gyokusen, K., and Ishii, H. R. (2017). Leaf water maintains daytime transpiration in young *Cryptomeria japonica* trees. Tree Physiology 37, 1394-1403.

Hochreiter, S. and Schmidhuber, J. (1997). Long short-term memory. Neural Computation 9, 1735-1780.

Jacobs, S.A., Dryden, N., Pearce, R., and Van Essen, B. (2017). Towards scalable parallel training of deep neural networks. In Proceedings of the Machine Learning on HPC Environments, 5.

Jang, D., Choi, k., Heo, J. and Kim, I. (2018). The effect of transplant age on growth and fruit yield in winter-planted paprika cultivation. Horticultural Science and Technology 36, 470-477.

Jensen, M.H. (1997). Food production in greenhouses. In Plant production in closed ecosystems (pp. 1-14). Springer, Dordrecht.

Ji, S., Zhang, C., Xu, A., Shi, Y., and Duan, Y. (2018). 3D convolutional neural networks for crop classification with multi-temporal remote sensing images. Remote Sensing 10, 75.

Jones, J.W., Antle, J.M., Basso, B., Boote, K.J., Conant, R.T., Foster, I., ... & Keating, B.A. (2017). Brief history of agricultural systems modeling. Agricultural Systems 155, 240-254.

Jones, J.W., Dayan, E., Allen, L.H., Van Keulen, H., and Challa, H. (1991). A dynamic tomato growth and yield model (TOMGRO). Transactions of the ASAE 34, 663-0672.

Jones, J.W., Hoogenboom, G., Porter, C.H., Boote, K.J., Batchelor, W.D., Hunt, L.A., ... & Ritchie, J.T. (2003). The DSSAT cropping system model. European Journal of Agronomy 18, 235-265.

Jovicich, E., Cantliffe, D.J., Stoffella, P.J., and Haman, D.Z. (2007). Bell pepper fruit yield and quality as influenced by solar radiation-based irrigation and container media in a passively ventilated greenhouse. HortScience 42, 642–652.

Jozefowicz, R., Zaremba, W., and Sutskever, I. (2015). An empirical exploration of recurrent network architectures. In International Conference on Machine Learning, 2342-2350.

Kalidindi, S., Bala, G., Modak, A., and Caldeira, K. (2015). Modeling of solar radiation management: a comparison of simulations using reduced solar constant and stratospheric sulphate aerosols. Climate Dynamics 44, 2909-2925.

Kamilaris, A., Kartakoullis, A., and Prenafeta-Boldú, F.X. (2017). A review on the practice of big data analysis in agriculture. Computers and Electronics in Agriculture 143, 23-37.

Kang, S., van Iersel, M. W., and Kim, J. (2019). Plant root growth affects FDR soil moisture sensor calibration. Scientia Horticulturae 252, 208-211.

Kanniah, K. D., Beringer, J., and Hutley, L. (2013). Exploring the link between clouds, radiation, and canopy productivity of tropical savannas. Agricultural and Forest Meteorology 182, 304-313.

Kim, J. (2012). Developing and integrating plant models for predictive irrigation. Irrigation Association, 2-6.

Kim, J. and van Iersel, M. W. (2011). Slowly developing drought stress increases photosynthetic acclimation of *Catharanthus roseus*. Physiologia Plantarum 143, 166-177.

Kim, J., Kang, W., Ahn, T., Shin, J., and Son, J. (2016). Precise, real-time measurement of the fresh weight of lettuce with growth stage in a plant factory using a nutrient film technique. Korean Journal of Horticultural Science and Technology 34, 77-83.

Klein, T., Cohen, S., Paudel, I., Preisler, Y., Rotenberg, E., and Yakir, D. (2016). Diurnal dynamics of water transport, storage and hydraulic conductivity in pine trees under seasonal drought. iForest-Biogeosciences and Forestry 9, 710.

Klepper, B., Browning, V. D., and Taylor, H. M. (1971). Stem diameter in relation to plant water status. Plant Physiology 48, 683-685.

Kingma, D. P. and Ba, J. (2014). Adam: A method for stochastic optimization. arXiv preprint arXiv:1412.6980.

Kohavi, R (1995). A study of cross-validation and bootstrap for accuracy estimation and model selection. In Ijcai, 14:1137-1145.

Körner, O. and Holst, N. (2015, October). An open-source greenhouse modelling platform. In V International Symposium on Applications of Modelling as an Innovative Technology in the Horticultural Supply Chain-Model-IT 1154, 241-248.

Küçükönder, H., Boyaci, S., and Akyüz, A. (2016). A modeling study with an artificial neural network: developing estimation models for the tomato plant leaf area. Turkish Journal of Agriculture and Forestry 40, 203-212.

Kumar, R., Chhabra, S., Verma, A.S., and Gupta, A. (2018). Analysis of load cell. International Journal of Applied Engineering Research 13, 274-277.

Kumar, K., Kumar, S., Sankar, V., Sakthivel, T., Karunakaran, G., and Tripathi, P. C. (2017). Non-destructive estimation of leaf area of durian (*Durio zibethinus*)–An artificial neural network approach. Scientia Horticulturae 219, 319-325.

Lena, B.P., Folegatti, M.V., Francisco, J., Santos, O.N.A., and Andrade, I.P.S. (2016). Performance of LAI-2200 plant canopy analyzer on leaf area index of Jatropha nut estimation. Journal of Agronomy 15, 191-197.

Li, T. and Yang, Q. (2015). Advantages of diffuse light for horticultural production and perspectives for further research. Frontiers in Plant Science 6, 704.

Llop, J., Gil, E., Llorens, J., Miranda-Fuentes, A., and Gallart, M. (2016). Testing the suitability of a terrestrial 2D LiDAR scanner for canopy characterization of greenhouse tomato crops. Sensors 16, 1435.

Lopes, D., Nunes, L., Walford, N., Aranha, J., Sette, C. J., Viana, H., and Hernandez, C. (2014). A simplified methodology for the correction of Leaf Area Index (LAI) measurements obtained by ceptometer with reference to Pinus Portuguese forests. iForest-Biogeosciences and Forestry, 7, 186.

Ma, L., Hoogenboom, G., Ahuja, L.R., Ascough Ii, J.C., and Saseendran, S.A. (2006). Evaluation of the RZWQM-CERES-Maize hybrid model for maize production. Agricultural Systems 87, 274-295.

Marcelis, L.F.M., Heuvelink, E., Baan Hofman-Eijer, L. R., Den Bakker, J., and Xue, L. B. (2004). Flower and fruit abortion in sweet pepper in relation to source and sink strength. Journal of Experimental Botany 55, 2261-2268.

Marcelis, L.F.M., Heuvelink, E., and Goudriaan, J. (1998). Modelling biomass production and yield of horticultural crops: a Review. Scientia Horticulturae 74, 83-111.

Marchiori, P.E., Machado, E.C., and Ribeiro, R.V. (2014). Photosynthetic limitations imposed by self-shading in field-grown sugarcane varieties. Field Crops Research 155, 30-37.

Martínez-Ruiz, A., López-Cruz, I.L., Ruiz-García, A., Pineda-Pineda, J., and Prado-Hernández, J.V. (2019). HortSyst: A dynamic model to predict growth, nitrogen uptake, and transpiration of greenhouse tomatoes. Chilean Journal of Agricultural Research 79, 1.

Mercado, L.M., Bellouin, N., Sitch, S., Boucher, O., Huntingford, C., Wild, M., and Cox, P.M. (2009). Impact of changes in diffuse radiation on the global land carbon sink. Nature 458, 1014.

Min, Q.,and Duan, M. (2005). Simultaneously retrieving cloud optical depth and effective radius for optically thin clouds. Journal of Geophysical Research: Atmospheres 110, 21.

Monsi, M. and Saeki, T. (2005). On the factor light in plant communities and its importance for matter production. Annals of Botany 95, 549-567.

Muangprathub, J., Boonnam, N., Kajornkasirat, S., Lekbangpong, N., Wanichsombat, A., and Nillaor, P. (2019). IoT and agriculture data analysis for smart farm. Computers and Electronics in Agriculture 156, 467-474.

Ngouajio, M., Auras, R., Fernandez, R. T., Rubino, M., Counts, J. W., and Kijchavengkul, T. (2008). Field performance of aliphatic-aromatic copolyester biodegradable mulch films in a fresh market tomato production system. HortTechnology 18, 605-610.

Nguyen, T., Slaughter, D., Max, N., Maloof, J., and Sinha, N. (2015). Structured light-based 3D reconstruction system for plants. Sensors 15, 18587-18612.

Nikolaou, G., Neocleous, D., Katsoulas, N., and Kittas, C. (2017). Effect of irrigation frequency on growth and production of a cucumber crop under soilless culture. Emirates Journal of Food and Agriculture 29, 863–871.

Ogbonnaya, C.I., Sarr, B., Brou, C., Diouf, O., Diop, N.N., and Roy-Macauley, H. (2003). Selection of cowpea genotypes in hydroponics, pots, and field for drought tolerance. Crop Science 43, 1114-1120.

O'Grady, M. J. and O'Hare, G. M. (2017). Modelling the smart farm. Information Processing in Agriculture 4, 179-187.

Oliphant, A.J., Dragoni, D., Deng, B., Grimmond, C.S.B., Schmid, H.P., and Scott, S.L. (2011). The role of sky conditions on gross primary production in a mixed deciduous forest. Agricultural and Forest Meteorology 151, 781-791.

Pantazi, X.E., Moshou, D., Alexandridis, T., Whetton, R.L., and Mouazen, A.M. (2016). Wheat yield prediction using machine learning and advanced sensing techniques. Computers and Electronics in Agriculture 121, 57-65.

Park, J.S., Tai, N.H., Ahn, T.I., Son, J.E. (2009) Analysis of moisture characteristics in rockwool slabs using time domain reflectometry (TDR) sensors and their applications to paprika cultivation. Journal of Bio-Environment Control 18, 238-243.

Paulus, S., Dupuis, J., Mahlein, A.K., and Kuhlmann, H. (2013). Surface feature based classification of plant organs from 3D laserscanned point clouds for plant phenotyping. BMC Bioinformatics 14, 238.

Paulus, S., Behmann, J., Mahlein, A.K., Plümer, L., and Kuhlmann, H. (2014). Low-cost 3D systems: suitable tools for plant phenotyping. Sensors 14, 3001-3018.

Peksen, E. (2007). Non-destructive leaf area estimation model for faba bean (*Vicia faba* L.). Scientia Horticulturae 113, 322-328.

Rajagopal, V., Balasubramanian, V., and Sinha, S.K. (1977). Diurnal fluctuations in relative water content, nitrate reductase and proline content in water-stressed and non-stressed wheat. Physiologia Plantarum 40, 69-71.

Ratto, M., Tarantola, S., and Saltelli, A. (2001). Sensitivity analysis in model calibration: GSA-GLUE approach. Computer Physics Communications 136, 212-224.

Rivera, C.M., Rouphael, Y., Cardarelli, M., and Colla, G. (2007). A simple and accurate equation for estimating individual leaf area of eggplant from linear measurements. European Journal of Horticultural Science 72, 228.

Roccia, J.P., Piaud, B., Coustet, C., Caliot, C., Guillot, E., Flamant, G., and Delatorre, J. (2012). SOLFAST, a Ray-tracing Monte-Carlo software for solar concentrating facilities. In Journal of Physics: Conference Series 369, 012029.

Rodríguez, F., Berenguel, M., Guzmán, J. L., and Ramírez-Arias, A. (2015). Modeling and control of greenhouse crop growth. Springer International Publishing.

Roger, M.J.R. (ed.). (2001). Handbook of plant ecophysiology techniques i9780792370536. Kluwer Academic Publishers.

Rouphael, Y., Rivera, C.M., Cardarelli, M., Fanasca, S., and Colla, G. (2006). Leaf area estimation from linear measurements in zucchini plants of different ages. Journal of Horticultural Science and Biotechnology 81, 238-241.

Rouphael, Y., Mouneimne, A.H., Ismail, A., Mendoza-De Gyves, E., Rivera, C.M., and Colla, G. (2010). Modeling individual leaf area of rose (*Rosa hybrida* L.) based on leaf length and width measurement. Photosynthetica 48, 9-15.

Sala, F., Arsene, G.G., Iordănescu, O., and Boldea, M. (2015). Leaf area constant model in optimizing foliar area measurement in plants: A case study in apple tree. Scientia Horticulturae 193, 218-224.

Salisbury, F.B. and Ross, C.W. (1992). Plant physiology. Fourth edition. Wadsworth Publishing Company, Belmont, California.

Schirrmann, M., Hamdorf, A., Giebel, A., Dammer, K.H., and Garz, A. (2015). A mobile sensor for leaf area index estimation from canopy light transmittance in wheat crops. Biosystems Engineering 140, 23-33.

Schwarz, D. and Kläring, H. P. (2001). Allometry to estimate leaf area of tomato. Journal of Plant Nutrition 24, 1291-1309.

Sezen, S.M., Yazar, A., and Eker, S. (2006). Effect of drip irrigation regimes on yield and quality of field grown bell pepper. Agricultural Water Management 81, 115-131.

Shamshiri, R., Ahmad, D., Zakaria, A., Ismail, W.I.W., Man, H.C., and Yamin, M. (2016). Evaluation of the reduced state-variable TOMGRO model using boundary data. Proceeding of ASABE, 162454205.

Shi, Y., Li, Y.N., Zhang, C., Bai, M.J., and Wang, Y.K. (2015). Development and Application of Decision Support System for Agro-technology Transfer DSSAT under Water Resources Management. Advanced Materials Research 1073, 1596-1603.

Shin, J.H. and Son, J.E. (2015) Development of a real-time irrigation control system considering transpiration, substrate electrical conductivity, and drainage rate of nutrient solutions in soilless culture of paprika (*Capsicum annuum* L.). European.Journal of.Horticulture.Science 80, 271-279.

Skierucha, W. and Wilczek, A. (2010). A FDR sensor for measuring complex soil dielectric permittivity in the 10–500 MHz frequency range. Sensors 10, 3314-3329.

Son, J.E., Kang, W.H., Kim, D.P., Hwang, I.H., and Kim, J.W. (2018). Development of functional-structural modeling techniques for advanced greenhouse crop growth modelling. iPET. (pp. 188).

Sonka, S. (2016). Big data: fueling the next evolution of agricultural innovation. Journal of Innovation Management 4, 114-136.

Spitters, C.J.T. and Schapendonk, A.H.C.M. (1990). Evaluation of breeding strategies for drought tolerance in potato by means of crop growth simulation. In Genetic aspects of plant mineral nutrition (pp. 151-161). Springer, Dordrecht.

Still, C.J., Riley, W.J., Biraud, S.C., Noone, D.C., Buenning, N.H., Randerson, J.T., and Farquhar, G.D. (2009). Influence of clouds and diffuse radiation on ecosystem-atmosphere CO_2 and $CO^{18}O$ exchanges. Journal of Geophysical Research 114, G01018.

Story, D. and Kacira, M. (2015). Design and implementation of a computer vision-guided greenhouse crop diagnostics system. Machine Vision and Applications 26, 495-506.

Suguiyama, V.F., da Silva, E.A., Meirelles, S.T., Centeno, D.D.C., and Braga, M.R. (2014). Leaf metabolite profile of the Brazilian resurrection plant *Barbacenia purpurea* Hook.(*Velloziaceae*) shows two time-dependent responses during desiccation and recovering. Frontiers in Plant Science 5, 96.

Takaichi, M., Shimaji, H., and Higashide, T. (1996). Monitoring of the change in fresh weight of plants grown in water culture. Acta Horticulturae 440, 413–418.

Toyota, M., Spencer, D., Sawai-Toyota, S., Jiaqi, W., Zhang, T., Koo, A. J., and Gilroy, S. (2018). Glutamate triggers long-distance, calcium-based plant defense signaling. Science 361, 1112-1115.

Ueda, M. and Nakamura, Y. (2007). Chemical basis of plant leaf movement. Plant and Cell Physiology 48, 900-907.

Uno, I., Yumimoto, K., Pan, X., Wang, Z., Osada, K., Itahashi, S., and Yamamoto, S. (2017). Simultaneous dust and pollutant transport over east asia: The tripartite environment ministers meeting march 2014 case study. SOLA, 13, 47-52.

Vieira, M.I., de Melo-Abreu, J.P., Ferreira, M.E., and Monteiro, A.A. (2009). Dry matter and area partitioning, radiation interception and radiation-use efficiency in open-field bell pepper. Scientia Horticulturae 121, 404-409.

Wang, L. (2005). A hybrid genetic algorithm–neural network strategy for simulation optimization. Applied Mathematics and Computation 170, 1329-1343.

Wang, H., Sánchez-Molina, J.A., Li, M., Berenguel, M., Yang, X.T., and Bienvenido, J.F. (2017). Leaf area index estimation for a greenhouse transpiration model using external climate conditions based on genetics algorithms, back-propagation neural networks and nonlinear autoregressive exogenous models. Agricultural Water Management 183, 107-115.

Wolfert, S., Ge, L., Verdouw, C., and Bogaardt, M.J. (2017). Big data in smart farming–a review. Agricultural Systems 153, 69-80.

Wu, G., Liu, Y., and Wang, T. (2007). Methods and strategy for modeling daily global solar radiation with measured meteorological data–A case study in Nanchang station, China. Energy Conversion and Management 48, 2447-2452.

Wyenandt, C.A., Kline, W.L., Ward, D.L., and Brill, N.L. (2017). Production system and cultivar effects on the development of skin separation or “silvering” in bell pepper fruit. HortTechnology 27, 37-44.

Yadav, S.B., Misra, A.K., Mishra, S.K., and Pandey, V. (2018). Crop growth simulation models (InfoCrop v. 2.1, DSSATv4. 5, WOFOSTv1. 5 and Cropsytv 4.19) software. Water and Energy Security in The Arena of Climate Change 34, 456-469.

Yamori, W., Makino, A., and Shikanai, T. (2016). A physiological role of cyclic electron transport around photosystem I in sustaining photosynthesis under fluctuating light in rice. Scientific Reports 6, 20147.

Yang, W., Duan, L., Chen, G., Xiong, L., and Liu, Q. (2013). Plant phenomics and high-throughput phenotyping: accelerating rice functional genomics using multidisciplinary technologies. Current Opinion in Plant Biology 16, 180-187.

Yao, W., Kelbe, D., Leeuwen, M., Romanczyk, P., and Aardt, J. (2016). Towards an improved LAI collection protocol via simulated and field-based PAR sensing. Sensors 16, 1092.

Zamora-Izquierdo, M.A., Santa, J., Martínez, J.A., Martínez, V., and Skarmeta, A.F. (2019). Smart farming IoT platform based on edge and cloud computing. Biosystems Engineering 177, 4-17.

CHAPTER 1

Estimating Leaf Area Index of Bell pepper According to Growth Stage Using Ray-tracing Simulation and Long Short-term Memory

ABSTRACT

Leaf area index (LAI), which represents crop-growth characteristics, is used to calculate canopy photosynthetic rate, set irrigation standards, and predict crop growth. LAI can be non-destructively and continuously estimated using the light-intensity ratio of the upper and lower crop canopy, but it is affected by solar altitude and external weather conditions. The objective of this study was to develop a method to estimate LAI using the light-intensity ratio of the upper and lower crop canopy via solar altitude and weather conditions. Growth stages and weather conditions with solar altitude were set using 3D-scanned plant models and ray-tracing simulation, respectively. The light intensities at each location of the canopy for given conditions were calculated using ray-tracing simulation. The relationship between light-intensity ratio and LAI was analyzed using long short-term memory (LSTM), which is a type of artificial neural network. According to our results, the ratio varied depending on solar altitude and external weather

conditions and exponentially decreased with increasing LAI. This LSTM algorithmic approach was able to quantitatively analyze this complex relationship; compared with a greenhouse experiment for validation, the algorithm was highly accurate (R^2=0.808). Accuracy further increased when solar altitude and weather conditions were added to the model. Therefore, we conclude that, using this method, LAI can be accurately measured in a non-destructive and continuous manner.

Additional keywords: continuous measurement, leaf area, light interception, paprika, recurrent neural network

INTRODUCTION

Crop leaves absorb light, produce biochemical energy, and exchange carbon and water; thus, they are important subjects for botanical, morphometrical, physiological, and ecological research (Cope et al., 2012; Sala et al., 2015). Among the various characteristics of leaves, the leaf area index (LAI), which is the leaf area per unit cultivation area, has a quantitative relationship with crop canopy photosynthesis and transpiration, so is used as a standard for irrigation and fertilization (Suguiyama et al., 2014; Yamori et al., 2016). Additionally, LAI is an important parameter for predicting crop growth and yield (Bertin and Heuvelink, 1993; Jones et al., 1991). Usually, crop leaf area data are collected through destructive means, which inherently limits the potential for continuous measurement of crop growth changes and affects crop growth and development due to changes in the amount of light interception by adjacent crops (Peksen, 2007). Therefore, further non-destructive approaches for estimating leaf area are necessary.

Simulation techniques offer an indirect method for estimating crop LAI (Rodríguez et al., 2015; Wang et al., 2017). However, simulation has a limited ability to estimate dynamic changes in leaf area because it cannot account for variable factors associated with cultivation. Although regression models offer a non-destructive approach for evaluating leaf area and leaf width for LAI (apples, Sala et al., 2015; cucumbers, Cho et al., 2006; eggplants, Rivera et al., 2007; roses, Rouphael et al., 2010; tomatoes, Schwarz and Klaring, 2001; and zucchini plants, Rouphael et al., 2006), this method requires a lot

of time and labor because the length and width of all leaves on every plant must be measured. Automated measurement is a fast, simple, and non-destructive way to measure dynamic changes in leaf area and to acquire large amounts of continuous crop growth data (Spitters, 1990). Recent examples of an automated continuous measurement of crop leaf area include 3D laser scanning, RGB camera, and thermal cameras that can record crop shape and form (Llop et al., 2016; Nguyen et al., 2015). However, these imaging methodologies require high cost for both measurement and analysis (El-Omari and Moselhi, 2011; Paulus et al., 2013) and require expensive platforms in commercial greenhouses (Paulus et al., 2014; Yang et al., 2013).

Thus, there is a need for a low-cost and practical continuous LAI measurement system. Monsi and Saeki (2005) showed that the light interception of the crop canopy is related to crop LAI, according to modifications of Lambert-Beer's equation. Using the differences between the upper and lower light intensities of the crop canopy, LAI can be estimated in forests or open fields (Fang et al., 2014; Lena et al., 2016; Lopes et al., 2014; Yao et al., 2016). However, in greenhouses, light conditions are changed by interactions between the greenhouse location and date, solar altitude by time, and various greenhouse structural factors, all of which can have different light characteristics compared with field contexts (Buck-Sorin et al., 2011; Gupta et al., 2012). Also, external weather conditions change the ratio of diffusive solar radiation, which has high light interception within crop canopies, and this can change light spatial distributions in the crop canopy (Li and Yang, 2015).

Therefore, to accurately estimate crop LAI, it is necessary to quantitatively analyze the light receiving patterns of greenhouse-cultivated crop canopies, while considering solar altitude and external weather conditions. Solar altitudes and external weather conditions are thought to be inevitable factors; thus, they are not yet possible to artificially control through experimentation. Recent studies have looked at various horticultural crops, such as cucumbers (Chen et al., 2014), tomatoes (de Visser et al., 2014), and roses (Buck-Sorlin et al., 2011), to analyze their spatial light distributions using a 3D graphic software and ray-tracing simulation on virtual light conditions. Ray-tracing simulation is an effective tool for quantitative analyses of crop canopy light receiving patterns.

The objective of this study was to develop a continuous LAI estimation system applicable to greenhouse cultivation of bell peppers using a ray-tracing method and long short-term memory (LSTM) that considers growth stage, solar altitude, and weather conditions.

MATERIALS AND METHODS

Use of 3D crop models and construction of greenhouse model

3D-scanned models of bell pepper (*Capsicum annuum* L.) developed by Son et al. (2018) were used. The growth stages of the models were 14, 21, 28, 35, 42, 49, 56, 63, 70, 77, and 84 days after transplanting (DAT) (Fig. 1-1). The crops were scanned by using a 3D scanner (GO! SCANTM; Creaform, Lévis, Quebec, Canada) and converted to a parametric model by using a scanning software (Vxelement; Creaform) and a reverse-engineering software (Geomagic Design X; 3D Systems, Rock Hill, SC, USA). The 3D models were reconstructed by using a 3D CAD software (SOLIDWORKS; Dassault Systèmes, Vélizy-Villacoublay, France).

The Venlo-type greenhouse model were constructed by using the 3D CAD software, and the 3D crop models were placed inside the greenhouse model (Fig 1-2). Optical simulations were carried out by using an optical simulation software (Optisworks, Optis, La Farlède, France). To apply the optical properties of the 3D crop models, crop leaf transmittance (Tr) and reflectance (Ref) were measured within a range of 400–700 nm in the integrating sphere combined with a radiospectrometer. Leaf absorbance (Abs) was calculated as: Abs = 1- (Tr + Ref). The optical properties of glass and iron were applied to account for the glass and frame components of the greenhouse model.

Estimation of light intensity during simulation conditions

Twelve weeks after transplantation, the plants were used for 3D crop modeling of a ray-tracing simulation, in which the solar radiation condition was determined by solar altitudes (latitude, longitude, date, time of the simulation set point, bearing, and ceiling direction) and microclimate environmental conditions. The location of the experimental farm at Seoul National University (Suwon, Korea, Lat. 37.3° N, long. 127° E) was used for the solar altitude as the validation experiment site. The orientation of the greenhouse was set as south-north-east, and the direction of the ceiling was set as horizontal to the height of the greenhouse. The dates of simulation were representative dates for spring, summer, autumn, and winter: April 15th, July 15th, October 15th, and January 15th, respectively. Seven times (09:00, 10:00, 11:00, 12:00, 14:00, 16:00, and 18:00) were set and analyzed for changes in daylight environment.

Another parameter for determining solar radiation was microclimate environmental condition, which indicates the degree of diffuse solar radiation allowed to pass through the atmosphere by clouds and aerosols. To estimate microclimate environments, the International Commission on Illumination (CIE) proposed a standard general sky, which classifies atmospheric conditions related to diffuse solar radiation into 15 standard states (Darula and Kittler 2002). Among the 15 CIE standard states, type 1 (standard overcast sky), type 6 (partly cloudy sky), and type 12 (standard clear sky) were selected for this study and were set to weather conditions corresponding to overcast, cloudy, and clear sky provided by the Korea Meteorological Administration.

Ray-tracing simulation was conducted on 1,008 conditions (12 growth stages * 4 seasons * 7 times of day * 3 weather conditions), and 5*108 rays were used in optical

simulation. Light intensity at the upper canopy (I_t), light intensity prior to crop-canopy interception at 20 cm above the top of the canopy, and light intensity at the lower canopy (I_b) at the height of the first main branch were measured.

Application of long short-term memory (LSTM)

The artificial neural network LSTM has been used to analyze sequential periodic data (Hochreiter and Schmidhuber 1997); a general network structure was used in this study (Fig. 1-3). The light-intensity ratio of the upper and lower crop canopies, weather conditions, seasons, and times of the day were used as input data, and LAI was used as output data. The time step, one of the parameters for LSTM, was set to seven. AdamOptimizer was used for model training (Kingma and Ba, 2014), and the hyperparameters for LSTM and AdamOptimizer were empirically changed to solve regression problems (Table 1-1). For model training, 70% of the total data were randomly selected, and the rest of the data were used for accuracy tests of the training results. To include all simulation conditions in the training, k-folds cross test with k = 5 was conducted (Kohavi 1995). The mean square error (MSE) was set as a cost for reducing computation. Training and test accuracy were verified using the coefficient of determination (R^2) and root mean squared error (RMSE). TensorFlow (v. 1.12.0, Google, Menlo Park, CA, USA) was used for computation and model construction (Abadi et al. 2016).

Cultivation conditions and LAI validation

A cultivation validation experiment was conducted to verify the algorithm for estimating LAI according to light intensities of the upper and lower crop canopy. The algorithm was developed through ray-tracing simulations and machine learning. The plants were cultivated in a Venlo-type greenhouse at the experimental farm from November 2016 to April 2017. Beginning when the plant formed its first main branch, three pyranometers (SP-110; Apogee Instruments Inc., Logan, Utah, USA) were installed in the upper crop canopy, and nine sensors were placed in each crop's first main branch to measure the light intensity in the upper canopy (I_t) and in the lower canopy (I_b) (Fig. 1-4). Leaf area and LAI were calculated and measured with an LAI meter (Li-3100; LI-COR, Lincoln, NE, USA) every five days on crops with installed sensors and similar leaf numbers and plant heights. External weather condition data were collected from the Suwon Korea Meteorological Administration (https://www.weather.go.kr/weather/climate/past_ table.jsp?stn=119). The accuracy of the algorithm was evaluated by comparing the machine-learned LSTM algorithm with ray-tracing simulation results to direct measurements of I_t, I_b, season, time, and weather data.

RESULTS AND DISCUSSION

Change in light intensity within the crop canopy

With regard to vertical spatial canopy light distribution of the greenhouse floor on DAT 63, the transmitted light intensity exponentially decreased from the upper to the lower crop canopy (Fig. 1-5). Because solar radiation is mainly absorbed in the leaves of the upper canopy, the light intercepting into the lower canopy was blocked (Hilker et al. 2008; Marchiori et al. 2014). The results in this study were consistent with those of previous studies that directly measured canopy light interceptions (Glenn et al. 2015; Schirrmann et al. 2015).

The daytime light intensities of the upper crop canopy continuously increased after sunrise, had highest intensity at 12:00, and decreased thereafter. Compared to the winter, light intensity was higher in the summer with longer daylight hours (Fig. 1-6A, DAT 63, clear sky condition), indicating that our ray-tracing simulations were well applied to the characteristics of solar radiation changes by time and season. Daytime changes in light intensity in the lower crop canopy were affected by the upper crop canopy, and the light intensity continuously increased after sunrise, reaching a peak at 12:00 before decreasing. However, the ranges of daytime light-intensity changed in the lower canopy were not greater than those in the upper crop canopy, which highly affected the light-intensity ratio of the upper and lower canopy (Fig. 1-6B, DAT 63, clear sky condition). During the daytime, the ratio did not show a constant pattern but was usually higher around sunrise and sunset. In contrast to open field cultivation, greenhouses crops are grown along the

lane for the convenience of workers, so the light-interception patterns of the upper and lower leaves are highly influenced by solar altitude. This trend was particularly significant at low solar altitudes with smaller light intensity differences between the upper and lower canopy. Even for crops with the same LAI, the light-intensity ratio of the upper and lower canopy changed according to the time of day.

Light intensities in the upper and lower canopy were highest under clear sky conditions, followed by cloudy sky conditions, and then overcast sky conditions, and showed smaller differences under low solar altitude conditions (Fig. 1-7A, DAT 63, summer). Solar radiation decreases as clouds block the solar radiation passing through the atmosphere (Min and Duan 2005). However, according to previous studies, clouds reduced the amount of total solar radiation but increased the ratio of diffuse solar radiation (Kanniah et al. 2013; Oliphant et al. 2011; Still et al. 2009). Clouds not only increased the ratio of diffuse solar radiation, which has higher light penetration within the crop canopy, but also affected the crop canopy's light interception pattern by changing primary growth productivity, net ecosystem exchange, and light-use efficiency. Studies of horticultural crop production that artificially increased the ratio of diffuse solar radiation in greenhouse conditions have been carried out (Hemming et al. 2008; Li et al. 2015), and an effect of increasing diffuse solar radiation was also observed in our simulation results. Under cloudy sky conditions, the light-intensity ratio of the upper and lower canopy was higher compared with clear sky conditions (Fig. 1-7B, DAT 63, summer). Direct solar radiation was mostly absorbed in the upper canopy and did not reach the lower canopy, but diffuse solar radiation reached the lower part of the canopy

as well, indicating that, even for crops with the same LAI, the light-intensity ratio can change according to external weather conditions.

With progressing crop growth stage, LAI and the daily average light-intensity ratio increased or decreased sigmoidally according to seasonal variation, but these differences were not significant (Fig. 1-8A, clear sky, average for all times). The daily average light-intensity ratio by DAT exponentially decreased with LAI (Fig. 1-8B, clear sky, average for all times). In previous studies (Fang et al. 2014; Lena et al. 2016; Lopes et al. 2014; Yao et al. 2016), LAI was estimated by measuring the light-intensity ratio. However, the relationship between LAI and light-intensity ratio of the upper and lower canopy showed different relational expression fittings at 12:00 and 18:00 (Figs. 1-8B, 1-9B). This implies that the optimum equation for LAI and the light-intensity ratio changes according to solar altitude. Also, meteorological conditions affected the optimum equation between LAI and the light-intensity ratio (Figs. 1-7B, 1-10B, 1-11B). For example, even though the light-intensity ratio was 0.3, the optimum equation for clear sky conditions estimated LAI to be 2.296, whereas the optimum equation for overcast sky conditions estimated LAI to be 2.559. Therefore, to estimate LAI according to light intensity in the upper and lower canopy, measurement time and weather conditions should be considered.

It is very difficult to experimentally set solar altitudes, external weather conditions, and crop growth stages (Buck-Sorlin et al. 2011; Roccia et al. 2012). Therefore existing products estimating LAI recommend to minimize these effects through manually methods. However, even with these experimental limitations, the combination of 3D crop modeling and ray-tracing simulation is highly useful for analyzing crops' light

intercepting patterns (Bailey 2018; de Visser et al. 2014; Henke and Buck-Sorlin 2018; Hitz et al. 2019). Using a 3D crop model and ray-tracing simulation, results for changes in light intensities according to various conditions, including solar altitude by season and time, external weather condition according to cloudiness, and crop growing stage, were obtained. This methodology can be useful for studying crops under various environmental and cultivation conditions.

LSTM accuracy

The average training accuracy of the LSTM was $R^2 = 0.990$. The test accuracy of each fold varied from 0.879 to 0.940 (Table 1-2). The average accuracy of the best test results was $R^2 = 0.937$, with RMSE = 1.48 (Fig. 1-12). LSTM was able to learn and estimate LAI with high accuracy by weekly scans of the 3D crop model according to season and weather conditions. LSTM, a type of recurrent neural network (RNN), is an optimum algorithm for analyzing data over time (Brunner et al. 2018). Daily solar radiation is comprised of patterned data over time, where it increases after sunrise, reaches the highest peak near noon, then decreases and reaches 0 after sunset. Therefore, LSTM was suitable for analyzing changes in daytime solar radiation.

LSTM algorithm learning efforts that excluded season and meteorological conditions had lower accuracy than algorithm tests that included these variables (Table 1-2). Previous estimates of crop LAI using difference in light intensities in the upper and lower canopy did not consider solar altitude or external weather conditions (Glenn et al. 2015; Schirrmann et al. 2015). Though there are limitations in the execution of

quantitative analysis of solar altitudes and weather conditions, this study quantitatively analyzed these parameters as input variables through LSTM.

Validation of LAI in a greenhouse

After verifying the LAI-estimating algorithm that was developed using ray-tracing simulation and LSTM, crop LAI was estimated to increase from 1.6 to 3.8, and the light-intensity ratio of the upper and lower canopy ranged from 0.138–0.479 from DAT 51 when measurement began to DAT 167 when measurement was completed (Fig. 1-13). Algorithm verification, which was performed by substituting daily seasonal and meteorological conditions into the ratio data for LAI and the light-intensity ratio of the upper and lower canopy, had an accuracy of R^2 = 0.808, and linearity error <5.517% (Fig.1-14). However, when LAI was estimated without meteorological data, algorithm accuracy significantly decreased to 0.426. Also, when LAI was estimated without seasonal data among the input variables, algorithm accuracy was 0.619, which was lower than that when all input parameters used. Not only did LAI and the light-intensity ratio of the upper and lower canopy affect the results from ray-tracing simulations, solar altitudes and external weather conditions also had an effect.

In this study, quantitative analyses of crop growth stage, season and time, and external weather conditions, which are difficult to control in actual experiments, were performed through ray-tracing simulations, and an accurate algorithm for estimating crop LAI was developed. However, this study has some limitations. First, only three weather conditions (clear, cloudy, overcast) were used in the simulation. Second, in addition to

atmospheric clouds, the diffuse solar-radiation ratio changes according to the amount of aerosol present (Kalidindi et al. 2015; Mercado et al. 2009). These aerosols change over time into fine dust, air pollution, etc. Recently, fine dust has become an important issue not only in Korea, but in other parts of East Asia as well (Uno et al. 2017). However, this study could not take into account the effect of aerosols because the Korea Meteorological Administration does not provide these information. If aerosols effects are included, the accuracy of the algorithm can be further improved.

LITERATURE CITED

Abadi, M., Barham, P., Chen, J., Chen, Z., Davis, A., Dean, J., and Kudlur, M. (2016). Tensorflow: A system for large-scale machine learning. In 12th {USENIX} Symposium on Operating Systems Design and Implementation 16, 265-283.

Bailey, B.N. (2018). A reverse ray-tracing method for modelling the net radiative flux in leaf-resolving plant canopy simulations. Ecological Modelling 368, 233-245.

Bertin, N. and Heuvelink, E. (1993). Dry-matter production in a tomato crop: comparison of two simulation models. Journal of Horticultural Science 68, 995-1011.

Buck-Sorlin, G., De Visser, P.H., Henke, M., Sarlikioti, V., Van Der Heijden, G.W., Marcelis, L.F., and Vos, J. (2011). Towards a functional–structural plant model of cut-rose: simulation of light environment, light absorption, photosynthesis and interference with the plant structure. Annals of Botany 108, 1121-1134.

Chen, T.W., Henke, M., De Visser, P.H., Buck-Sorlin, G., Wiechers, D., Kahlen, K., and Stützel, H. (2014). What is the most prominent factor limiting photosynthesis in different layers of a greenhouse cucumber canopy ?. Annals of botany 114, 677-688.

Cho, Y.Y., Oh, S., Oh, M.M., and Son, J.E. (2007). Estimation of individual leaf area, fresh weight, and dry weight of hydroponically grown cucumbers (*Cucumis sativus* L.) using leaf length, width, and SPAD value. Scientia Horticulturae 111, 330-334.

Cope, J.S., Corney, D., Clark, J.Y., Remagnino, P., and Wilkin, P. (2012). Plant species identification using digital morphometrics: A review. Expert Systems with Applications 39, 7562-7573.

Darula, S. and Kittler, R. (2002). CIE general sky standard defining luminance distributions. Proceedings eSim, 11-13.

De Visser, P.H.B., van der Heijden, G., and Buck-Sorlin, G. (2014). Optimizing illumination in the greenhouse using a 3D model of tomato and a ray tracer. Frontiers in Plant Science 5, 48.

El-Omari, S. and Moselhi, O. (2011). Integrating automated data acquisition technologies for progress reporting of construction projects. Automation in Construction 20, 699-705.

Fang, H., Li, W., Wei, S., and Jiang, C. (2014). Seasonal variation of leaf area index (LAI) over paddy rice fields in NE China: Intercomparison of destructive sampling, LAI-2200, digital hemispherical photography (DHP), and AccuPAR methods. Agricultural and Forest Meteorology 198, 126-141.

Glenn, D.M., Bassett, C.B., Tworkoski, T., Scorza, R., and Miller, S.S. (2015). Tree architecture of pillar and standard peach affect canopy transpiration and water use efficiency. Scientia Horticulturae 187, 30-34.

Gupta, R., Tiwari, G N., Kumar, A., and Gupta, Y. (2012). Calculation of total solar fraction for different orientation of greenhouse using 3D-shadow analysis in Auto-CAD. Energy and Buildings 47, 27-34.

Hemming, S., Dueck, T., Janse, J., and van Noort, F. (2007, October). The effect of diffuse light on crops. In International Symposium on High Technology for Greenhouse System Management: Greensys2007, 801:1293-1300.

Henke, M. and Buck-Sorlin, G.H. (2018). Using a full spectral ray tracer for calculating light microclimate in functional-structural plant modelling. Computing and Informatics 36, 1492-1522.

Hilker, T., Coops, N.C., Schwalm, C.R., Jassal, R.P.S., Black, T.A., and Krishnan, P. (2008). Effects of mutual shading of tree crowns on prediction of photosynthetic light-use efficiency in a coastal Douglas-fir forest. Tree physiology 28, 825-834.

Hitz, T., Henke, M., Graeff-Hoenninger, S., and Munz, S. (2019). Three-dimensional simulation of light spectrum and intensity within an LED growth chamber. Computers and Electronics in Agriculture 156, 540-548.

Hochreiter S, Schmidhuber J (1997) Long short-term memory. Neural Computation 9:1735-1780.

Jones, J.W., Dayan, E., Allen, L.H., Van Keulen, H., and Challa, H. (1991). A dynamic tomato growth and yield model (TOMGRO). Transactions of the ASAE 34, 663-0672.

Kalidindi, S., Bala, G., Modak, A., and Caldeira, K. (2015). Modeling of solar radiation management: a comparison of simulations using reduced solar constant and stratospheric sulphate aerosols. Climate Dynamics 44, 2909-2925.

Kanniah, K.D., Beringer, J., and Hutley, L. (2013). Exploring the link between clouds, radiation, and canopy productivity of tropical savannas. Agricultural and Forest Meteorology 182, 304-313.

Kingma, D.P. and Ba, J. (2014). Adam: A method for stochastic optimization. arXiv preprint arXiv:1412.6980.Kohavi R (1995) A study of cross-validation and bootstrap for accuracy estimation and model selection. In Ijcai 14:1137-1145

Lena, B.P., Folegatti, M.V., Francisco, J., Santos, O.N.A., and Andrade, I.P.S. (2016). Performance of LAI-2200 plant canopy analyzer on leaf area index of Jatropha nut estimation. Journal of Agronomy 15, 191-197.

Li, T. and Yang, Q. (2015). Advantages of diffuse light for horticultural production and perspectives for further research. Frontiers in Plant Science 6, 704.

Llop, J., Gil, E., Llorens, J., Miranda-Fuentes, A., and Gallart, M. (2016). Testing the suitability of a terrestrial 2D LiDAR scanner for canopy characterization of greenhouse tomato crops. Sensors 16, 1435.

Lopes, D., Nunes, L., Walford, N., Aranha, J., Sette, C.J., Viana, H., and Hernandez, C. (2014). A simplified methodology for the correction of Leaf Area Index (LAI) measurements obtained by ceptometer with reference to Pinus Portuguese forests. iForest-Biogeosciences and Forestry 7, 186.

Marchiori, P.E., Machado, E.C., and Ribeiro, R.V. (2014). Photosynthetic limitations imposed by self-shading in field-grown sugarcane varieties. Field Crops Research 155, 30-37.

Mercado, L.M., Bellouin, N., Sitch, S., Boucher, O., Huntingford, C., Wild, M., and Cox, P.M. (2009). Impact of changes in diffuse radiation on the global land carbon sink. Nature 458, 1014.

Min, Q. and Duan, M. (2005). Simultaneously retrieving cloud optical depth and effective radius for optically thin clouds. Journal of Geophysical Research: Atmospheres 110, D21.

Monsi, M. and Saeki, T. (2005). On the factor light in plant communities and its importance for matter production. Annals of Botany 95, 549-567.

Nguyen, T., Slaughter, D., Max, N., Maloof, J., and Sinha, N. (2015). Structured light-based 3D reconstruction system for plants. Sensors 15, 18587-18612.

Oliphant, A.J., Dragoni, D., Deng, B., Grimmond, C.S.B., Schmid, H.P., and Scott, S.L. (2011). The role of sky conditions on gross primary production in a mixed deciduous forest. Agricultural and Forest Meteorology 151, 781-791.

Paulus, S., Dupuis, J., Mahlein, A.K., and Kuhlmann, H. (2013). Surface feature based classification of plant organs from 3D laserscanned point clouds for plant phenotyping. BMC bioinformatics 14, 238.

Paulus, S., Behmann, J., Mahlein, A.K., Plümer, L., and Kuhlmann, H. (2014). Low-cost 3D systems: suitable tools for plant phenotyping. Sensors 14, 3001-3018.

Peksen, E. (2007). Non-destructive leaf area estimation model for faba bean (*Vicia faba* L.). Scientia Horticulturae 113, 322-328.

Rivera, C.M., Rouphael, Y., Cardarelli, M., and Colla, G. (2007). A simple and accurate equation for estimating individual leaf area of eggplant from linear measurements. European Journal of Horticultural Science 72, 228-230.

Roccia, J.P., Piaud, B., Coustet, C., Caliot, C., Guillot, E., Flamant, G., and Delatorre, J. (2012). SOLFAST, a Ray-Tracing Monte-Carlo software for solar concentrating facilities. In Journal of Physics: Conference Series 369: 012029.

Rodríguez, F., Berenguel, M., Guzmán, J.L., and Ramírez-Arias, A. (2015). Modeling and control of greenhouse crop growth. Springer International Publishing.

Rouphael, Y., Rivera, C.M., Cardarelli, M., Fanasca, S., and Colla, G. (2006). Leaf area estimation from linear measurements in zucchini plants of different ages. Journal of Horticultural Science and Biotechnology 81, 238-241.

Rouphael, Y., Mouneimne, A.H., Ismail, A., Mendoza-De Gyves, E., Rivera, C.M., and Colla, G. (2010). Modeling individual leaf area of rose (*Rosa hybrida* L.) based on leaf length and width measurement. Photosynthetica 48, 9-15.

Sala, F., Arsene, G.G., Iordănescu, O., and Boldea, M. (2015). Leaf area constant model in optimizing foliar area measurement in plants: A case study in apple tree. Scientia Horticulturae 193, 218-224.

Schirrmann, M., Hamdorf, A., Giebel, A., Dammer, K.H., and Garz, A. (2015). A mobile sensor for leaf area index estimation from canopy light transmittance in wheat crops. Biosystems Engineering 140, 23-33.

Schwarz, D. and Kläring, H.P. (2001). Allometry to estimate leaf area of tomato. Journal of Plant Nutrition 24, 1291-1309.

Son, J.E., Kang, W.H., Kim, D.P., Hwang, I.H., Kim. J.W, (2018). Development of functional-structural modeling techniques for advanced greenhouse crop growth modelling, p188, iPET.

Spitters, C. J. T. and Schapendonk, A.H.C.M. (1990). Evaluation of breeding strategies for drought tolerance in potato by means of crop growth simulation. In Genetic aspects of plant mineral nutrition (pp. 151-161). Springer, Dordrecht.

Still, C.J., Riley, W.J., Biraud, S.C., Noone, D.C., Buenning, N.H., Randerson, J.T., and Farquhar, G.D. (2009). Influence of clouds and diffuse radiation on ecosystem-

atmosphere CO_2 and $CO^{18}O$ exchanges. Journal of Geophysical Research, 114, G01018.

Suguiyama, V.F., da Silva, E.A., Meirelles, S.T., Centeno, D.D.C., and Braga, M.R. (2014). Leaf metabolite profile of the Brazilian resurrection plant *Barbacenia purpurea* Hook.(*Velloziaceae*) shows two time-dependent responses during desiccation and recovering. Frontiers in Plant Science 5, 96.

Uno, I., Yumimoto, K., Pan, X., Wang, Z., Osada, K., Itahashi, S., and Yamamoto, S. (2017). Simultaneous dust and pollutant transport over east Asia: The tripartite environment ministers meeting March 2014 case study. SOLA 13, 47-52.

Wang, H., Sánchez-Molina, J.A., Li, M., Berenguel, M., Yang, X.T., and Bienvenido, J.F. (2017). Leaf area index estimation for a greenhouse transpiration model using external climate conditions based on genetics algorithms, back-propagation neural networks and nonlinear autoregressive exogenous models. Agricultural Water Management 183, 107-115.

Yamori, W., Makino, A., and Shikanai, T. (2016). A physiological role of cyclic electron transport around photosystem I in sustaining photosynthesis under fluctuating light in rice. Scientific Reports 6, 20147.

Yang, W., Duan, L., Chen, G., Xiong, L., and Liu, Q. (2013). Plant phenomics and high-throughput phenotyping: accelerating rice functional genomics using multidisciplinary technologies. Current Opinion in Plant Biology 16, 180-187.

Yao, W., Kelbe, D., Leeuwen, M., Romanczyk, P., and Aardt, J. (2016). Towards an improved LAI collection protocol via simulated and field-based PAR sensing. Sensors 16, 1092.

Table 1-1. Hyperparameters for long short-term memory and AdamOptimizer.

Parameter	Value	Description
Learning rate	0.035	Learning rate used by the optimizer
β_1	0.9	Exponential mass decay rate for momentum estimates
β_2	0.999	Exponential velocity decay rate for momentum estimates
E	0.0001	A constant for numerical stability
Forget bias	1.0	Probability of forgetting information in the previous dataset
Number of perceptrons		The number of perceptrons used for the hidden layer of LSTM and FC
Time step		Number of datasets that the LSTM will see at one time

Table 1-2. Comparison of LSTM test accuracy in case of using all variables, excluding seasonal variables, and excluding weather variables.

Input variable	Test 1[z]	Test 2	Test 3	Test 4	Test 5	Average
All	0.940	0.940	0.931	0.879	0.930	0.937a[y]
No season	0.904	0.945	0.921	0.930	0.934	0.927ab
No weather	0.879	0.920	0.892	0.930	0.923	0.901b

[z]Test data-set number in a 5-fold cross test

[y]Different letters within columns indicate significant differences ($p < 0.05$) by Duncan's multiple range test

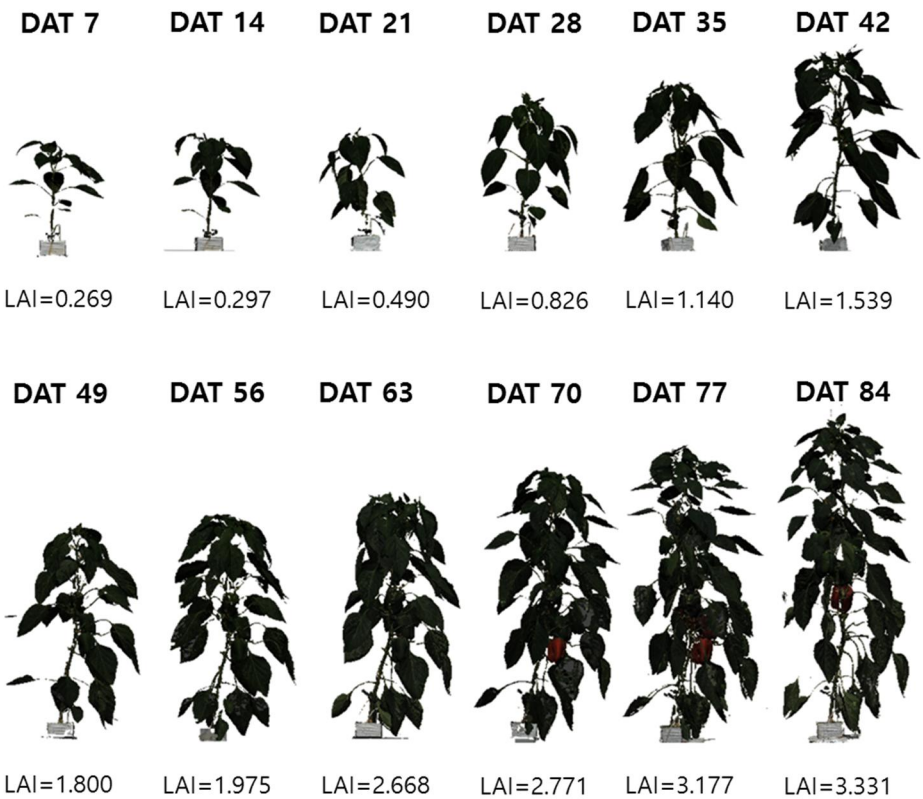

Fig. 1-1. 3D structural model and leaf area index (LAI) of paprika by growth stage.

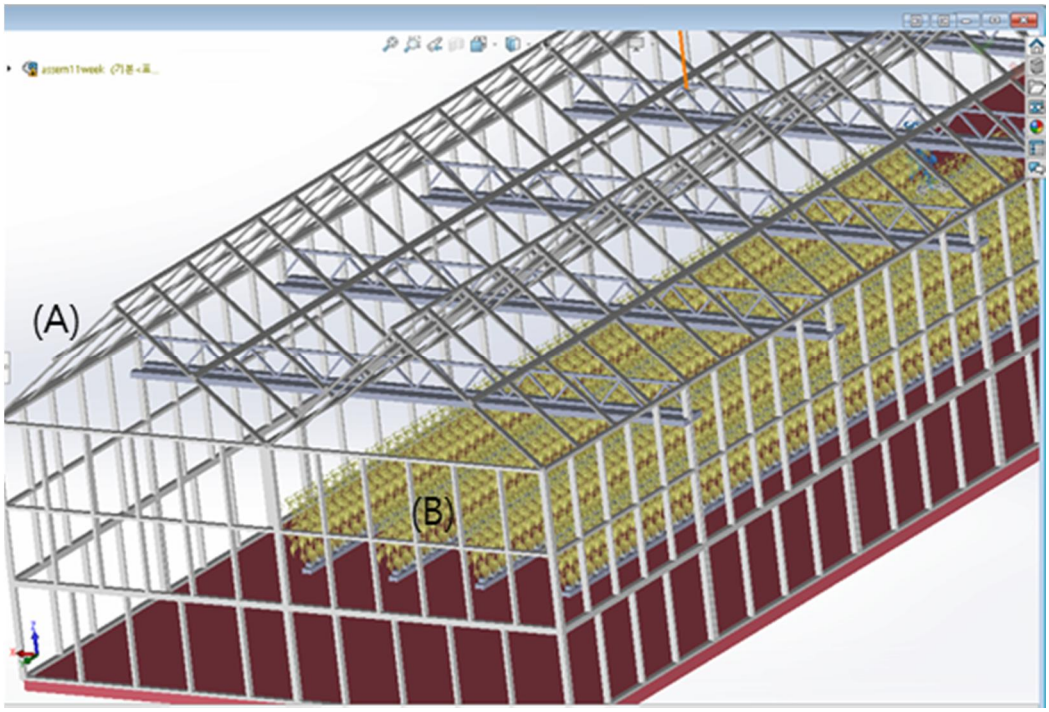

Fig. 1-2. Combination of greenhouse CAD model (A) with 3D crop model (B).

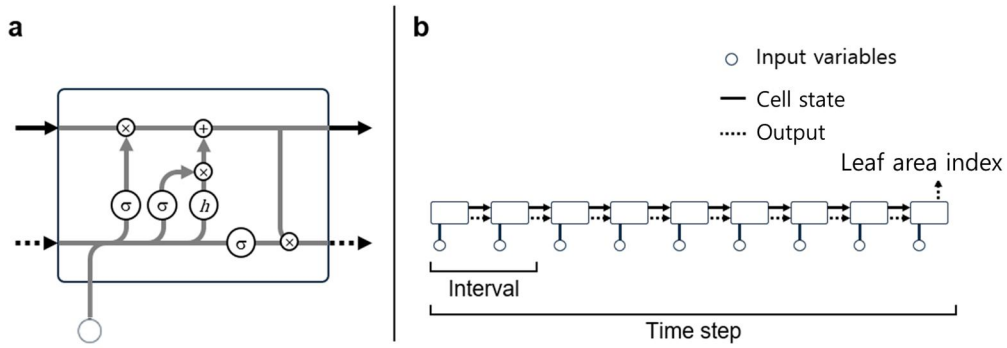

Fig. 1-3. A structure of long short-term memory (A) and a diagram of the model work (B). h and σ represent hidden layers with a hyperbolic tangent and sigmoid as an activation function, respectively.

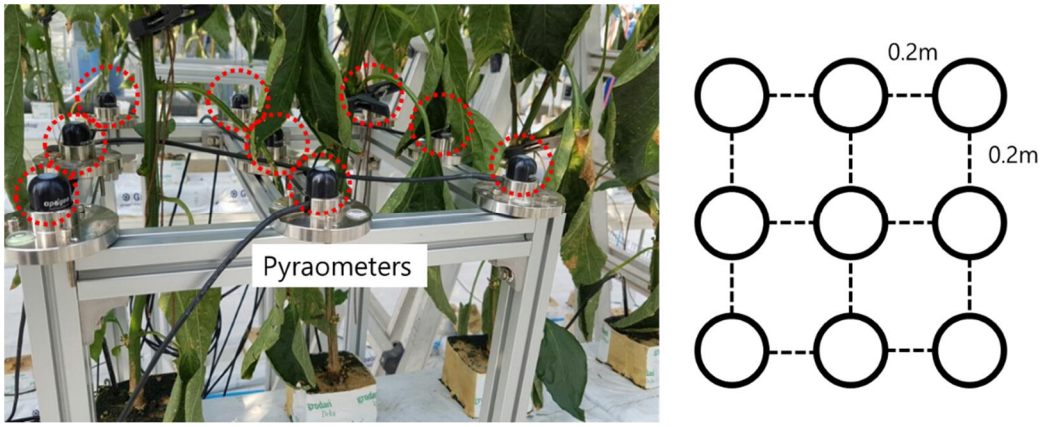

Fig. 1-4. Nine sensors installed for measuring light intensities of the lower canopy.

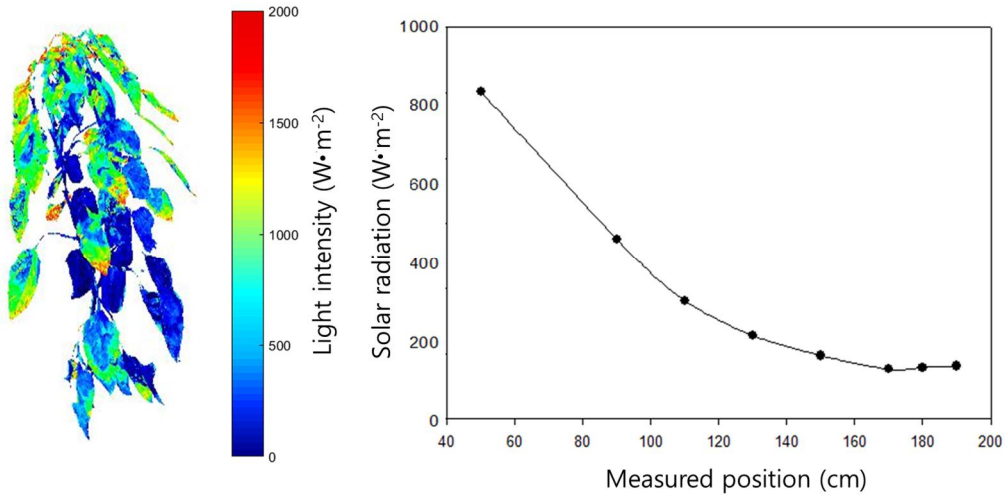

Fig. 1-5. Spatial light distribution (A) and light intensity by vertical position (B) in the canopy.

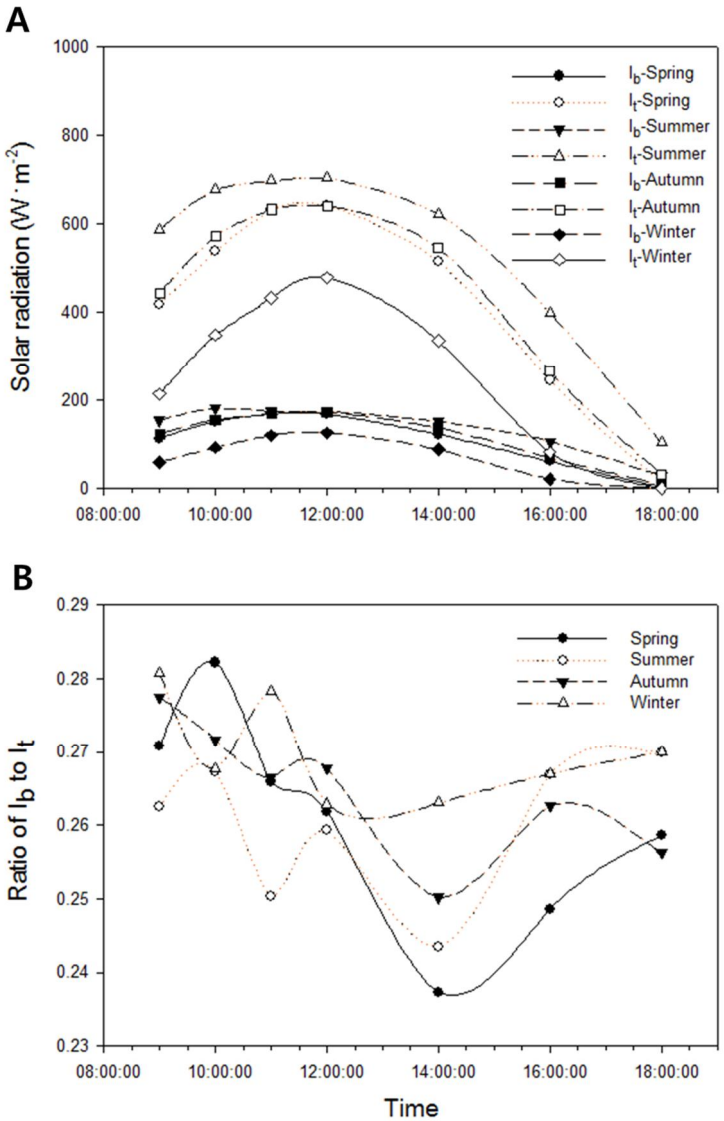

Fig. 1-6. Diurnal change in light intensities of the upper (I_t) and lower (I_b) canopy (A), and the ratio of I_t and I_b (B) 63 days after transplanting (DAT) during clear sky conditions.

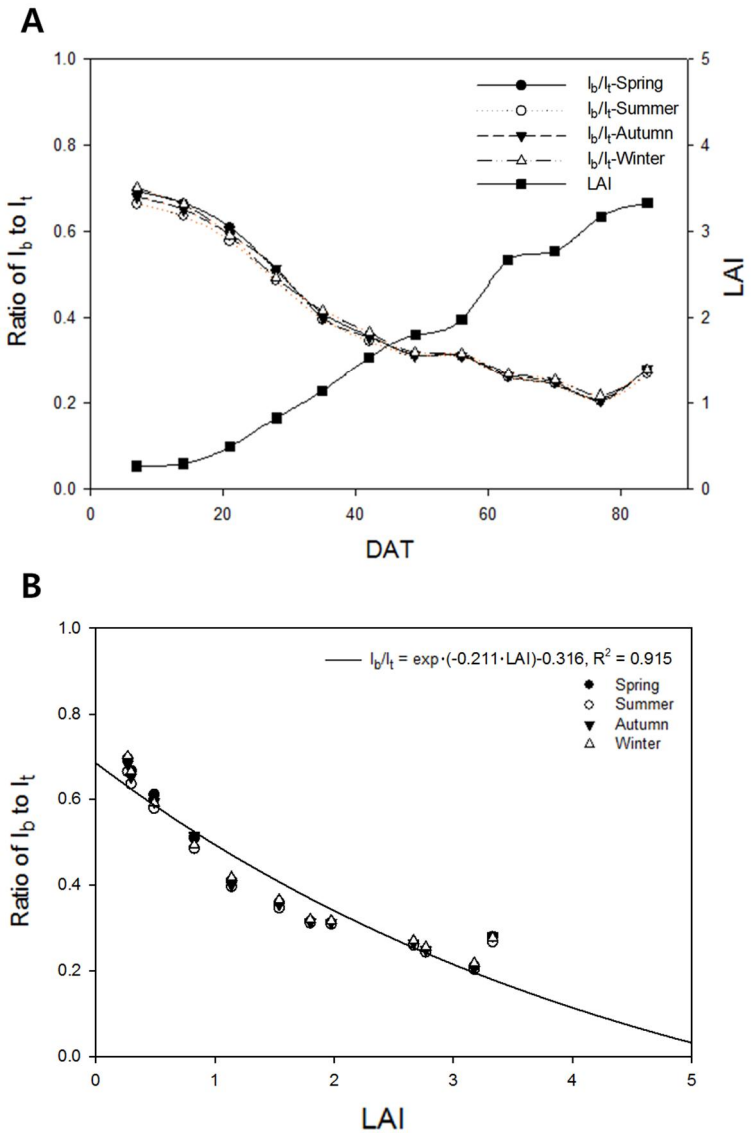

Fig. 1-7. Diurnal change in the average light-intensity ratio of the upper (I_t) and lower (I_b) canopy days after transplanting (DAT, A), and the relationship between I_t / I_b and leaf area index (LAI, B) during clear sky conditions.

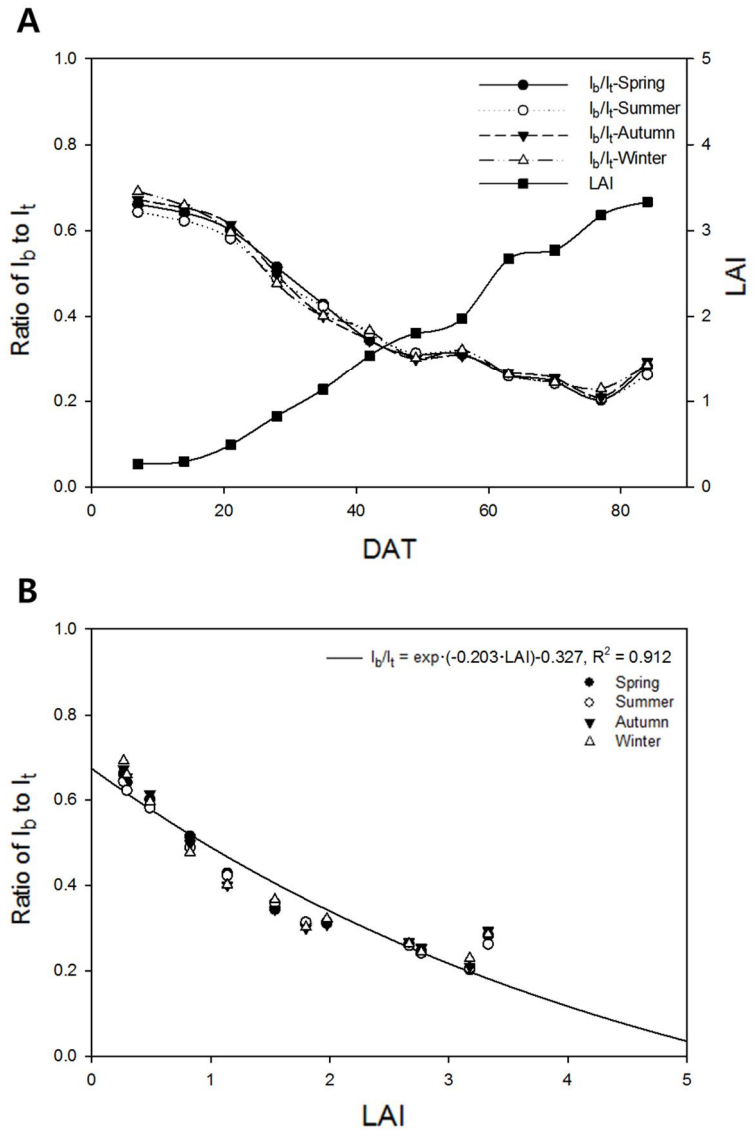

Fig. 1-8. Diurnal change in the light-intensity ratio of the upper (I_t) and lower (I_b) canopy days after transplanting (DAT, A), and the relationship between I_t / I_b and leaf area index (LAI, B) at 12:00 during clear sky conditions.

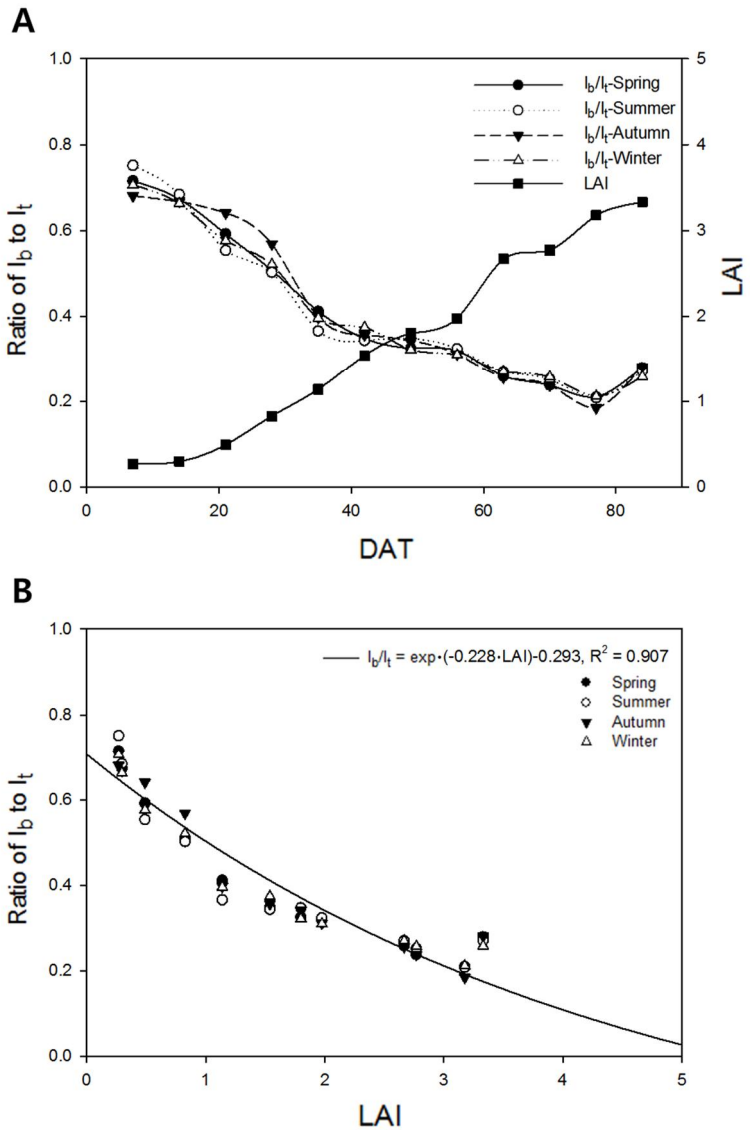

Fig. 1-9. Diurnal change in the light-intensity ratio of the upper (I_t) and lower (I_b) canopy days after transplanting (DAT, A), and the relationship between I_t / I_b and leaf area index (LAI, B) at 18:00 during clear sky conditions.

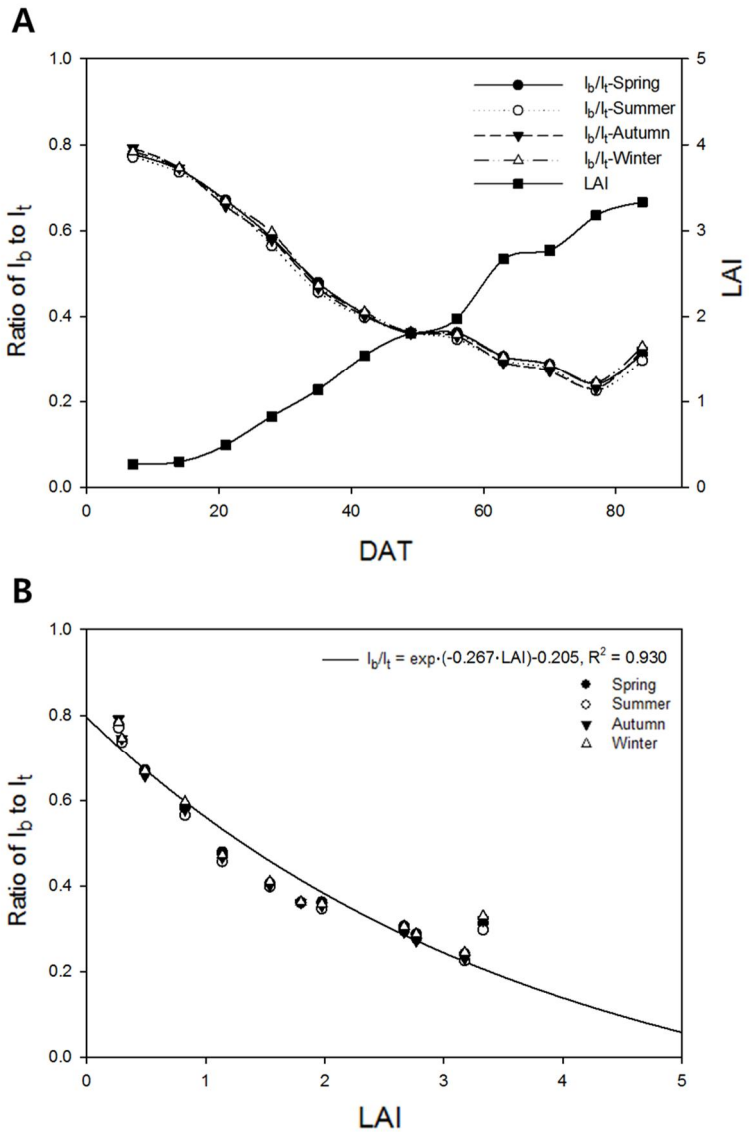

Fig. 1-10. Diurnal change in the average light-intensity ratio of the upper (I_t) and lower (I_b) canopy days after transplanting (DAT, A), and the relationship between I_t / I_b and leaf area index (LAI, B) during overcast conditions.

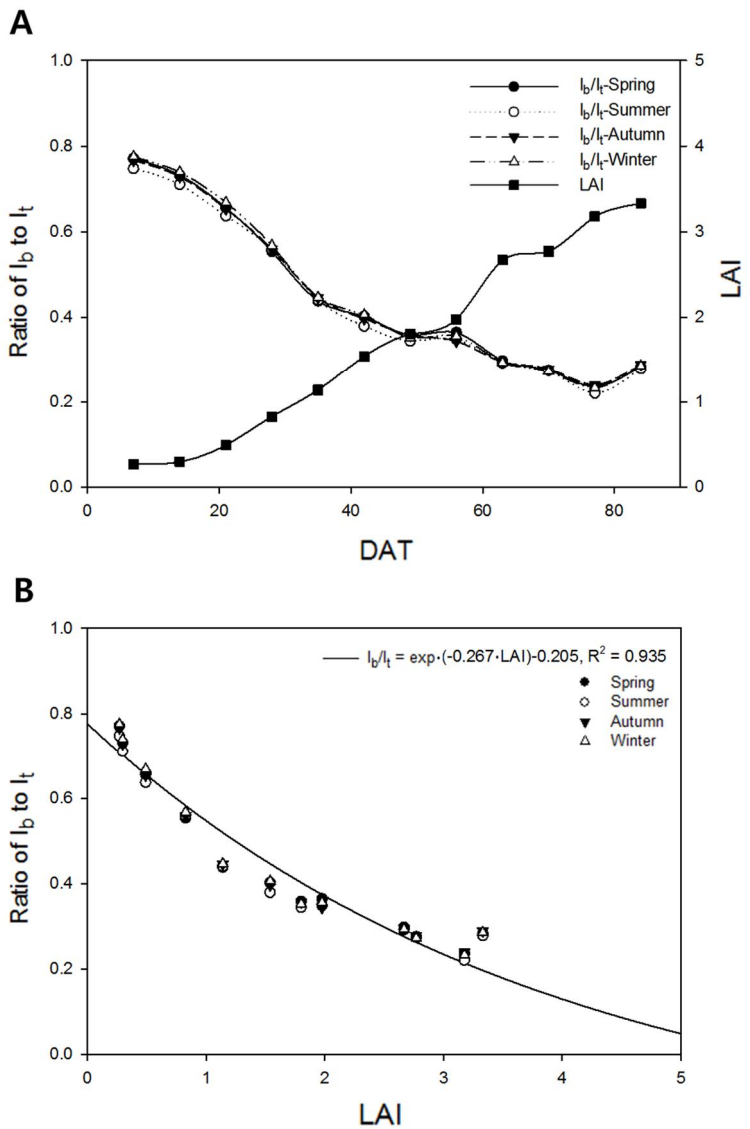

Fig. 1-11. Diurnal change in the average light-intensity ratio of the upper (I_t) and lower (I_b) canopy days after transplanting (DAT, A), and the relationship between I_t / I_b and leaf area index (LAI, B) during cloudy conditions.

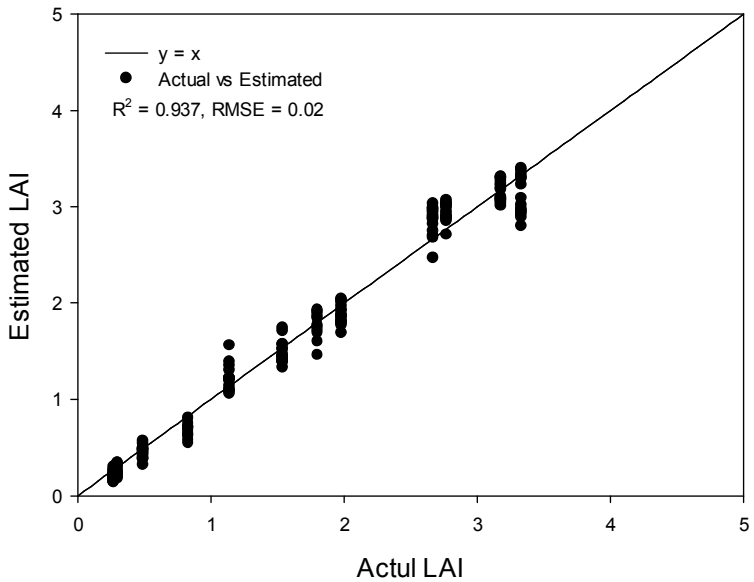

Fig. 1-12. Comparison of leaf area index (LAI) directly measured and estimated by LSTM algorithm.

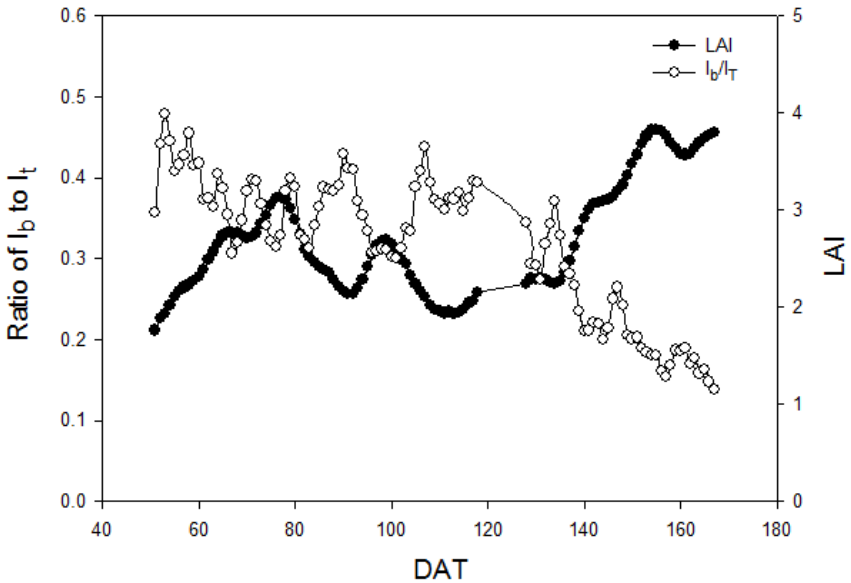

Fig. 1-13. The light-intensity ratio of the upper (It) and lower (Ib) canopy and the leaf area index (LAI) days after transplanting (DAT) in the validation experiment.

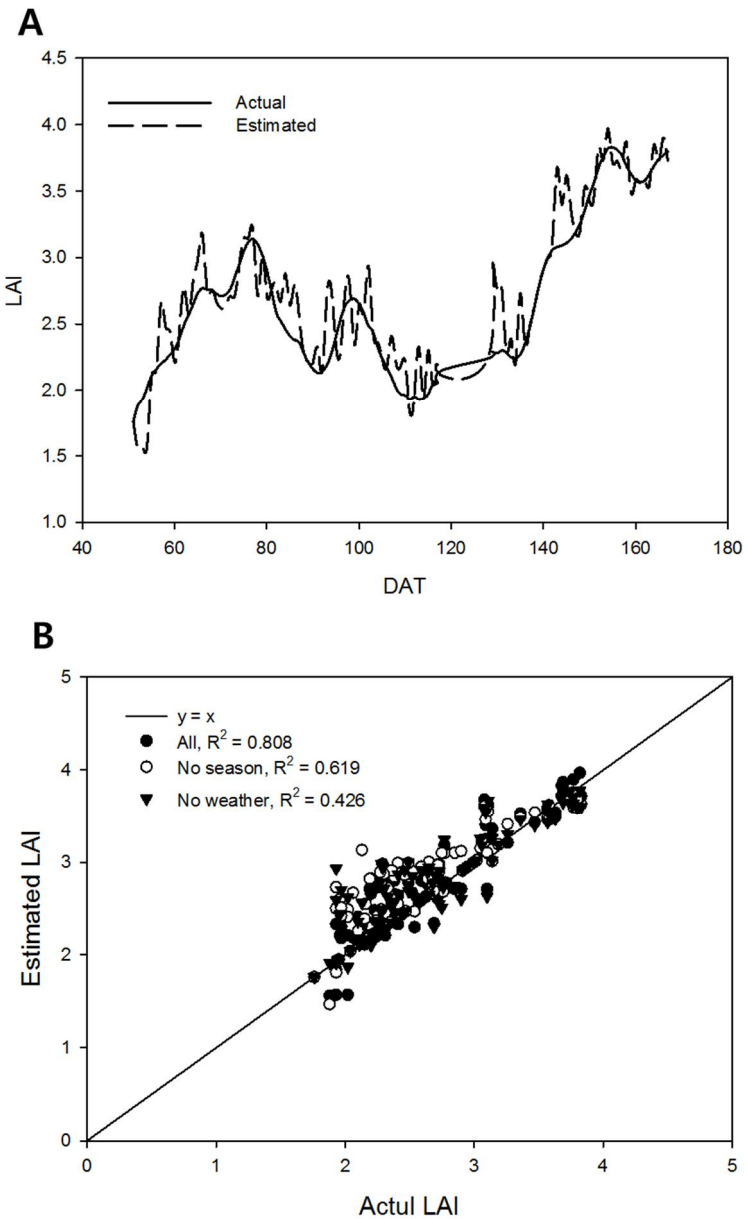

Fig. 1-14. Leaf area idex (LAI) directly measured and estimated by LSTM algorithm days after transplanting (DAT, A), and validation accuracy in case of using all variables (black circle), excluding seasonal variables (black triangle), and excluding weather variables (white circle) (B).

CHAPTER 2

Nondestructive and continuous measurement of fresh weights of Hydroponically-grown Bell Pepper

ABSTRACT

Fresh weight is a direct index of the crop growth, however, it is difficult to continuously measure the fresh weight of bell peppers grown in in hydroponic cultures due to the difficulty in identifying moisture condition of crops and growing media. The objective of this study was to develop a continuous and nondestructive measuring system for the fresh weight of bell pepper in hydroponic culture considering the moisture content in the growing media. The developed system simultaneously measured the supported weight from the trellis string and the gravitational weight using a tensile load cell. The weight of moistures in the growing media was calibrated by using the changes in moisture content before and after the irrigation at a specific time during the growth period. The most stable time-zone for the measurement was determined by analyzing the diurnal change of relative water content. To verify the accuracy of the developed system, the fresh weight of the fruits, stems, leaves, and roots were measured manually. The fresh weights measured by the system showed good agreements with actual fresh weight.

From the results, it is confirmed that the system can stably measure the fresh weights of bell peppers grown in hydroponic culture with high accuracy. This method can be applied to the continuous data collection of crop growth information in hydroponic cultures.

Additional Keywords: automated measurement, crop growth, frequency domain reflectometry (FDR) sensor; load cell, soilless culture

INTRODUCTION

Bell pepper (*Capsicum annuum* L.) is an economically important vegetable widely consumed due to its high mineral and vitamin contents with various colors (Castro et al., 2008; Frans et al., 2018; Wyenandt et al., 2017). As its high sensitivity to environmental conditions, most of the bell peppers were grown in hydroponic culture systems where microclimate is precisely controlled greenhouse (Jang et al., 2018; Ngouajio et al., 2008; Sezen et al., 2006; Shin and Son, 2015). In these cultivation conditions, environmental control and cultivation techniques in the greenhouse are carried out to optimize the growth of crops. Therefore, it is important to measure crop growth reactions to various environmental control and cultivation techniques.

Among the crop growth factors, the crop weight is an indicator of the crop growth itself and used as a key parameter for crop growth models (Heuvelink, 1999; Jones et al., 1991; Katsoulas et al., 2015; Martínez-Ruiz et al., 2019). The most common method to collect the crop weight is to manually measure it through destructive growth surveys, which is not only destructive, but also laborious (Yeh et al., 2014). Therefore, an automated and continuous measurement system that measures the crop weight during the whole growth period need to be developed.

Studies on development of systems continuously measure the crop fresh weight have been conducted. Chen et al. (2016) and Kim et al. (2016) installed a compressive force load cell to measure the fresh weight of the leafy vegetables in deep flow hydroponic culture. However, this method can be used only in a deep flow hydroponic cultivation in

which the moisture in the sponge block is always saturated. It is not applicable for general hydroponic cultivation for bell peppers where the moisture in the growing media continuously changes by irrigation, drainage, or water uptake from the crops. Baas and Slooweg (2004) installed a compressive load cell under the gerbera-planted rockwool media, and crop fresh weight was calculated by excluding the moisture weight in the rockwool media using frequency domain reflectometry (FDR) sensors. This methodology can be used to revise the moisture weight in the growing media that continuously changes throughout the day. However this methodology, using a compressive load cell, can only be applied to crops that have only gravitational weight and it is difficult to apply to large crops such as bell pepper which partial crop weight is supported by the string trellis. Therefore, it is necessary to develop a system that can measure the crop weight containing the weight supported by the string trellis.

CropAssist is a system developed to measure the weight of large crop, supported by the string trellis (Helmer et al., 2005). It measures the crop fresh weight through the tensile load cell (upper load cell) installed between the aluminum bar where the string trellis are fixed and the greenhouse frame. In addition, the moisture change in the growth media is measured using a compressive load cell (lower load cell) installed under the growth media. It has been used to measure the crop growth and the transpiration cultivated in various environment and cultivation conditions. (Ahmad et al., 2013; Battista et al., 2015; Ehret et al., 2011; Story and Kacira, 2015). However, Cropassist is limited to tomatoes or cucumber where the crop weights are entirely supported by the string trellis. In case of bell pepper, some of the crop weight is supported on the string

trellis, while some weight has the gravitational weight (downward force) conditions. Therefore, in order to continuously measure the fresh weight of bell pepper, it is appropriate to calculate the weight of crops by measuring the total weight of the cultivation system, including the growth medium, and revising the moisture content in the growing media. The objective of this study was to develop a continuous and nondestructive measuring system for the fresh weight of bell pepper in hydroponic culture considering the moisture content in the growing media.

MATERIALS AND METHODS

Fresh Weight Measurement System in hydroponic Culture

The developed instrument consists of four components: an outer frame, an inner frame, a load cell, and an FDR sensor (Fig. 2-1), the outer frame serves as the main framework which supports the overall system. “The rockwool growing media was on the lower part of the inner frame and 4 bell peppers were planted on the growing media. The crop was supported by string trellis which was fixed by the upper part of the inner frame. With this structure, both the gravitational weight of the crop and rockwool growing media (downward force) and the weight supported by the string trellis (upward force) are all supported by the inner frame. These inner frame and the outer frame were connected using four load cells. S-beam type tensile load cells were used for measuring the crop fresh weight. In this research, LDB-2kg load cells (SBA-25, CAS, Yangju, Korea) were used, with the resolution of 1g, and the measurement capability from 0 to 25 kg. The load cell was connected to an amplifier and conditioner module (CI-1500A, CAS, Yangju, Korea) which amplified and converted the electric signal to a proportional weight value. This weight signal is then sent to the data logger (CR-1000, Campbell Scientific, Logan, USA). To measure the changes in moisture content of the growing media, FDR sensors (WT100B, Mi-Rae Sensor, Seoul, Korea) were installed vertically in the middle of the rockwool media. The moisture content in the growing media was also collected in the equivalent data logger.

Cultivation Conditions

The experiments were conducted in a Venlo-type glasshouse located in the experimental farm of Seoul National University, Suwon, Korea (latitude, 37.3°N; longitude, 127.0°E). The vents on the roof and sidewall were automatically opened when the temperature was higher than 26°C during the day. Bell pepper seedlings (*Capsicum annuum* L. 'Sirocco') at 40 days post-sowing on rockwool cubes (Grodan delta, Grodan, Roermond, Netherlands) in a seedling chamber were used. On February 8th, 2018 (cultivation period 1), and on October 30th, 2018 (cultivation period 2), were transplanted into 0.9·0.15 0.07m (L·W·H) rockwool media (Grotop GT Master Dry, Grodan, Roermond, Netherlands) with a plant density of 3.3 plants·m^2 after 2 weeks of acclimatization to the irrigation system at a nutrient concentration of 2.0 dS·m^{-1}, the bell pepper seedlings with 5-6 nodes. The EC and pH in the nutrient solutions were maintained at 2.6-3.0 dS·m^{-1} and 5.5-6.5, respectively. The plants were pruned to maintain two main stems, which were vertically trellised to a 'V' canopy system (Jovicich et al., 2004). The environmental factors in greenhouse, such as solar radiation [Pyranometer (SP-110, Apogee Instruments, Logan, USA)], temperature (CS220, Campbell Scientific, UT, USA), and relative humidity (PCMini70, Gilwoo Trading, Seoul, Korea) were measured.

Fresh Weight Calculation

The FDR sensor measured the volumetric moisture content (v/v, %) in the growing media. Therefore, the weight-moisture contents revision factor is required to estimate the

moisture weight in the growing media. The revision factor was calculated using the change of the cultivation system weight measured by the load cell and the change of the moisture content in the growing media measured by the FDR sensor before and after the first irrigation daily [Equation (1)].

$$A = \frac{SW_a - SW_b}{MC_a - MC_b} \quad \text{(Eq. 2-1)}$$

where, A is the weight-moisture content revision factor, SW_a, the system weight after irrigation, SW_b, the system weight before irrigation, MC_a, the moisture content after irrigation, and MC_b, the moisture content before irrigation.

The fresh weight of a crop during the day depends on the measured time, since the water content in the crops varies depending on the weather and crop conditions (Ueda and Nakamura, 2007). Thus, the diurnal changes of relative water content (RWC) in the crops were measured for the time zone selection that can represent the fresh weight of the crops. RWC was measured hourly for 24hours using Equation (2), during the period when the night heating in the greenhouse operated (Feb. 27th, DAT 20) and when the night heating did not operate (Apr. 28th, DAT 80).

$$RWC = \frac{FW - DW}{TW - DW} * 100 \quad \text{(Eq. 2-2)}$$

where, FW (fresh weight) is the weight of the sample after harvest and TW (fully turgid weight).

The saturated weight of the sample in 4°C distilled water for 4 hours, and *DW* (dry weight), the dry weight of the sample after oven-drying at 70°C for 48 hours (Roger, 2001).

Growth Survey and Verification

To verify the crop fresh weight measured by developed systems, destructive crop growth survey was carried out. The fresh weight of the stem and leaf, for the crops that are similar in size and shape of the system, were measured every 2 weeks during the cultivation period. Fruit diameter and fruit length were measured every 2 weeks and fruit weight were estimated by substituting in Equation (3).

$$\mathrm{FFW} = 290.74 * \mathrm{WF}^2 * \mathrm{LF} + 0.342 \qquad \text{(Eq. 2-3)}$$

where, *FFW* is the fruit fresh weight, *WF*, the fruit length, LF, the fruit diameter.

Also, both of the weight of the harvested crops and the weight of pinched crops in the developed system were measured during the cultivation period. The roots of crops are closely connected to the rockwool media structures (Fig. 2-2), thus, actual measurement of the roots fresh weight was impossible. Therefore, the rockwool media including the roots was harvested and dried in the oven at 70°C for 48 hours on DAT 10, 30, 75, 113. After oven-drying, the initial rock wool media weight was excluded from the dried rockwool media and the roots weight. The root fresh weight was calculated indirectly with the ratio of the dry and fresh root weight. The total fresh weights with destructive

measurements were compared to measured crop fresh weight by the developed system for verification.

RESULTS AND DISCUSSION

Diurnal Change in RWC and Selection of Appropriate Time for Fresh Weight Calculation

The changes in RWC and greenhouse environment data during the days when the nighttime heating was on (Feb. 27th, DAT 20) and when the nighttime heating was off (Apr. 28th, DAT 80) are shown in Fig. 2-3 and 4. On DAT 20, daytime RWC decreased from sunrise to the lowest at noon and gradually increased. These results are consistent with the results of previous studies on various crops of measured daytime RWC (Himeno et al., 2017; Klepper et al., 1971; Rajagopal et al., 1977). In the nighttime heating conditions, the temperature and humidity changed rapidly which caused relatively unstable RWC. Recent studies have shown that there is a time lag between crop water uptake and transpiration, and as this time lag, RWC of crop changes (Himeno et al., 2017). The loss of water in crops continued during the daytime, but after the sunset, crops stored the water and contain them constant after midnight (Klein et al., 2016). The average RWC of crops does not have a significant difference due to the recovery of water contents at night unless there is an extreme water stress condition (Flexas et al., 2006). In hydroponic culture, changes of water content in crops are low as the moisture content in the media is always contained at an optimum level (Ogbonnaya et al., 2003). The results in this experiment showed that the nighttime RWC values were relatively unstable in the nighttime heating condition, but the changes in RWC was less than 3% from 03:00 until

sunrise. Therefore, the appropriate time for the crop fresh weight calculation was selected as after 03:00 to before the transpiration begins.

Weight-Moisture Content Revision and Fresh Weight Calculation

The changes of FDR sensor and load cell weight before and after the daily first irrigation was analyzed (Fig. 2-5). When the irrigation started, the moisture content in the growing media and the total system weight increased by the irrigation, decreased by the drainage, and stayed constant after drainage. As the transpiration rate is less than $0.5 g \cdot min^{-1}$ on the time of first irrigation in the morning (Shin and Son, 2015), changes of moisture content in the growing media and total system weight by the transpiration was disregarded. The calculated system weight-media moisture content revision factor using Equation (1) were 0.072 ± 0.003 (cultivation period 1), and 0.068 ± 0.002 (cultivation period 2), respectively. The revision factor was slightly different depending on the cultivation period, which is considered to be due to the characteristics of installation direction, location and depth of the FDR sensor (Park et al., 2009).

According to previous researches (Kang et al., 2019; Skierucha and Willczek, 2010), the absolute value of FDR sensor is affected by the cultivation period and environmental factors. However, in this study, the revision factor did not change significantly between the cultivation periods. In hydroponic cultivation conditions, when the amount of irrigation is proportional to the amount of radiation, the underground parts are stably maintained (Jovicich et al., 2007; Nikolaou et al., 2017). The calculated weight-moisture content revision factor was substituted into the moisture content at the determined

appropriate time to calculate the crop fresh weight excluding the moisture weight in the growing media.

The total system weight, media moisture content, and calculated crop fresh weight measured during 2018.04.02-04.17 are shown in Fig. 2-6. The total weight of the system measured by the load cell varies with the media moisture content, but the crop fresh weight calculated with the weight-moisture content revision factor increased throughout the period. In hydroponic cultivation conditions, the weight of moisture in the growing media was high proportion among the total cultivation system weight. Therefore, the weight of moisture in the growing media should be excluded for accurate crop fresh weight measurement.

Destructive Crop Growth Survey

The root samples of the crops taken from the rockwool media on DAT 10, 30, 75, and 113 are shown in Table 1. The ratio of dry-fresh weight of the root samples was about 0.132, which showed no significant difference depending on the growth stages. To calculate the fresh weight of the roots by the growth stages, the ratio of dry-fresh weight of the root was multiplied on the measured root dry weight (Table 2). The fresh weight of the roots at the early growth stage was about 14% of the total crop fresh weight. As the growth continues, the proportion decreased to less than 10% after the middle growth stage.

More than 60% of the fresh weight at the last growth stages were reproductive parts including the fruit. In bell pepper, both vegetative and reproductive growth

simultaneously occurs and the fruit is the most rapidly changing organ of the whole crop during the cultivation period (Marcelis et al., 2004). Unlike the continuous increase in fresh weight of the roots, stems and leaves during the cultivation periods, fruit abortion and harvest caused discontinuously increase of total crops weight. Therefore, fruit fresh weight is considered to be the most important factor in the crop fresh weight measurements.

Continuous Changes in Fresh Weight and its Verification

The crop fresh weight was nondestructively measured with the selection of appropriate time (03:00~sunrise) and the substitution of weight-moisture content revision factor. This allowed daily monitoring and recording of crop growth during the cultivation periods. Fig. 2-7 shows the fresh weight growth curves of bell peppers during the growth period.

In the early stages of growth, the fresh weight changes were relatively small. As the growth progressed, the rate of growth increased and then decreased again, indicating a sigmoid growth curve. In general greenhouse cultivation conditions, bell pepper grows in sigmoidal form (Gijzen et al., 1997), and this growth from was confirmed by the developed system. There was a significant decrease in the crop fresh weight during the cultivation period, which was consistent with the fruits harvest date.

The comparisons between the crop fresh weight measured by the system and actual crop fresh weight are shown in Fig. 2-8. As a result of verification, R^2 showed high

linearity with 0.978-0.969 and also d-statistic, which shows the accuracy of the absolute value, was 0.948-935 by growth periods, and linearity error <1.725%.

This accuracy was relatively lower than the recent studies in which crop weights were measured using load cells (Avotins et al., 2018, error<1.5%; Chen et al., 2016, R^2 = 0.997; Kim et al., 2016, R^2 = 0.998). Since these studies have been conducted under deep flow hydroponic cultivation conditions with the roots being free from the growing media, the crop weight including the roots can be easily measured through the load cell. However, comparing to the previous studies of crop fresh weight measurements using load cell similar where the crop roots are fixed in the solid growing media or soil (Baas and Slootweg, 2004, Helmer et al., 2005), the developed system in this experiment accuracy was higher. In addition, the developed system was the suitable system for measuring the crop fresh weight of bell peppers grown in hydroponic culture. Also, the application of this development is not only limited to bell pepper cultivation, but also available to use in various crop cultivation.

As the growth of crops was continuously measured through the developed system, additional possibilities were presented for the analysis of the growth of crops according to environmental conditions. The crop growth response to the environment is determined by accumulated time series change of environmental factors. Generally, it was not possible to analyse the chronic relationship between this environment and the growth of the crops in discontinuous crop growth surveys. The developed system was able to analyse the chronic relationship between the environment and the growth of crops. Fig. 2-9 is a continuous change in the growth and environment of continuously measured

crops during cultivation. Correlation analysis allowed to interpret the continuous relationship between the growth of crops and the environment (Table 3). This relationship may be useful in later studies that analyze big data for agriculture.

Instrument advantages and limitations

Recently, the demand for agricultural big data has increased due to the emergence of smart farm where ICT technology is applied to agriculture (Muangprathub et al., 2019; O'Grady and O'Hare, 2017). Among these agricultural big data, information of environmental factors can be easily measured and collected through various sensors. However, there are still limitations on the information of crop growth. The developed system can monitor the crop response to the environmental condition continuously, automatically, and non-destructively.

Load cell was the main sensor used in this developed system. Load cells are durable, easy to interact with various data collection systems, and require little maintenance after installation (Kumar et al., 2018). In general, crops are grown with high planting density in greenhouses. In these dense conditions, crops are affected by the worker's activities (Helmer et al., 2005). However, the developed system in this study can be installed in coexistence with crop canopy under dense conditions, which does not affect the crop environment or any adjacent crops.

There are also limitations on the developed system. In hydroponic cultivation conditions, the weight of moisture in growing media changes by irrigation, drainage, and water uptake of crops are several kilograms, but the growth rate of daytime crops is very

low. In order to detect such a minute changes, a load cell operating in a fine range is required. However, because the cultivation system of a crop is heavy for its structural stability, a load cell capable of sustaining a high load is required. A load cell having both high resolution and high maximum weight conditions increases in price, so it is necessary to select an appropriate level of load cell for the purpose.

Also, this developed system does not provide information on the growth of specific plant organs, such as leaves, stem, and fruit. Existing formula-based crop growth prediction models estimated total biomass by biomass distribution to each organs (Heuvelink et al., 1999; Martínez-Ruiz et al., 2019). Therefore, in order to discuss the crop growth using the changes in fresh weight collected through developed system, new algorithm for predicting the crop growth should be needed.

LITERATURE CITED

Ahmad, U., Subrata, D.M., and Arif, C. (2013). Speaking Plant Approach for Automatic Fertigation System in Greenhouse. *arXiv preprint arXiv*:1303.1869.

Avotins, A., Gruduls, J., Apse-Apsitis, P., and Potapovs, A. (2018). Crop weight measurement sensor for IoT based industrial greenhouse systems. Agronomy Research 16, 952-957.

Baas, R., Straver, N.A., Shmulevich, I., Galili, I., Seginer, J., Bailey, B., and Gieling, T. (2001). In situ monitoring water content and electrical conductivity in soilless media using a frequency-domain sensor. In Proceedings of the Third International Symposium on Sensors in Horticulture (pp. 295-303).

Baas, R. and Slootweg, C. (2004). On-line acquisition of plant related and environmental parameters (plant monitoring) in gerbera: determining plant responses. Acta Horticulturae 654, 139–146. doi: 10.17660/ActaHortic.2004.654.14

Castro, S.M., Saraiva, J.A., Lopes-da-Silva, J.A., Delgadillo, I., Van Loey, A., Smout, C., and Hendrickx, M. (2008). Effect of thermal blanching and of high pressure treatments on sweet green and red bell pepper fruits (*Capsicum annuum* L.). Food Chemistry 107, 1436-1449.

Chen, W.T., Yeh, Y.H.F., Liu, T.Y., and Lin, T.T. (2016). An automated and continuous plant weight measurement system for plant factory. Frontiers in Plant Science 7, 392.

Ehret, D.L., Hill, B.D., Helmer, T., and Edwards, D.R. (2011). Neural network modeling of greenhouse tomato yield, growth and water use from automated crop monitoring data. Computers and Electronics in Agriculture 79, 82-89.

Flexas, J., Ribas-Carbó, M., Bota, J., Galmés, J., Henkle, M., Martínez-Cañellas, S., and Medrano, H. (2006). Decreased Rubisco activity during water stress is not induced by decreased relative water content but related to conditions of low stomatal conductance and chloroplast CO_2 concentration. New Phytologist 172, 73-82.

Frans, M., Moerkens, R., Van Gool, S., Sauviller, C., Van Laethem, S., Luca, S., ... and Ceusters, J. (2018). Modelling greenhouse climate factors to constrain internal fruit rot (*Fusarium* spp.) in bell pepper. Journal of Plant Diseases and Protection 125, 425-432.

Gijzen, H., Heuvelink, E., Challa, H., Marcelis, L.F.M., Dayan, E., Cohen, S., and Fuchs, M. (1997). HORTISIM: a model for greenhouse crops and greenhouse climate. Acta Horticulturae 456, 441-450.

Helmer, T., Ehret, D.L., and Bittman, S. (2005). CropAssist, an automated system for direct measurement of greenhouse tomato growth and water use. Computers and electronics in Agriculture 48, 198-215.

Heuvelink, E. (1999). Evaluation of a dynamic simulation model for tomato crop growth and development. Annals of Botany 83, 413-422.

Himeno, S., Azuma, W., Gyokusen, K., and Ishii, H.R. (2017). Leaf water maintains daytime transpiration in young *Cryptomeria japonica* trees. Tree physiology 37, 1394-1403.

Jang, D., Choi, k., Heo, J., and Kim, I. (2018). The effect of transplant age on growth and fruit yield in winter-planted paprika cultivation. Horticultural Science and Technology 36, 470-477.

Jovicich, E., Cantliffe, D.J., Stoffella, P.J., and Haman, D.Z. (2007). Bell pepper fruit yield and quality as influenced by solar radiation-based irrigation and container media in a passively ventilated greenhouse. HortScience 42, 642–652.

Kang, S., van Iersel, M. W., and Kim, J. (2019). Plant root growth affects FDR soil moisture sensor calibration. Scientia Horticulturae 252, 208-211.

Kim, J., Kang, W., Ahn, T., Shin, J., and Son, J. (2016). Precise, real-time measurement of the fresh weight of lettuce with growth stage in a plant factory using a nutrient film technique. Korean Journal of Horticultural Science and Technology 34, 77-83.

Kim, J. and van Iersel, M.W. (2011). Slowly developing drought stress increases photosynthetic acclimation of *Catharanthus roseus*. Physiologia Plantarum 143, 166-177.

Kim, J. (2012). Developing and integrating plant models for predictive irrigation. Irrigation Association. November, 2-6.

Klein, T., Cohen, S., Paudel, I., Preisler, Y., Rotenberg, E., and Yakir, D. (2016). Diurnal dynamics of water transport, storage and hydraulic conductivity in pine trees under seasonal drought. iForest-Biogeosciences and Forestry 9, 710.

Klepper, B., Browning, V.D., and Taylor, H.M. (1971). Stem diameter in relation to plant water status. Plant Physiology 48, 683-685.

Kumar, R., Chhabra, S., Verma, A.S., and Gupta, A. (2018). Analysis of load cell. International Journal of Applied Engineering Research 13, 274-277.

Marcelis, L.F.M., Heuvelink, E., Baan Hofman-Eijer, L.R., Den Bakker, J., and Xue, L.B. (2004). Flower and fruit abortion in sweet pepper in relation to source and sink strength. Journal of Experimental Botany 55, 2261-2268.

Martínez-Ruiz, A., López-Cruz, I.L., Ruiz-García, A., Pineda-Pineda, J., and Prado-Hernández, J.V. (2019). HortSyst: A dynamic model to predict growth, nitrogen uptake, and transpiration of greenhouse tomatoes. Chilean Journal of Agricultural Research 79, 1.

Muangprathub, J., Boonnam, N., Kajornkasirat, S., Lekbangpong, N., Wanichsombat, A., and Nillaor, P. (2019). IoT and agriculture data analysis for smart farm. Computers and Electronics in Agriculture 156, 467-474.

Ngouajio, M., Auras, R., Fernandez, R.T., Rubino, M., Counts, J.W., and Kijchavengkul, T. (2008). Field performance of aliphatic-aromatic copolyester biodegradable mulch films in a fresh market tomato production system. HortTechnology 18, 605-610.

Nikolaou, G., Neocleous, D., Katsoulas, N., and Kittas, C. (2017). Effect of irrigation frequency on growth and production of a cucumber crop under soilless culture. Emirates Journal of Food Agriculture 29, 863–871.

Ogbonnaya, C.I., Sarr, B., Brou, C., Diouf, O., Diop, N.N., and Roy-Macauley, H. (2003). Selection of cowpea genotypes in hydroponics, pots, and field for drought tolerance. Crop Science 43, 1114-1120.

O'Grady, M.J. and O'Hare, G.M. (2017). Modelling the smart farm. Information Processing in Agriculture 4, 179-187.

Park, J.S., Tai, N.H., Ahn, T.I., and Son, J.E. (2009). Analysis of moisture characteristics in rockwool slabs using time domain reflectometry (TDR) sensors and their applications to paprika cultivation. Journal of Bio-Environment Control 18, 238-243.

Rajagopal, V., Balasubramanian, V., and Sinha, S.K. (1977). Diurnal fluctuations in relative water content, nitrate reductase and proline content in water-stressed and non-stressed wheat. Physiologia Plantarum 40, 69-71.

Roger, M.J.R. (ed.). (2001). Handbook of plant ecophysiology techniques (No. Sirsi) i9780792370536). Kluwer Academic Publishers.

Salisbury, F.B. and Ross, C.W. (1992). Plant physiology. Fourth edition. Wadsworth Publishing Company, Belmont, California.

Sezen, S.M., Yazar, A., and Eker, S. (2006). Effect of drip irrigation regimes on yield and quality of field grown bell pepper. Agricultural Water Management 81, 115-131.

Shamshiri, R., Ahmad, D., Zakaria, A., Ismail, W.I.W., Man, H.C., and Yamin, M. (2016). Evaluation of the reduced state-variable TOMGRO model using boundary data. In 2016 ASABE Annual International Meeting (p. 1). American Society of Agricultural and Biological Engineers.

Shin, J.H. and Son, J.E. (2015). Development of a real-time irrigation control system considering transpiration, substrate electrical conductivity, and drainage rate of nutrient solutions in soilless culture of paprika (*Capsicum annuum* L.). European Journal of Horticultural Science 80, 271-279.

Skierucha, W. and Wilczek, A. (2010). A FDR sensor for measuring complex soil dielectric permittivity in the 10–500 MHz frequency range. Sensors 10, 3314-3329.

Story, D. and Kacira, M. (2015). Design and implementation of a computer vision-guided greenhouse crop diagnostics system. Machine Vision and Applications 26, 495-506.

Takaichi, M., Shimaji, H., and Higashide, T. (1996). Monitoring of the change in fresh weight of plants grown in water culture. Acta Horticulturae 440, 413–418. doi: 10.17660/ActaHortic.1996.440.72

Ueda, M. and Nakamura, Y. (2007). Chemical basis of plant leaf movement. Plant and Cell Physiology 48, 900-907.

Wyenandt, C.A., Kline, W.L., Ward, D.L., and Brill, N.L. (2017). Production system and cultivar effects on the development of skin separation or “silvering” in bell pepper fruit. HortTechnology 27, 37-44.

Table 2-1. Fresh and dry weights of root samples according to the day after transplanting (DAT).

DAT	Fresh weight (A)	Dry weight (B)	A/B
10	0.098	0.013	0.133
30	1.206	0.165	0.137
75	1.935	0.248	0.128
113	1.117	0.147	0.132

Table 2-2. Growth survey results of fresh or dry weight (kg) of roots, leaves, stems and fruits according to the day after transplanting in different cultivation periods.

Cultivation period	DAT	Root dry weight	Root fresh weight	Leaf fresh weight	Stem fresh weight	Fruit fresh weight
1	20	2.599	19.647	79.116	35.864	1.738
	34	2.589	19.465	89.609	40.159	4.729
	48	5.629	42.327	160.264	121.916	7.857
	68	19.171	144.149	662.7493	499.739	237.180
	76	29.023	218.220	1195.476	788.339	182.413
	91	29.067	218.550	1204.076	782.739	3049.593
	104	29.173	219.348	1248.828	708.880	3513.915
2	29	2.599	17.998	53.273	29.581	2.271
	44	4.620	37.3153	238.392	189.991	110.930
	58	15.629	120.227	531.352	397.048	556.845
	71	19.171	162.223	707.071	559.803	1216.035
	85	27.684	212.954	807.608	604.624	50.136
	101	28.644	220.308	1034.282	785.096	197.835
	113	29.001	226.677	1361.963	800.076	643.727
	127	41.564	319.723	1685.632	1207.760	1048.149

Table 3. Correlation analysis of time series variables in the growth and environment factors.

Value	Temperature	CO_2 concentration	Radiation	Relative humidity
Average[a]	0.510**	0.157	0.545**	0.639**
Maximum[b]	-0.187*	0.179	0.547**	0.692**
Minimum[c]	0.061	-0.288**	-	0.353**

*, ** Pearson correlation (r) significant at 0.05 and 0.01, respectively

[a] Average value of the day

[b] Maximum value of the day

[c] Minimum value of the day

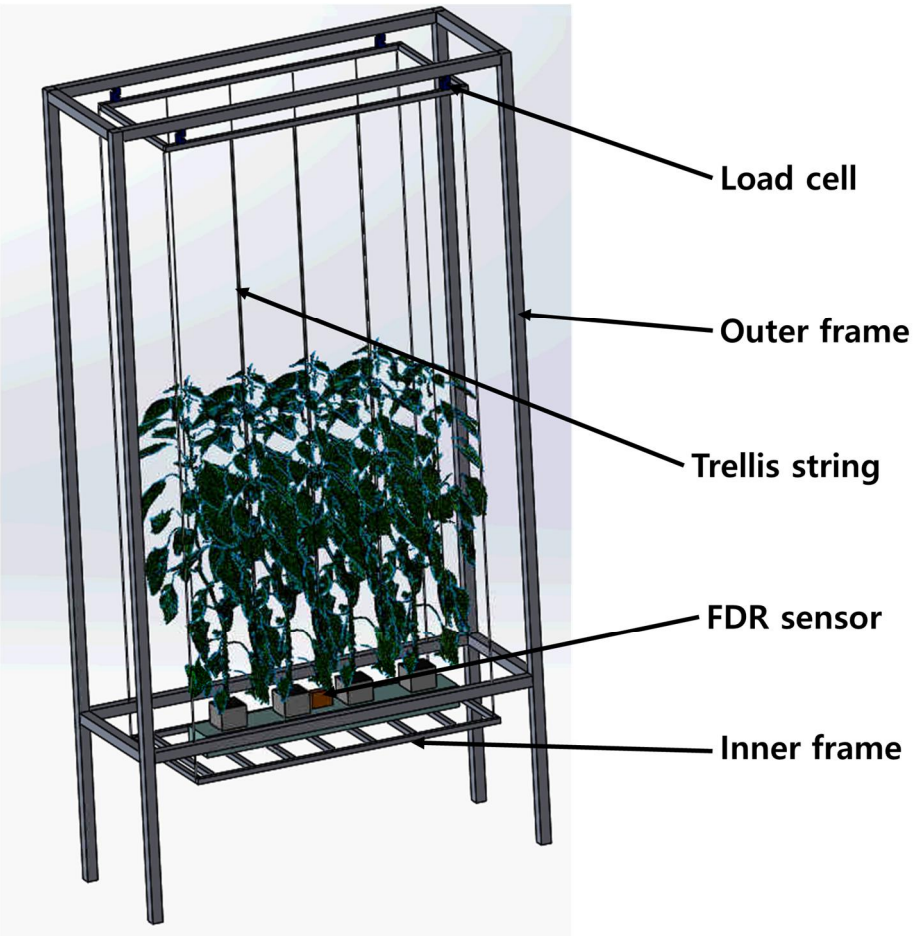

Fig. 2-1. A schematic diagram of the fresh weight measuring system using load cell and frequency domain reflectometry (FDR) sensors.

Fig. 2-2. Distribution of roots inside the rockwool substrate.

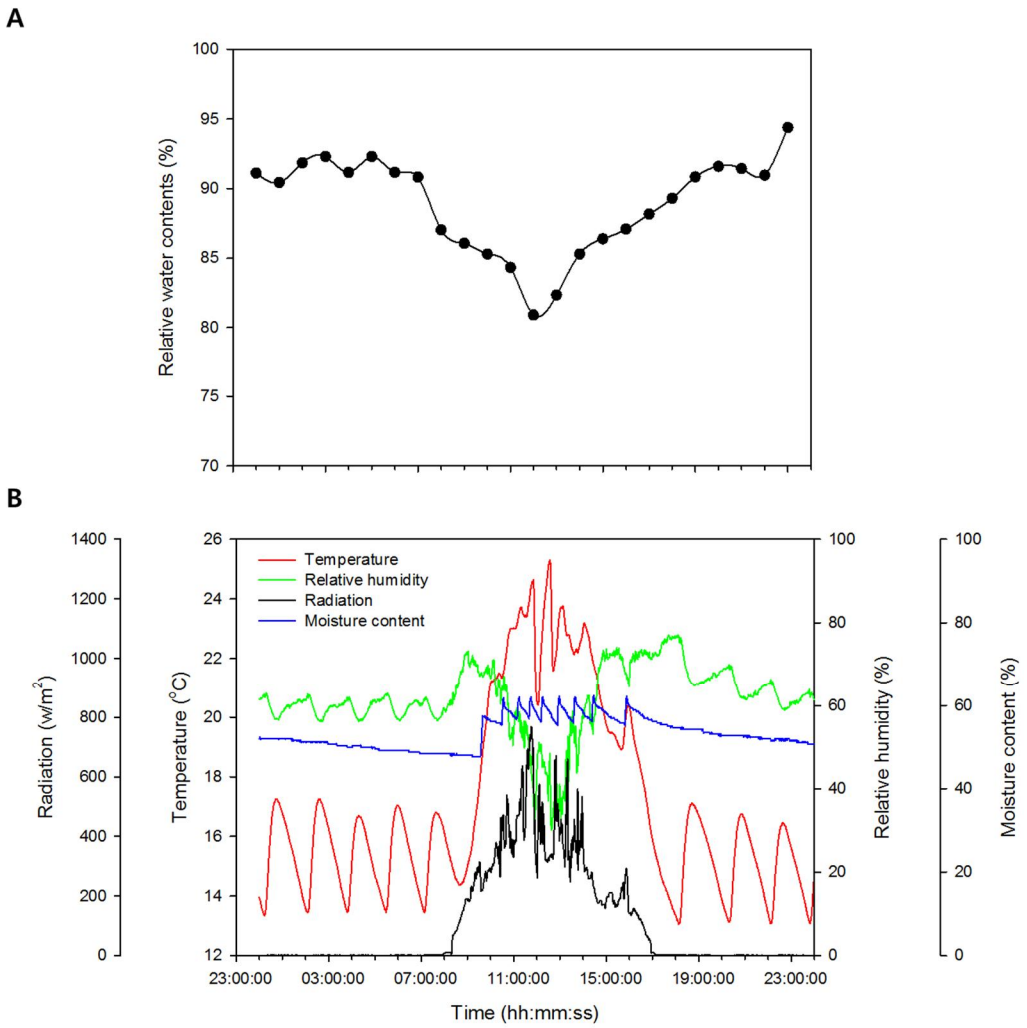

Fig. 2-3. Diurnal changes in relative water content (A) and environmental factors (B) in heated condition at night (Feb. 27, 2018).

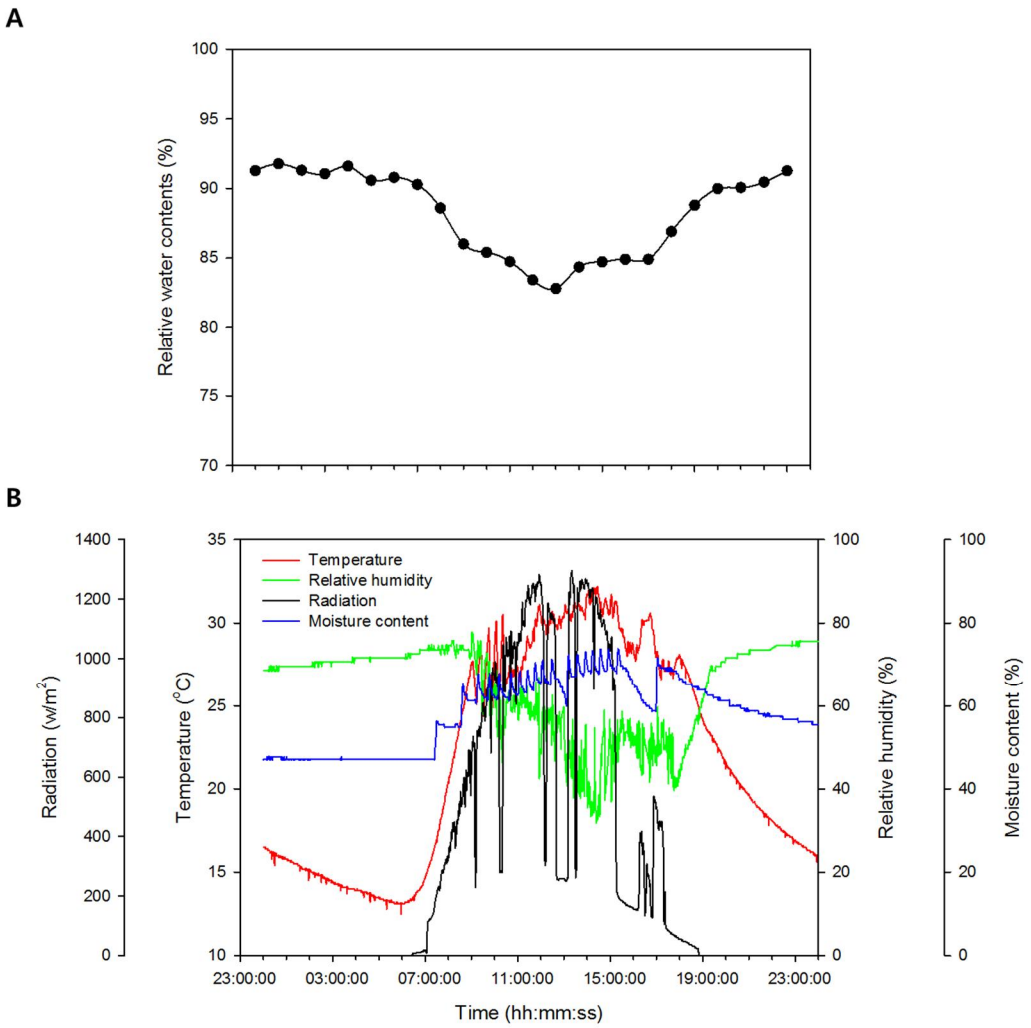

Fig. 2-4. Diurnal changes in relative water content (A) and environmental factors (B) in unheated condition at night (Apr. 28, 2018).

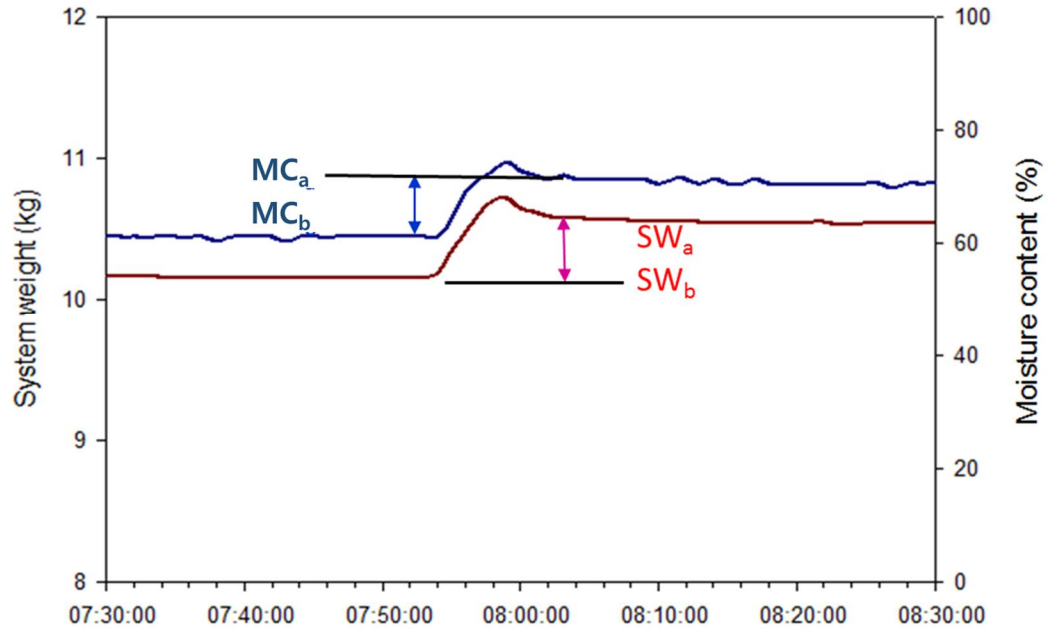

Fig. 2-5. Changes in system weight (SW) and moisture content (MC) measured by load cells and frequency domain reflectometry sensors, respectively, before and after the irrigation. Subscripts a and b mean after and before irrigation, respectively.

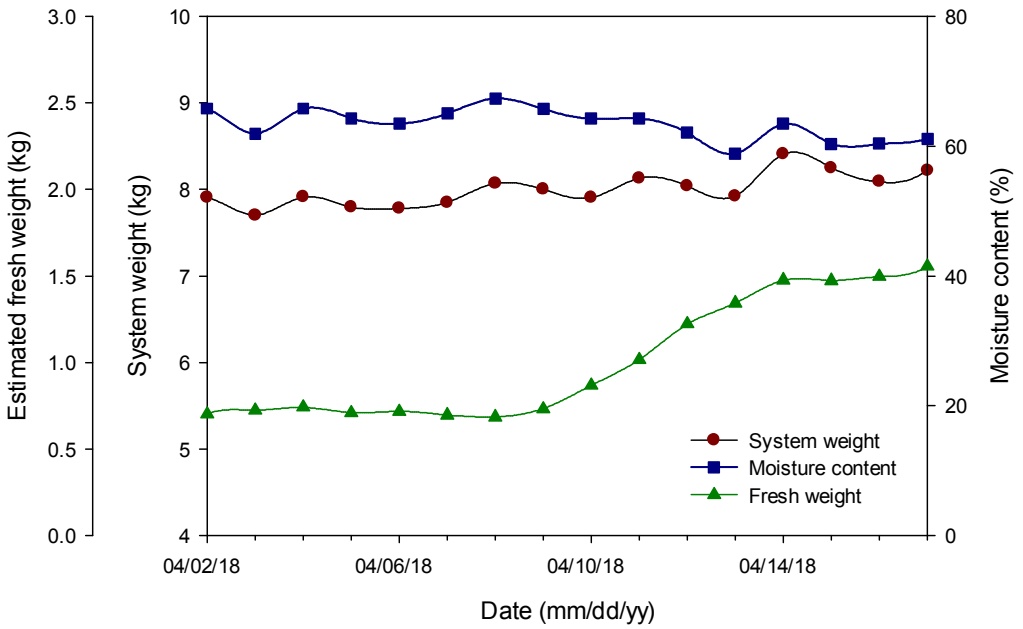

Fig. 2-6. Changes in total system weight, moisture content, and fresh weight from Apr. 2 to 17, 2018.

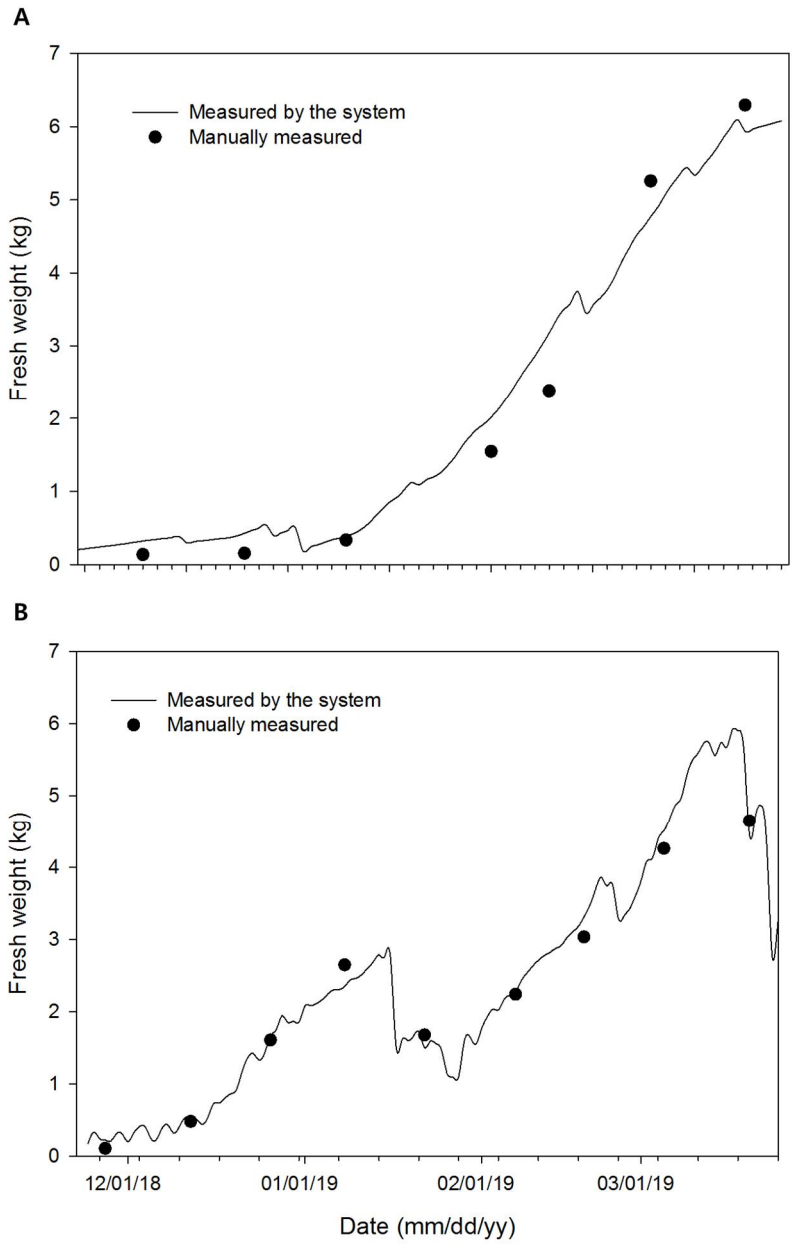

Fig. 2-7. Changes in crop fresh weights measured by the developed system (line) and actually measured (dot). A and B mean cultivation periods 1 and 2, respectively.

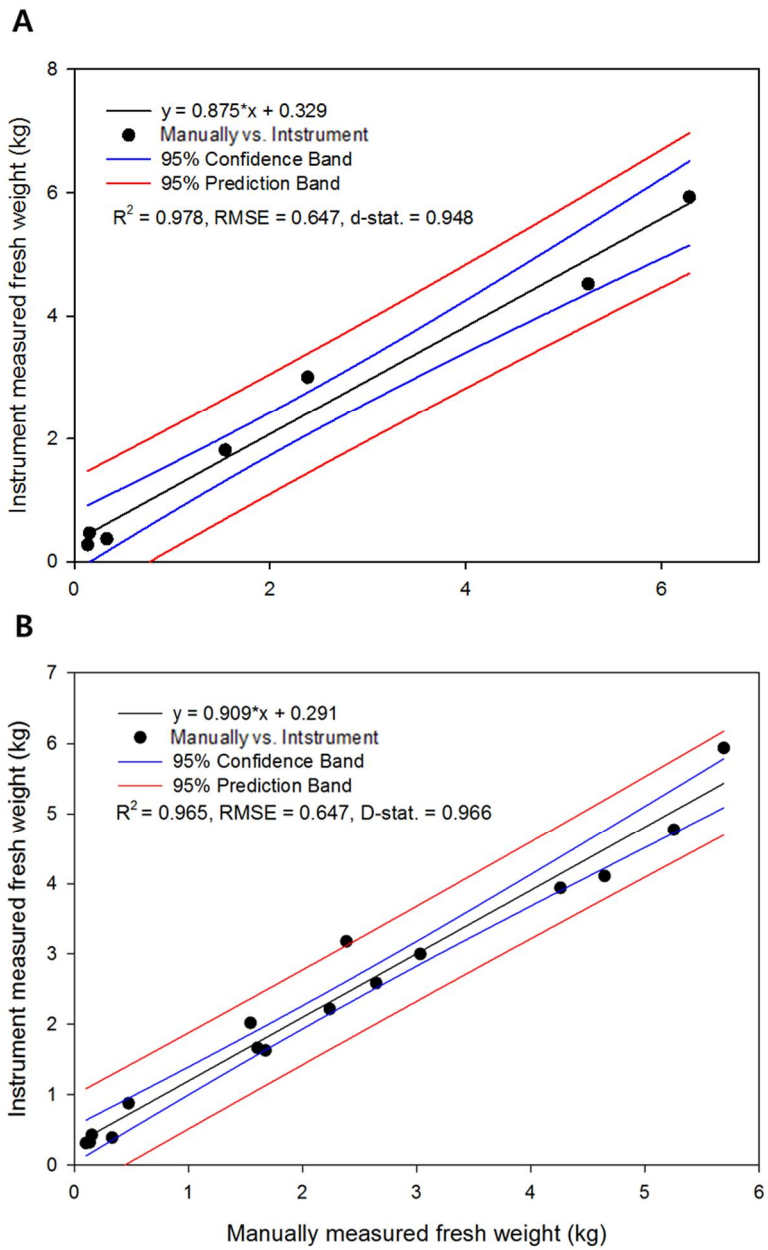

Fig. 2-8. Comparison of crop fresh weights measured by the developed system and actually measured.

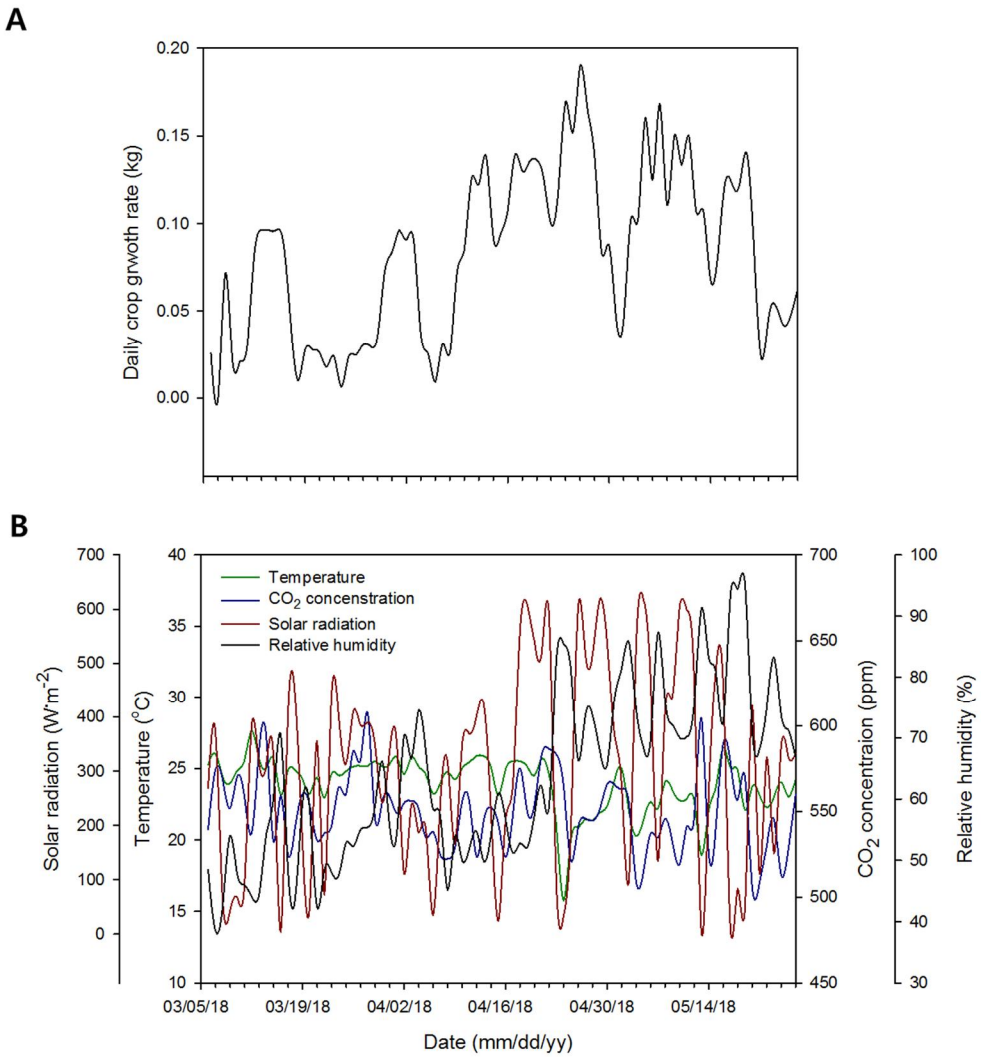

Fig. 2-9. Comparison of crop fresh weights measured by the developed system and actually measured.

CHAPTER 3

Development of Growth Estimation Algorithms for Hydroponically-grown Bell Pepper Crops Based on Recurrent Neural Network

ABSTRACT

For the efficient use of big data for smart farms, quantitative analysis of complex, diverse and unpredictable relationships between crop growth and the environment conditions are required. The objective of this study was to develop an algorithm that can interpret the crop growth response to environmental factors based on recurrent neural network (RNN). The algorithms were trained with data from three growth periods. The developed measurement methods were used to measure the growth characteristics of bell peppers. As the crop growth was affected by cumulative changes of environmental factors, a RNN algorithm, specialized in chronologically data analysis, was selected. Using the training accuracy, major environmental factors were selected and an optimal algorithm was developed. Long short term memory (LSTM) algorithm was selected as an optimal algorithm among the RNN algorithms. The algorithm consisted of eight environmental variables, and three crop growth characteristics as input variables and the

weekly crop growth rate as output variables. The training accuracies varied from 0.748 to 0.806 in all growth periods. The estimated crop growths showed linearly good agreements with the actual ones. The algorithm developed in this study are expected to be useful in estimation of crop fresh weight by using the relationship between crop growth and environment conditions in greenhouses.

Additional keywords: agricultural big data, crop monitoring system, long short term memory (LSTM), machine learning, smart farming

INTRODUCTION

Smart farms are emerging as new digital technologies such as remote sensing (Atzberger, 2013), cloud computing (Zamora-Izquierdo et al., 2019), and internet of things (IoT) (Baoyun, 2009) are being applied to agricultural technologies. For efficient use of big data for the smart farms, it is necessary to understand more about the complex, diverse, and unpredictable relationship between crop growth, and environmental factors. The emerging digital technologies can contribute to this understanding with continuous monitoring and measurement by generating large amounts of data at unprecedented rates (Chi et al., 2016; Sonka, 2016). So quantitative analysis of big data collected from these diverse sources is required (Hashem et al., 2015).

Many studies have been conducted using process based models (PBMs) to quantitatively analyze the relationship between crops growth, and the environment (Jones et al., 2017). PBM consists of many modules that various physiological process of crops (e.g. photosynthesis, respiration, biomass assimilation, biomass distribution, and stress response). PBM simulated the crop growth through various process modules according to input variables. Since PBM aims to include all biochemical functions of plants, various modules are subjected to complicated calculations for even a single variable, and calibration of many indexes is required (Dayan et al., 1993; Marcelis et al., 1998). In addition, it is important to measure the each crop organs growth to simulate accurate models, since PBM estimates the biomass production through the distribution to each

organ (Heuvelink et al., 1999; Martznez-Ruiz et al., 2019; Shamshiri et al., 2016). In these respects, PBM is not optimized to interpret agricultural big data.

Artificial neural network (ANN) provides a way of analyzing complex, nonlinear, and multi-dimensional datasets from big data (Wang, 2005), and could abstract quantitative relationship from raw data (LeCun et al., 2015). ANN has been widely used in agricultural research for the purpose of analyzing the biochemical, and physiological characteristics of various crop cultivations (Arab et al., 2010; Eftekhari et al., 2018; Ehret et al., 2011; Kucukonder et al., 2016). Among ANN algorithm, recurrent neural network (RNN) is useful for analyzing the chronological data, and this algorithm shows better accuracy than previous algorithms (Adavanne et al., 2017; Ororbia et al., 2017).

Recurrent neural network has an advantage of inputting big data of relatively long period, and the length of output values is also unlimited theoretically (Hochreiter and Schmidhuber, 1997).The crop growth response to the environment is determined by accumulated time series change of environmental factors. Therefore, RNN would be useful algorithm to estimate the crop growth response to cumulative environmental changes. The objective of this study was to develop an algorithm to estimate the crop growth respond to various environment factors in hydroponically-grown bell pepper.

MATERIALS AND METHODS

Greenhouse and crop cultivation conditions

The experiments were conducted in Venlo-type glasshouses located in the experimental farm of Seoul National University, Suwon, Korea (growth period 1, and 2; latitude, 37.3°N; longitude, 127.0°E), and, the experimental farm of Nong-woo, Ansung, Korea (growth period 3; latitude, 37.0°N; longitude, 127.0°E). The vents on the roof, and sidewall were automatically opened when the temperature was higher than 26°C during the day. Bell pepper seedlings (*Capsicum annuum* L. 'Sirocco') at 40 days post-sowing on rockwool cubes (Grodan delta, Grodan, Roermond, Netherlands) in a seedling chamber were used for the experiment. After 2 weeks of acclimatization to the irrigation system at a nutrient concentration of 2.0 $dS \cdot m^{-1}$, the bell pepper seedlings with 5-6 nodes were transplanted into 0.9·0.15 0.07m (L·W·H) rockwool slabs (Grotop GT Master Dry, Grodan, Roermond, Netherlands), and placed on the gutters with a plant density of 3.3 $plants \cdot m^{-2}$. The electrical conductivity (EC) and pH of nutrient solutions were maintained at 2.6-3.0 $dS \cdot m^{-1}$ and 5.5-6.5, respectively. The crops were pruned to maintain two main stems, which were vertically trellised to a 'V' canopy system (Jovicich et al., 2004). The fruit yields were harvested when the coloring were completed. The weight of fruit abortion that had fallen before the harvest was measured. The environmental factors in greenhouse, such as amount of solar radiation [Pyranometer (SP-110, Apogee Instruments, Logan, USA)], temperature (CS220, Campbell Scientific, UT, USA), relative humidity (PCMini70, Gilwoo Trading, Seoul, Korea) were measured. The

environmental factors in root-zone, such as substrate temperature, EC of the substrate, and moisture content of the substrate, were measured using a multiple sensor [WT1000B, Frequency Domain Reflectometry (FDR), Mi-Rae Sensor, Seoul, Korea] located at the middle of substrate. A pH sensor (DPH-1, DIK electronics, Bucheon, Korea) were installed in the middle of the drainage tube.

Crop growth monitoring

Crop growth characteristics [leaf area index (LAI), fresh weight] monitoring systems were installed during cultivation. The LAI measurement system measured the light intensity at the top, and bottom of the crop canopy using pyranometer (SP-110; Apogee Instruments Inc., Logan, Utah, USA), and calculated the LAI using the light intensity ratio at the top and bottom of the canopy. In accordance with Chap.1, the LAI of crops was estimated, including both the external weather condition data, collected from the Korea Meteorological Administration, and measurement time conditions. Because the LAI measurement system was developed taking into account the effects of adjacent crops, it was installed in the middle of the greenhouse plantation area. Through this methodology, daily changes of LAI were continuously monitored.

The fresh weight measurement system was designed to support the whole crop cultivation system in accordance with Chap. 2, and the weight of the whole system was measured using tensile load cells. In addition, the water weight in substrate was corrected to derive only the fresh weight of the crop. The crop fresh weight at the dawn time zone (03:00 - 05:00) when the relative moisture content of the crops is stable was selected as a

representative fresh weight of the day. Through this methodology, daily changes of fresh weight were continuously monitored. All crop growth characteristics monitoring systems were installed using 30mm * 30mm aluminium frames to minimize the restriction of greenhouse workers activity, and the shadow caused by the frame.

Recurrent neural network analysis

The RNN has been used to analyze the crop growth respond to various environment factors. Among various RNN algorithm, long short-term memory (LSTM) could solve the vanishing gradient problem of RNN (Hochreiter and Schmidhuber, 1997). The LSTM algorithm has a cell with several gates (Fig. 3-1). LSTM accepts previous data with addition operation, so vanishing gradient or exploding gradient problem is not occurred. Therefore, LSTM can analyze long time data than simple RNN.

Long short-term memory cells can retain, save, and load information about previous data. LSTM receives current input, and previous output simultaneously, and the received information is operated through the gates. Previous information is saved as cell state, so sequenced data can be analyzed based on cell state. Gates are divided into three parts: input, forget, and output. The input gate determines how to select the data. The forget gate decides how much data should be forgotten and passes suitably forgotten previous data through a hyperbolic tangent function. The output gate combines cell state and input data and the combined output is sent to the next cell. The final output is printed when the predetermined time step is reached.

A modified LSTM algorithm called a gated recurrent unit (GRU) was developed (Cho et al., 2014). GRU has a similar structure to LSTM, except that it consists of update and reset gates. Since GRU has only two gates, it reduces computational complexity while retaining the advantages of LSTM. A specific RNN algorithm does not always yield the best prediction in all situations (Greff et al., 2015; Jozefowicz et al., 2015). Therefore, LSTM and GRU, the most well-known RNN algorithms, were compared. Similar to ordinary ANNs, RNN has hidden layers of perceptrons with activation function. In this study, input and output activation functions were set to hyperbolic tangent function, and gate activation function was set to sigmoidal function.

The environment factors in greenhouse, the environment factors in root-zone, and crop growth characteristics were used as input data, and weekly crop growth was used as output data. The environment factors in greenhouse were consist of atmospheric temperature, relative humidity, light intensity, and CO_2 concentration. The environment factors in root-zone were consist of moisture content, EC, substrate temperature, and drainage pH. Crop growth characteristics were consist of LAI, fresh weight, and days after transplanting (DAT). Crop growth was calculated with weekly change of fresh weight. The time step, one of the parameters for LSTM, was set to seven. AdamOptimizer was used for algorithm training (Kingma and Ba, 2014), and the hyperparameters for LSTM, and AdamOptimizer were empirically changed to solve regression problems (Table 3-1). 70% of the total data were randomly selected, and were used for algorithm training, and the rest of the data were used for accuracy tests of the training results. To include all cultivation data, 5-folds cross test was conducted (Kohavi

1995). The mean square error (MSE) was set as a cost for reducing computation. TensorFlow (v. 1.12.0, Google, Menlo Park, CA, USA) was used for computation and model construction (Abadi et al. 2016).

Statistical analysis

A regression analysis was using the SPSS statistical package (IBM, New York, NY, USA) and a graph of the model was drawn using Sigmaplot (Systat Software, San Jose, CA, USA).

RESULTS AND DISCUSSION

Collecting variables of RNN algorithm

Environmental variables were collected using sensors in the greenhouse during cultivation (Fig. 3-2). The average temperature of growth period 1, grown from February to June, was more than 6 degrees higher than that of growth period 2, grown from October to March. This was affected by ambient air temperature. Despite the difference in average temperature by growth periods, the solar radiation did not vary by growth periods. In general open field cultivation, the solar radiation is highly correlated with the average temperature. There are studies that use these relationships to estimate solar radiation through the relationship with temperature variables without measuring (Beshara et al., 2013; Wu et al., 2007). However, in greenhouse conditions, the relationship between temperature, and solar radiation is not linear because of the light screen, the heating curtain, etc. (De Gelder et al., 2012). Therefore, greenhouse crops should be used as independent variables for temperature, and solar radiation. The substrate moisture contents did not change rapidly because the amount of irrigation was adjusted to account for the solar radiation and the crop growth stage.

The LAI, and fresh weight of the crop were measured using the crop growth characteristics measurement methods developed in chap. 1, and 2 (Fig. 3-3A, C, and E). The LAI, and fresh weight of the crops showed growth in the form of sigmoidal according to DAT. A drastic decrease in fresh weight occurred during the growth period 2 (Fig. 3-3C, 2019.01.16). The crop wires on the top of the system were snapped, which

damaged main stems of the bell pepper. This accident was monitored by the fresh weight measurement system.

The fruits yield, and abortion weigh of the crops grown on the fresh weight measurement system were measured weekly (Fig. 4-4A). In growth period 3, the fruits were kept without harvest until the end of the data collection. The algorithm could estimate that the crop growth was negatively, since the fruits harvest, and abortions caused drastic the fresh weight reduce. Therefore, calibrated fresh weight values, used in the previous studies conducted in bell pepper (Cosic et al., 2017; Sønchez-Molina et al., 2015), were calculated. Calibrated weight was calculated as adding the weight of fruit harvested, or abortion to the weight of the current crop (Fig. 3-4B, D, and F). The crop growth was calculated as weekly changes of the calibrated weight, and used it as an output variable of the algorithm.

Optimal RNN Algorithm Selection

The results of comparing the various RNN algorithms test accuracy to select the optimal RNN algorithm are shown in Table 3-2. Among all RNN structures, LSTM showed the highest accuracy. Although the RMSE of all structures ranged from 0.01 to 0.03, the single-layered LSTM showed the highest test accuracy with $R^2 = 0.78$. Multi-layers did not improve the accuracy of RNN models. LSTM showed the higher accuracy than GRU.

The contribution of each input variable was evaluated by excluding each input variable to train the RNN algorithm, and comparing the accuracy of the results with all

input variables (Table 3-3). All variables of the environmental factors in greenhouse conditions (atmospheric temperature, relative humidity, light intensity, and CO_2 concentration) showed high contribution levels. Among the environmental factors in root-zone, substrate moisture content variable showed high contribution, whereas EC, temperature of substrate, and, drainage pH were relatively low contribution. Among the growth characteristics, LAI and fresh weight variables showed high contribution, whereas DAT were relatively low contribution. An ANN, optimized to analyze the relationship among nonlinear interactions of different variables, does not decrease accuracy as input variable increase (Moon et al., 2018). Considering the economic costs, high-contribution variables, such as atmospheric temperature, relative humidity, light intensity, and CO_2 concentration, and DAT variables that do not require additional sensors were selected as algorithm input variables.

Crop growth estimation

The trained algorithm estimated the actual crop growth, although there was some deviation between the estimated, and the measurement (Fig. 3-5). The calibrated fresh weight of the crop, calculated as integrating the growth estimated by the algorithm, was similar to the actual calibrated fresh weight (Fig. 3-6). The d-statistic, which indicates the estimation accuracy, was 0.749, 0.748, and 0.806, respectively, depending on the growth periods. From these results, the developed algorithm was possible to estimate the actual crop growth. PBM should calibrate various parameters to estimate crop growth response to environmental factors. To calibrate the PBM, destructive growth survey should be

required. High level of labor, time and cost were needed to collect agricultural big data with destructive growth surveys. In this study, the crop growth were measured, and collected non-destructively using continuous measurement method for LAI and fresh weight. ANN was used for analysis of such collected data. However, the data collected from the several growth periods were not enough to train the ANN. ANN training using insufficient data cause overfitting (Jacobs et al., 2017). In this study, the continuously collected data were divided into one week intervals, and the growth characteristics, and environmental factors of each interval were used for RNN training. Through this process, accuracy was high even though relatively small numbers of data were used. The methodology would be expected to be used to estimate the crop growth response to various environmental factors, and cultivation technology under limited big data collection.

During growth period 2, on 2019.01.16 the crop stem was broken, the rate of crop growth was dramatically reduced, and then recovered after about two weeks (Fig. 3-7). When a plant is physically injured, the stress-defensive mechanism begins (Toyota et al., 2018) with increased transport of calcium ions through phloem, and this defense mechanism causes the crop growth reduction. Also, the physical injury increase the maintenance respiration (Fonseca et al., 2002). Therefore, physical injury causes the crop growth reduction over several days as well as reduction in the instantaneous fresh weight. The RNN, specialized in interpreting data with time intervals between input, and output variables (Jozefowicz et al., 2015). The RNN-based growth algorithm developed estimated the current crop growth based on the input variables from the past week. The

time interval between input, and output variables of RNN affect the estimation accuracy during crop physical injury, and its recovery (Fig. 3-7). The actual growth rate of the crops has been rapidly decreased after 2019.01.16, and recovered after several days. The algorithm estimated higher than the actual growth until 2019.01.22, which used the growth characteristics before the physical injury. From 2019.01.23, which used the growth characteristics after the physical injury, a decrease of crop growth was estimated. RNN, which estimated the current situation (output variables) with information from the past (input variables), has the advantage of analyzing the cumulative effect of environmental factors, but also has disadvantages that it is difficult to react immediately to unexpected changes in conditions.

LITERATURE CITED

Ahmadi, H., and Golian, A. (2010b). The integration of broiler chicken threonine responses data into neural network models. Poultry Science 89, 2535–2541. doi: 10.3382/ps.2010-00884

Arab, M.M., Yadollahi, A., Shojaeiyan, A., and Ahmadi, H. (2016). Artificial neural network genetic algorithm as powerful tool to predict and optimize in vitro proliferation mineral medium for g × n15 rootstock. Frontiers in Plant Science 7:1526. doi: 10.3389/fpls.2016.01526

Atzberger, C. (2013). Advances in remote sensing of agriculture: Context description, existing operational monitoring systems and major information needs. Remote Sensing 5, 949-981.

Baoyun, W. (2009). Review on internet of things [J]. Journal of Electronic Measurement and Instrument 12, 1-7.

Besharat, F., Dehghan, A.A., and Faghih, A.R. (2013). Empirical models for estimating global solar radiation: A review and case study. Renewable and Sustainable Energy Reviews 21, 798-821.

Chi, M., Plaza, A., Benediktsson, J.A., Sun, Z., Shen, J., and Zhu, Y. (2016). Big data for remote sensing: Challenges and opportunities. Proceedings of the IEEE 104(11), 2207-2219.

Ćosić, M., Stričević, R., Djurović, N., Moravčević, D., Pavlović, M., and Todorović, M. (2017). Predicting biomass and yield of sweet pepper grown with and without plastic

film mulching under different water supply and weather conditions. Agricultural Water Management 188, 91-100.

Dayan, E., Van Keulen, H., Jones, J. W., Zipori, I., Shmuel, D., and Challa, H. (1993). Development, calibration and validation of a greenhouse tomato growth model: I. Description of the model. Agricultural Systems 43, 145-163.

De Gelder, A., Dieleman, J.A., Bot, G.P.A., and Marcelis, L.F.M. (2012). An overview of climate and crop yield in closed greenhouses. Journal of Horticultural Science and Biotechnology 87, 193-202.

Eftekhari, M., Yadollahi, A., Ahmadi, H., Shojaeiyan, A., and Ayyari, M. (2018). Development of an Artificial Neural Network as a Tool for Predicting the Targeted Phenolic Profile of Grapevine (*Vitis vinifera*) Foliar Wastes. Frontiers in Plant Science 9, 837.

Ehret, D.L., Hill, B.D., Helmer, T., and Edwards, D.R. (2011). Neural network modeling of greenhouse tomato yield, growth and water use from automated crop monitoring data. Computers and Electronics in Agriculture 79, 82-89.

Fonseca, S.C., Oliveira, F.A., and Brecht, J.K. (2002). Modelling respiration rate of fresh fruits and vegetables for modified atmosphere packages: a review. Journal of Food Engineering 52, 99-119.

Hashem, I.A.T., Yaqoob, I., Anuar, N.B., Mokhtar, S., Gani, A., and Khan, S.U. (2015). The rise of “big data” on cloud computing: Review and open research issues. Information Systems 47, 98-115.

Jacobs, S.A., Dryden, N., Pearce, R., and Van Essen, B. (2017, November). Towards scalable parallel training of deep neural networks. In Proceedings of the Machine Learning on HPC Environments (p. 5). ACM.

Jones, J.W., Antle, J.M., Basso, B., Boote, K.J., Conant, R.T., Foster, I., ... and Keating, B.A. (2017). Brief history of agricultural systems modeling. Agricultural Systems 155, 240-254.

Jovicich, E., Cantliffe, D.J., Stoffella, P.J., and Haman, D.Z. (2007). Bell pepper fruit yield and quality as influenced by solar radiation-based irrigation and container media in a passively ventilated greenhouse. HortScience 42, 642–652.

Jozefowicz, R., Zaremba, W., and Sutskever, I. (2015, June). An empirical exploration of recurrent network architectures. In International Conference on Machine Learning (pp. 2342-2350).

Kamilaris, A., Kartakoullis, A., and Prenafeta-Boldú, F.X. (2017). A review on the practice of big data analysis in agriculture. Computers and Electronics in Agriculture 143, 23-37.

Küçükönder, H., Boyaci, S., and Akyüz, A. (2016). A modeling study with an artificial neural network: developing estimation models for the tomato plant leaf area. Turkish Journal of Agriculture and Forestry 40, 203-212.

Marcelis, L.F.M., Heuvelink, E., and Goudriaan, J. (1998). Modelling biomass production and yield of horticultural crops: a Review. Scientia Horticulturae 74, 83-111.

O'Grady, M.J. and O'Hare, G.M. (2017). Modelling the smart farm. Information Processing in Agriculture 4, 179-187.

Sonka, S. (2016). Big data: fueling the next evolution of agricultural innovation. Journal of Innovation Management 4, 114-136.

Toyota, M., Spencer, D., Sawai-Toyota, S., Jiaqi, W., Zhang, T., Koo, A. J., ... and Gilroy, S. (2018). Glutamate triggers long-distance, calcium-based plant defense signaling. Science 361, 1112-1115.

Wang, L. (2005). A hybrid genetic algorithm-neural network strategy for simulation optimization. Applied Mathematics and Computation 170, 1329–1343. doi: 10.1016/j.amc.2005.01.024

Wu, G., Liu, Y., and Wang, T. (2007). Methods and strategy for modeling daily global solar radiation with measured meteorological data–A case study in Nanchang station, China. Energy Conversion and Management 48, 2447-2452.

Zamora-Izquierdo, M.A., Santa, J., Martínez, J.A., Martínez, V., and Skarmeta, A.F. (2019). Smart farming IoT platform based on edge and cloud computing. Biosystems Engineering 177, 4-17.

Table 3-1. Hyperparameters for recurrent neural network (RNN) and AdamOptimizer.

Parameter	Value	Description
Learning rate	0.001	Learning rate used by the AdamOptimizer
β1	0.9	Exponential mass decay rate for the momentum estimates
β2	0.999	Exponential velocity decay rate for the momentum estimates
E	1e-0.8	A constant for numerical stability
Forget bias∗	1.0	Probability of forgetting information in the previous dataset
Time step	2–24	Number of datasets that the LSTM will see at one time

Table 3-2. Test accuracies and root mean square errors (RMSEs) of trained recurrent neural network (RNN) algorithms.

Type of RNN	Test accuracy (R^2)	Test RMSE (kg)
Long short-term memory (LSTM)	0.78	0.325
Gated recurrent unit (GRU)	0.68	0.472
Multi-layered LSTM	0.70	0.427
Multi-layered GRU	0.71	0.386

Table 3-3. Test accuracies of the long short-term memory (LSTM) after excluding input data.

Excluded data	Test accuracy (R^2)
Atmospheric temperature (°C)	0.75 (-0.03)
Relative humidity (%)	0.73 (-0.04)
CO_2 concentration (μmol·mol^{-1})	0.76 (-0.02)
Solar radiation (W/m^2)	0.75 (-0.03)
Moisture content of substrate (%)	0.73 (-0.05)
Substrate temperature (°C)	0.77 (-0.01)
Electrical conductivity (EC) of substrate (dS·m^{-1})	0.77 (-0.01)
Drainage pH	0.77 (-0.01)
Day after transplanting (DAT)	0.77 (-0.01)
Leaf area index (LAI)	0.74 (-0.04)
Fresh weight (kg)	0.75 (-0.03)

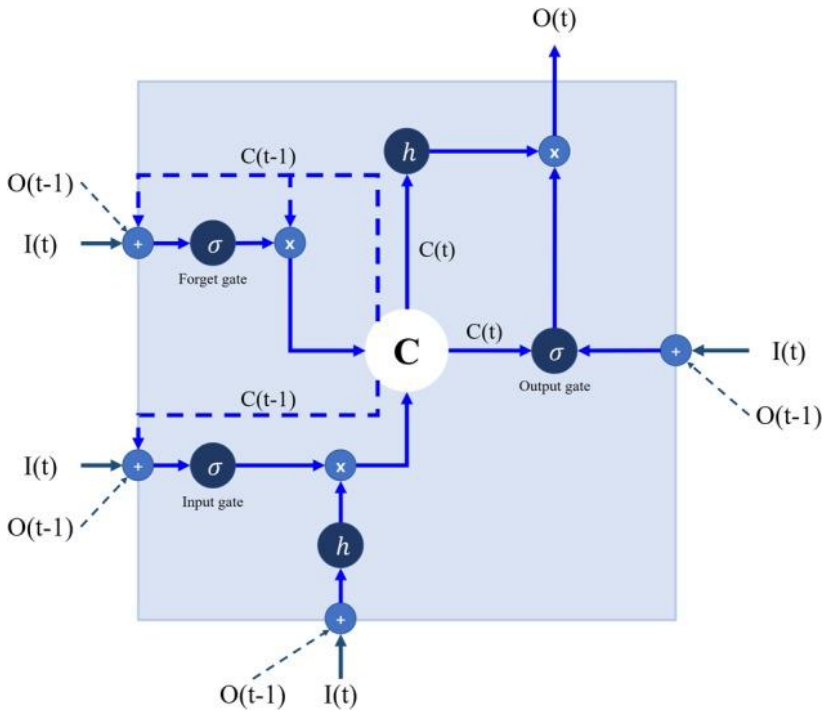

Fig. 3-1. A structure of a long short-term memory (LSTM). I, input vectors; O, output vectors; C, cell state; *h*, tanh for input and output activation function; σ, sigmoidal function for gate activation function; *t* and *t*–1, current and previous times, respectively.

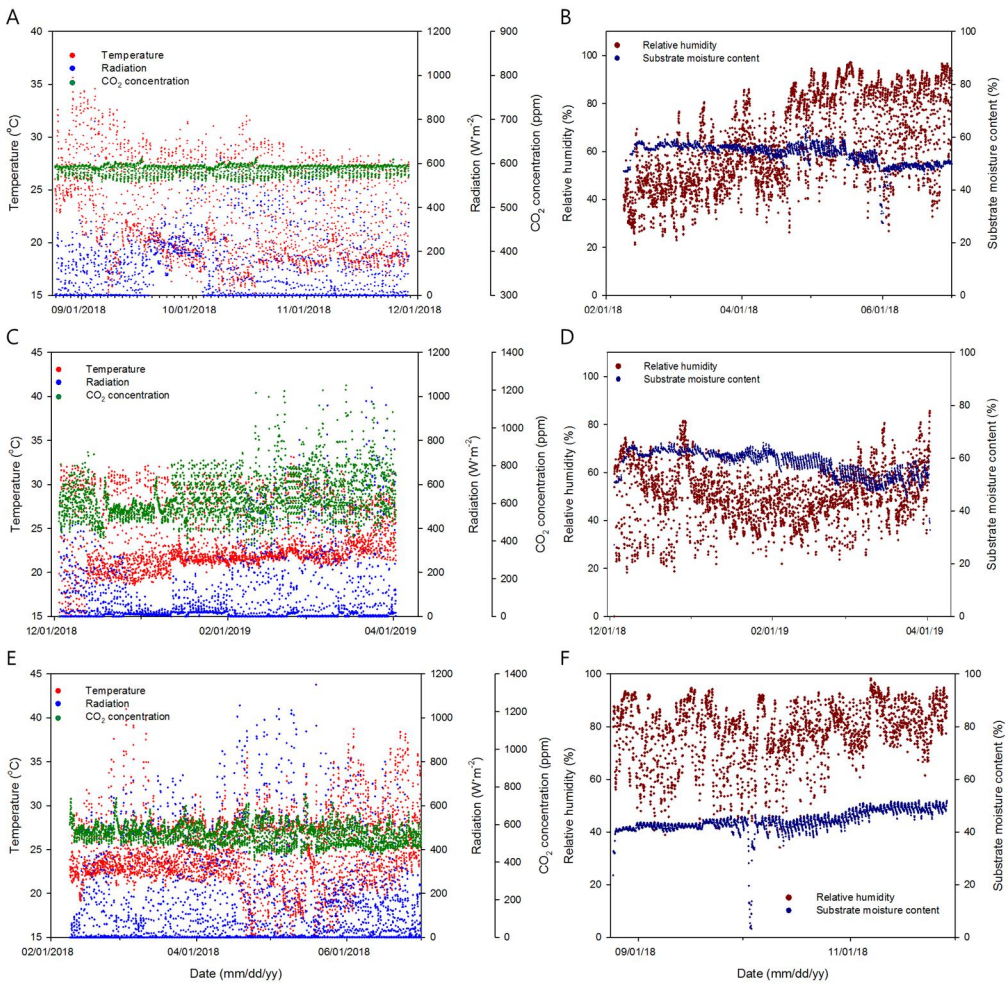

Fig. 3-2. Environmental conditions in the greenhouse during growth period 1 (Sept 1 – Dec 01, 2018; A and B), growth period 2 (Dec 01, 2018 – Apr 01, 2019; C and D), and growth period 3 (Feb 01 – June 01, 2018; E and F).

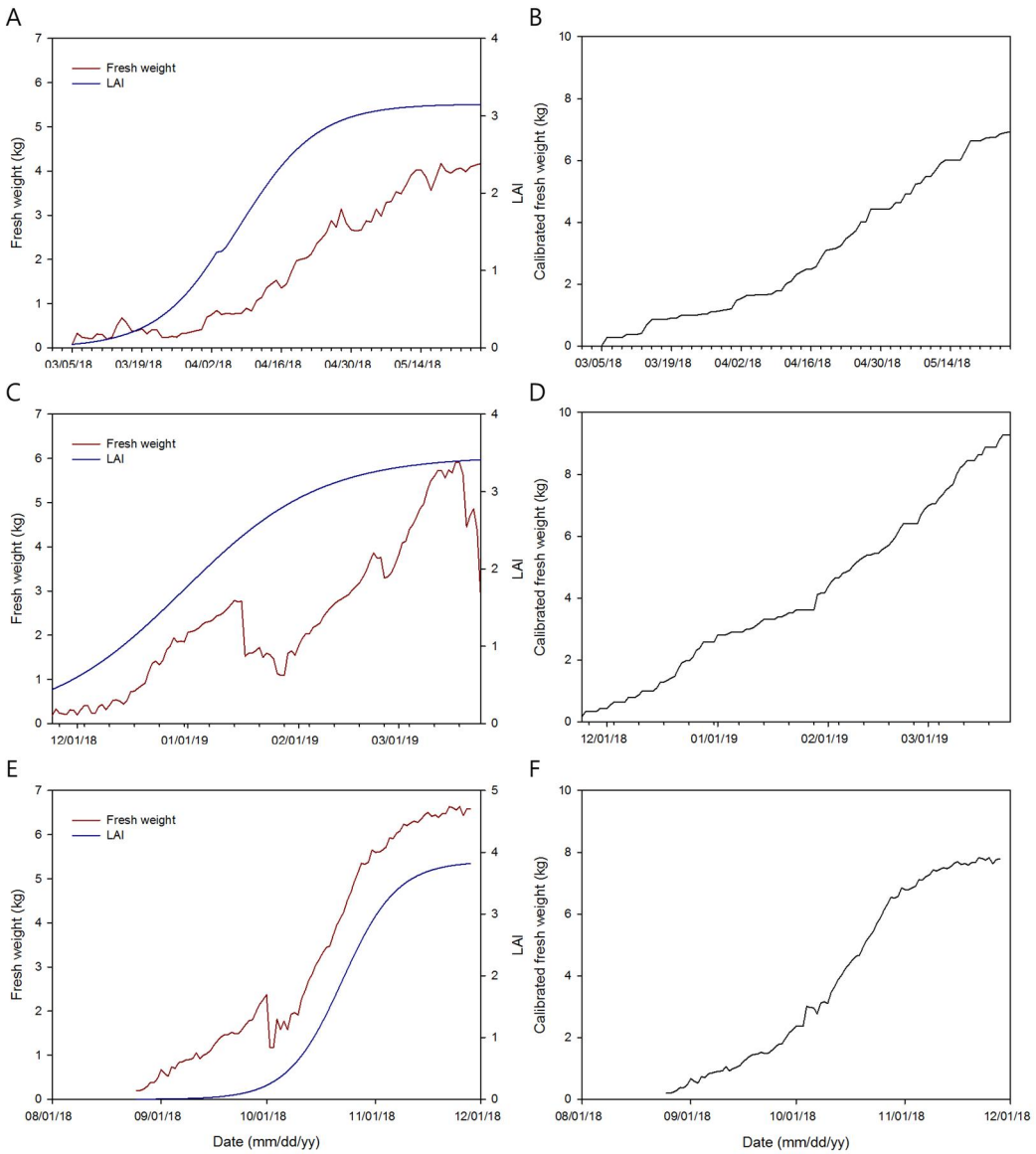

Fig. 3-3. Changes in fresh weight and leaf area index (LAI) during growth period 1 (Sept 1 – Dec 01, 2018; A), growth period 2 (Dec 01, 2018 – Apr 01, 2019; C), and growth period 3 (Feb 01 – June 01, 2018; E). B, D, and F represent the calibrated fresh weights during growth periods 1, 2, and 3, respectively

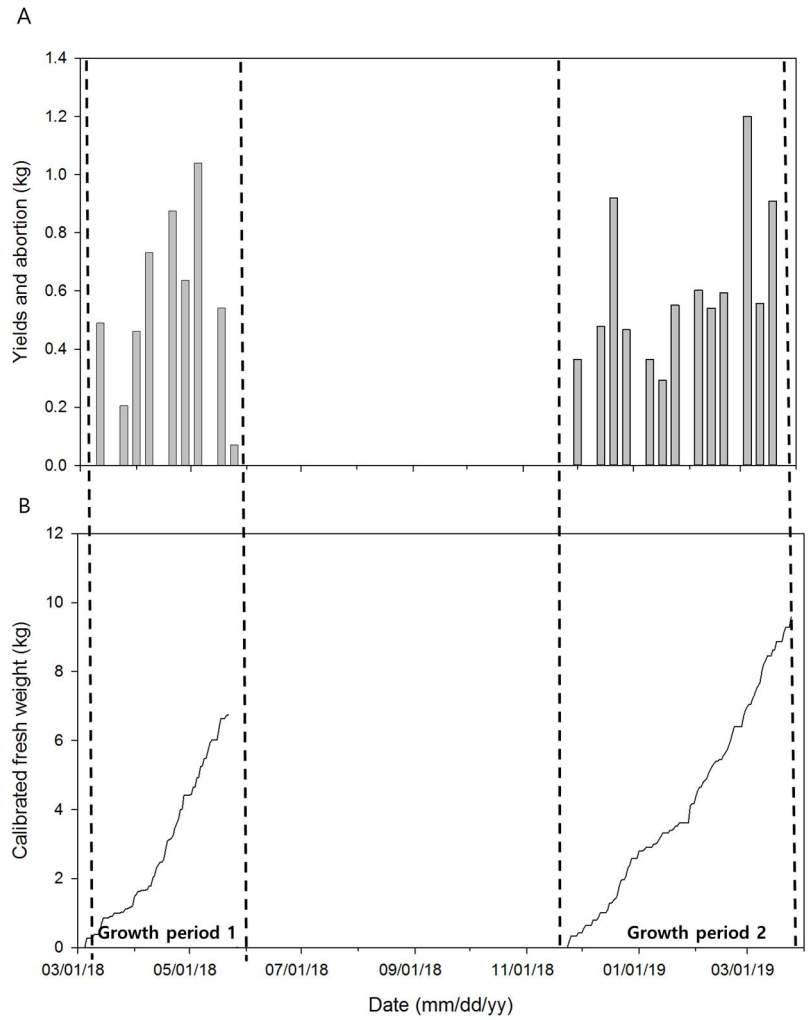

Fig. 3-4. Fruit yield and abortion at one-week interval (A) and calibrated crop fresh weight considering fruit yield and abortion (B).

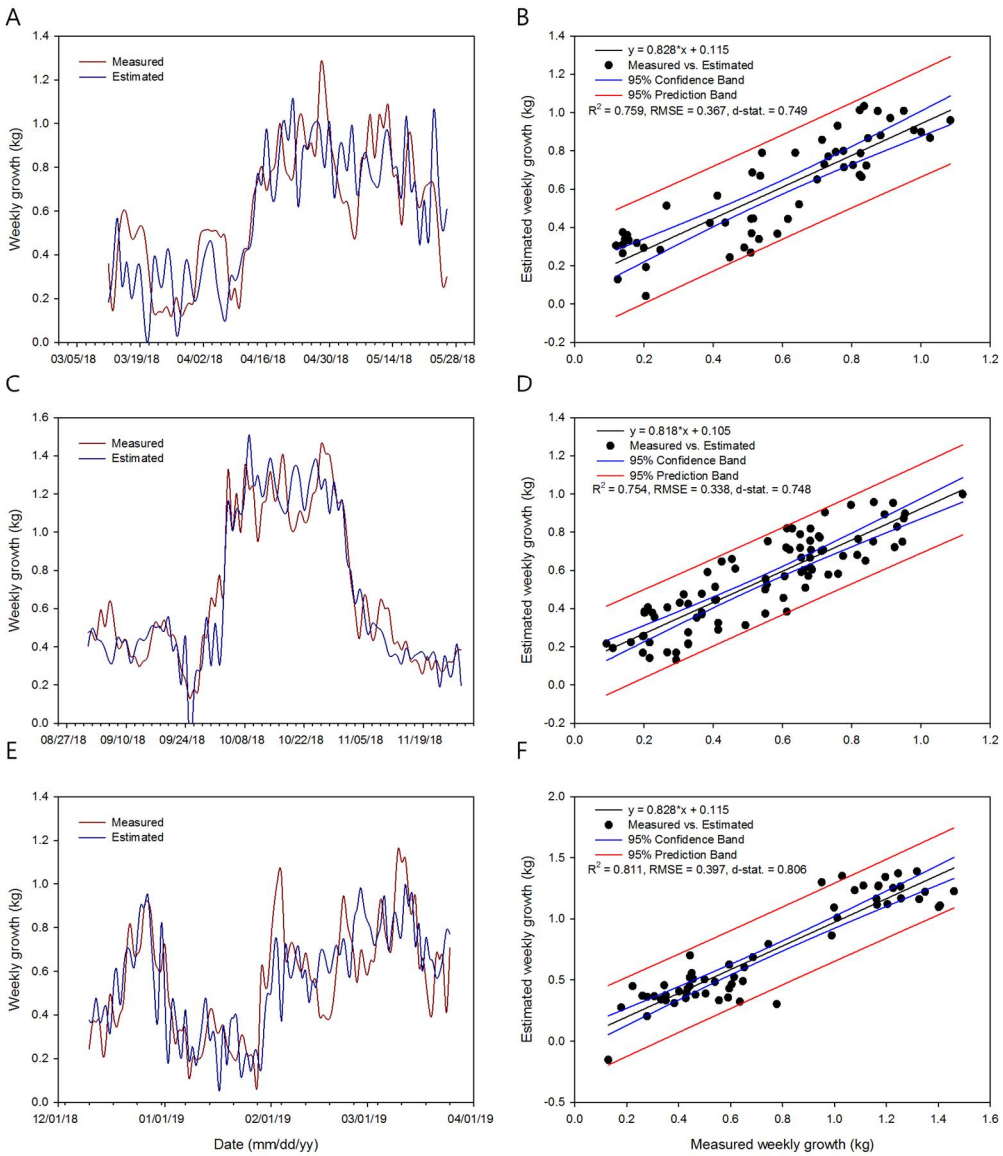

Fig. 3-5. Comparison of weekly crop growth rates measured by the system and estimated by the algorithm during growth periodq (Sept 1 – Dec 01, 2018; A and B), growth period 2 (Dec 01, 2018 – Apr 01, 2019; C and D), and growth period 3 (Feb 01 – June 01, 2018; E and F). B, D, and F represent the test accuracies of the algorithms during growth periods 1, 2, and 3, respectively.

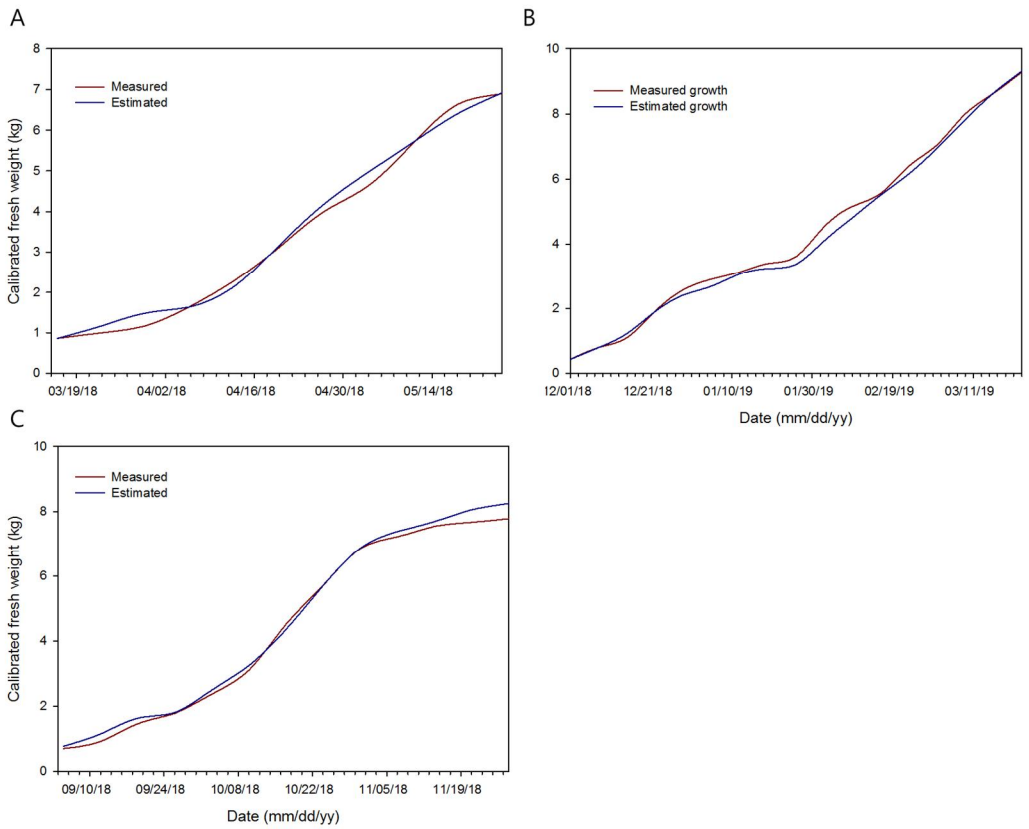

Fig. 3-6. Comparisons of crop fresh weights measured by the system and estimated by accumulated crop growth rate during the growth periods from Mar. 19 to Dec 01, 2018 (A, growth period 1), from Dec 01, 2018 to Mar 24, 2019 (B, growth period 2), and from Sep 5 to 28, 2018 (C, growth period 3).

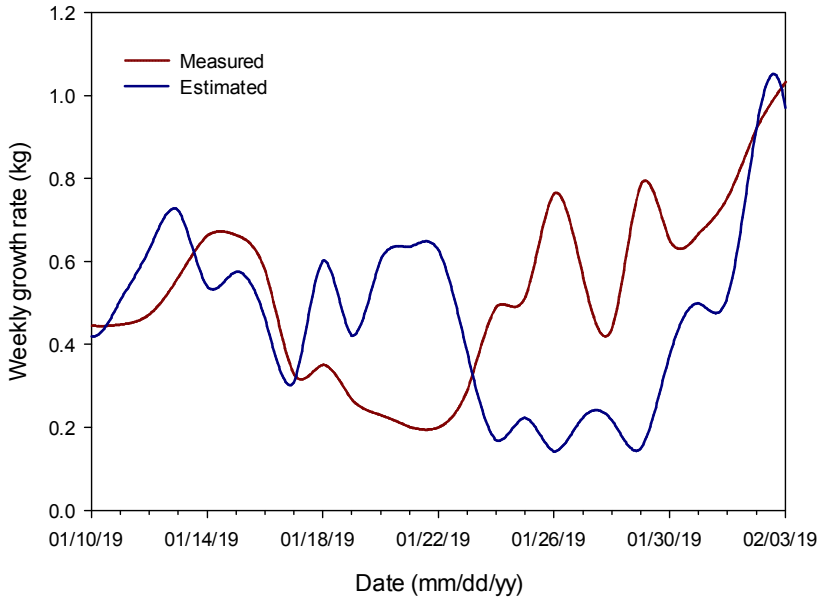

Fig. 3-7. Comparison of weekly crop growth rates measured by the system and estimated by the algorithm during growth period from Jan. 10, 2019 to Feb. 3, 2019.

CHAPTER 4

Validation and Evaluation of Growth Estimation Algorithm for Hydroponically-grown Bell Pepper Crops Based on Recurrent Neural Network

ABSTRACT

Since recurrent neural network (RNN) has a 'black box' hidden layers inside the algorithm, it is impossible to manually calibrate the parameters unlike process-based model (PBM). Validation process is essential in evaluation of the algorithm developed. The objectives of this study were to validate the developed algorithm in greenhouses and evaluate the accuracy of the algorithm compared to the PBM. Validation of the RNN-based crop growth prediction algorithm was carried out using the data collected from a large commercial greenhouse. The CropGro-bell pepper model was applied to compare and evaluate the accuracy of the developed algorithm. The parameters of the PBM were calibrated using the growth survey data collected during growth period for the algorithm training. As a result of the validation, it was confirmed that a reliable level of accuracy was achieved in commercial greenhouses. The PBM was able to simulate the growth of

each organ, however the output was estimated as dry weight. In order to compare the accuracy with the developed algorithms, it was converted to fresh weight using the ratio of dry and fresh weights of each organ. The accuracy of the developed algorithm showed higher than that of the PBM.

Additional keywords: comparative analysis, crop monitoring system, CropGro, machine learning, process-based model (PBM)

INTRODUCTION

Smart farm technologies have been introduced to identify the relationship between crops and environments from various aspects (Wolfert et al., 2017). Due to the demands of modeling and quantitative technologies for big data (Hashem et al., 2015), previous studies have attempted to estimate the crop growth using algorithms based on machine learning (Ehret et al., 2011; Gupta et al., 2015; Gi et al., 2018; Kumar et al., 2017). These studies used machine learning to produce meaningful results in areas of data that were previously difficult to interpret, or to indicate an improvement in the accuracy of predictions compared to previous studies.

The growth prediction models, or algorithms developed through various studies are incorporated into the platform (e.g. AquaCrop, DSSAT, HORTSIM) to simulate the crop growth, or yield response to environmental factors. Ideally, such simulated results can be used to infer the real systems results (Asseng et al., 2013; Körner et al., 2015; Yadav et al., 2018). Virtual experiments (simulations) using the models can complement actual experiments, but there is a need to improve model responses relative to real system responses for a range of conditions to establish confidence in the model (Jones et al., 2017). Little has been done to establish uncertainty of agricultural systems models (Rosenzweig et al., 2013a, Rosenzweig et al., 2013b, Asseng et al., 2013).

In process based crop models (PBMs), the parameters of the model were determined to reflect the physiological crop characteristics. THRSH, for example, is a widely used parameter in the growth of *Fabaceae* (CropGro-soybean, Ma et al., 2006), an indicator of

the weight ratio of seeds, and whole fruits. It is possible to calculate these parameters automatically through an overall crop growth survey. In general, in the process of estimating parameters, certain coefficients may be outside the normal range, depending on the developer purpose. However, it is possible to manually adjust these parameters by hand calibrating them to the value estimated empirically by the users of the model.

Although in many studies artificial neural networks (ANN)s have been shown to exhibit superior predictive power compared to traditional approaches, they have also been labeled a “black box” because they provide little explanatory insight into the relative influence of the independent variables in the prediction process. Therefore, the RNN algorithm requires a different validation process than the PBM. A strategy is needed for validating crop estimation algorithm in each crop period using datasets independent of those used for algorithm training. The objectives of this study were to collect data from additional growth conditions, validate the developed algorithms, and evaluated the developed algorithm comparing with the widely-used PBM of bell peppers.

MATERIALS AND METHODS

Growth cultivation for validation

The validation were conducted in two Venlo-type glasshouse located commercial farm, Jinju, Korea (validation 2, latitude, 35.1°N; longitude, 128.0°E). Environmental control, and crop cultivation management in the greenhouse was carried out in the same way as in Chap 3. The environmental factors in greenhouse, such as amount of solar radiation [Pyranometer (SP-110, Apogee Instruments, Logan, USA)], temperature (CS220, Campbell Scientific, UT, USA), relative humidity (PCMini70, Gilwoo Trading, Seoul, Korea) were measured. The moisture content of the substrate, were measured using a multiple sensor [WT1000B, Frequency Domain Reflectometry (FDR), Mi-Rae Sensor, Seoul, Korea] located at the middle of substrate.

A growth survey was conducted every one week. The LAI of the crop was calculated by substituting the measured leaf length (L), leaf width (W), and node numbers (N) for the Eq. 4-1.

$$LA = -0.266 + 0.563 * L * W + 0.232 * N \quad \text{(Eq. 4-1)}$$

The fresh weight of the stem and leaf were measured weekly during the cultivation period. Fruit weight with fruit diameter, and fruit length were measured every week, and calculated by substituting in Eq. 4-2.

$$FFW = 286.30 * WF^2 * LF + 1.136 \quad \text{(Eq. 4-2)}$$

where, *FFW* is the fruit fresh weight, *WF*, the fruit length, *LF*, the fruit diameter. The weight of the harvested crops and the weight of pinched crops in the developed system were measured during the cultivation period.

Growth estimation algorithm

The RNN-based growth estimation algorithm, which was trained in chap. 3 was used. The test accuracy of algorithm training was 0.768.

Bell pepper PBM

The PBM selected for comparison to evaluate the accuracy of the algorithm is the CropGro-Bell Pepper. CropGro is a PBM platform that applies models to various crops such as soybean, peanut, dry bean, faba bean, macuna, chickpea, cowpea, velvet bean, cotton, pasture, etc., starting with development of PBM for tomato (Jones et al., 1991; Shi et al., 2015). CropGro-Bell Pepper is a variant of the soybean model that reflects the genotype, and ecotype of the bell pepper.

The model parameters (Table 4-1, and 4-2) were calculated from the growth survey results investigated in Chap. 2, and auto calibrated with the GLUE cofficient estimator (Ratto et al., 2001).

Validation of RNN algorithm and comparison of growth prediction to PBM

To validate the developed algorithm, the weekly crop growth was estimated with the environmental variables, and crop growth characteristics collected in validation growth period. The crop fresh weight was calculated by integrating the estimated crop growth. To validate the PBM, Decision Support Systems for Agrotechnology Transfer v4.7 (DSSAT, Jones et al., 2003; Hoogenboom et al., 2012) was used to simulate the bell pepper growth response to environment. Since the output value of the PBM were as the dry matter state of each organ (leaves, stems, roots, and fruits), the fresh weight was calculated with the ratio of the dry, and fresh weight by organs, and growth stages. Accuracy was evaluated by comparing the fresh weight of a crop predicted by the RNN algorithm, and PBM with the actual fresh weight.

RESULTS AND DISCUSSION

Environmental factors for validation

Environmental data were collected using sensors in the greenhouse throughout the validation growth period (Fig. 4-1). The validation growth period, which completed a year of bell pepper cultivation, was included within the temperature range of algorithm trained cultivation. The temperature range was maximum of 40.31°C, and minimum of 14.37°C. In validation cultivation, high level of environmental control was applied to all other environmental factors, thus, humidity, light intensity, and CO_2 concentration were all within the range of algorithm trained cultivation conditions. ANN accuracy reduce for data out range of the data used for training (Da Silva et al., 2017). Therefore, this validation dataset was available.

Growth characteristic for validation

During the validation cultivation period, the measurements were conducted by the actual growth measurements. The fresh weight was discontinuous due to the fruit harvest (Fig.4-2). The crop LAI increased as sigmoid form by DAT.

The fruits yield weight during the growth period was shown as Fig. 4-3. Calibrated fresh weight was calculated as Chp. 3. Calibrated fresh weight increased continuously as sigmoid from by DAT (Fig. 4-4).

PBM calibration

CropGro-bell pepper model was calibrated using the growth measurements collected from algorithm learned and applied cultivation period (Tables 3 and 4). The automatically calculated parameters were re-calibrated by hand to match the results of the previous study (Csizinszky, 1999) and empirical values. For LFMAX, maximum leaf photosynthesis rate at 30°C, 350 vpm CO_2, and high light (mg $CO_2 \cdot m^{-2} \cdot s$) and SIZLF, maximum size of full leaf, the values recorded from simple measurement were entered. In CropGro, the crop growth stages are divided into 7 stages, and it estimates no further growth after the crop reaches the R7 stage. Also, when the photothermal day is above a certain value, it is estimated that the growing point no longer develops resulting in no appearance of new nodes (Boote et al., 1998). However, bell pepper grows infinitely during the growth period under greenhouse conditions (Jensen, 1997), the effect on this parameter should be minimized. Boote et al. (2012) revised the infinite values of SD-PM, time between first seed (R3), and physiological maturity (R7), and FL-VS, time from first flower to last leaf on main stem, for greenhouse grown tomatoes to represent the tomato growth curve as an infinite form. Therefore, in this study, SD-PM, and FL-VS were set to 330 because the growth, and development of bell peppers continued until the end of the measurement.

Validation and evaluation

As a result of the validation, the developed algorithm was able to estimate the growth similarly to the actual crop growth (Fig. 4-5). Although the accuracy was relatively low compared to training test, validation results showed the crops growth with reliable level

of accuracy. These results presented the possibility for the use of the developed algorithms even from the data with growth survey, currently being used in most agricultural studies.

Calibrated PBM was able to simulate organ-specific growth of crops (Fig. 4-7). In the early days of growth, roots grew faster, but soon decreased, and the growth of stem, and leaves grew rapidly. From the time of the first fruit development, the growth of fruit was a major factor in the whole crop growth. This is because fruits sink strength was very high compared to other organs of bell pepper (Vieira et al., 2009).

The ratio of dry-fresh weight was highest in fruits, and lowest in roots (Fig. 4-8). In other crop organs, the ratio of dry-fresh weight did not change depending on the growth stages, except for stem, where the ratio was highest in the initial growth stage, and maintained constant after the middle growth stage. Because PBM calculated the crop growth based on dry weight, fresh weight was calculated with the ratio of dry-fresh weight measured during every growth stages. The fresh weight comparison results of the RNN algorithm, and the PBM estimated results are shown in Fig. 4-9. The RNN algorithm estimated the fresh weight with higher accuracy than PBM. The RNN algorithm had lower RMSE value than the PBM, and the d-statistic was also higher than the PBM. Although the amount of data used to optimize RNN training was insufficient, the algorithms developed were more accurate than PBMs. Rather than PBM, which calculated the parameters through the weekly growth survey, the developed algorithm trained the RNN through the automatically measured crop growth characteristics daily, so algorithm developed could reflect the changes of environment more precisely. Also in

PBM, the crop growth was estimated using only temperature, CO_2 concentration, and light intensity, while in the RNN algorithm, relative humidity, and substrate moisture contents were added. Relative humidity, and growth rate were not environmental factors that directly affect photosynthesis rate, but they were environmental factors that affect the water content of crops. As most of the horticultural crops were sold fresh in the markets, it is imported to measure the crop fresh light (Marcelis et al., 1998). Therefore, quantitative analysis of more diverse environmental factors is required for the growth of horticultural crops growth. However, the developed algorithm could not estimate the each organ growth. Therefore, further study is required on the development of algorithms to estimate the growth of the target organ.

LITERATURE CITED

Asseng, S., Ewert, F., Rosenzweig, C., Jones, J.W., Hatfield, J.L., Ruane, A.C., ... and Brisson, N. (2013). Uncertainty in simulating wheat yields under climate change. Nature Climate Change 3, 827.

Boote, K.J., Jones, J.W., Batchelor, W.D., Nafziger, E.D., and Myers, O. (2003). Genetic coefficients in the CROPGRO–soybean model. Agronomy Journal 95, 32-51.

Boote, K.J., Jones, J.W., Hoogenboom, G., and Pickering, N.B. (1998). Simulation of crop growth: CROPGRO model. Agricultural Systems Modeling and Simulation 18, 651-692.

Boote, K.J., Rybak, M.R., Scholberg, J.M., and Jones, J.W. (2012). Improving the CROPGRO-tomato model for predicting growth and yield response to temperature. HortScience 47, 1038-1049.

Csizinszky, A.A. (1999). Yield and Nutrient Uptake ofCapistrano'Bell Peppers in Compost-Amended Sandy Soil. In Proceedings-Florida State Horticultural Society 112, 333-336.

Da Silva, I.N., Spatti, D.H., Flauzino, R.A., Liboni, L.H.B., and dos Reis Alves, S.F. (2017). Artificial neural networks. Cham: Springer International Publishing.

Ehret, D.L., Hill, B.D., Helmer, T., and Edwards, D.R. (2011). Neural network modeling of greenhouse tomato yield, growth and water use from automated crop monitoring data. Computers and Electronics in Agriculture 79, 82-89.

Gupta, D.K., Kumar, P., Mishra, V.N., Prasad, R., Dikshit, P.K.S., Dwivedi, S.B., ... and Srivastava, V. (2015). Bistatic measurements for the estimation of rice crop variables using artificial neural network. Advances in Space Research 55, 1613-1623.

Hsiao, T.C., Heng, L., Steduto, P., Rojas-Lara, B., Raes, D., and Fereres, E. (2009). AquaCrop—the FAO crop model to simulate yield response to water: III. Parameterization and testing for maize. Agronomy Journal 101, 448-459.

Hashem, I.A.T., Yaqoob, I., Anuar, N.B., Mokhtar, S., Gani, A., and Khan, S.U. (2015). The rise of "big data" on cloud computing: Review and open research issues. Information Systems 47, 98-115.

Jensen, M.H. (1997). Food production in greenhouses. In Plant production in closed ecosystems (pp. 1-14). Springer, Dordrecht.

Ji, S., Zhang, C., Xu, A., Shi, Y., and Duan, Y. (2018). 3D convolutional neural networks for crop classification with multi-temporal remote sensing images. Remote Sensing 10, 75.

Jones, J.W., Antle, J.M., Basso, B., Boote, K.J., Conant, R.T., Foster, I., ... and Keating, B.A. (2017). Brief history of agricultural systems modeling. Agricultural Systems 155, 240-254.

Jones, J.W., Dayan, E., Allen, L.H., Van Keulen, H., and Challa, H. (1991). A dynamic tomato growth and yield model (TOMGRO). Transactions of the ASAE 34, 663-0672.

Jones, J.W., Hoogenboom, G., Porter, C.H., Boote, K.J., Batchelor, W.D., Hunt, L.A., ... and Ritchie, J.T. (2003). The DSSAT cropping system model. European Journal of Agronomy 18, 235-265.

Körner, O. and Holst, N. (2015, October). An open-source greenhouse modelling platform. In V International Symposium on Applications of Modelling as an Innovative Technology in the Horticultural Supply Chain-Model-IT 1154 (pp. 241-248).

Kumar, K., Kumar, S., Sankar, V., Sakthivel, T., Karunakaran, G., and Tripathi, P.C. (2017). Non-destructive estimation of leaf area of durian (Durio zibethinus)–An artificial neural network approach. Scientia Horticulturae 219, 319-325.

Ma, L., Hoogenboom, G., Ahuja, L.R., Ascough Ii, J.C., and Saseendran, S.A. (2006). Evaluation of the RZWQM-CERES-Maize hybrid model for maize production. Agricultural Systems 87, 274-295.

Pantazi, X.E., Moshou, D., Alexandridis, T., Whetton, R.L., and Mouazen, A.M. (2016). Wheat yield prediction using machine learning and advanced sensing techniques. Computers and Electronics in Agriculture 121, 57-65.

Ratto, M., Tarantola, S., and Saltelli, A. (2001). Sensitivity analysis in model calibration: GSA-GLUE approach. Computer Physics Communications 136, 212-224.

Shi, Y., Li, Y.N., Zhang, C., Bai, M.J., and Wang, Y.K. (2015). Development and application of decision support system for agro-technology transfer DSSAT under water resources management. Advanced Materials Research 1073, 1596-1603. .

Vieira, M.I., de Melo-Abreu, J.P., Ferreira, M.E., and Monteiro, A.A. (2009). Dry matter and area partitioning, radiation interception and radiation-use efficiency in open-field bell pepper. Scientia Horticulturae 121, 404-409.

Wolfert, S., Ge, L., Verdouw, C., and Bogaardt, M.J. (2017). Big data in smart farming–a review. Agricultural Systems 153, 69-80.

Yadav, S.B., Misra, A.K., Mishra, S.K., and Pandey, V. (2018). Crop growth simulation models (InfoCrop v. 2.1, DSSATv4. 5, WOFOSTv1. 5 and Cropsytv 4.19) software. Water and Energy Security in The Arena of Climate Change, 34, 456-469.

Table 4-1. Bell pepper genotype coefficientsin CropGro-pepper.

Index	Description (unit)
PPSEN	Slope of the relative response of development to photoperiod with time (positive for shortday plants) (1/hour)
EM-FL	Time between plant emergence and flower appearance (R1) (photothermal days)
FL-SH	Time between first flower and first pod (R3) (photothermal days)
FL-SD	Time between first flower and first seed (R5) (photothermal days)
SD-PM	Time between first seed (R5) and physiological maturity (R7) (photothermal days)
FL-LF	Time between first flower (R1) and end of leaf expansion(photothermal days)
LFMAX	Maximum leaf photosynthesis rate at 30 C, 350 vpm CO_2, and high light (mg CO_2/m^2-s)
SLAVR	Specific leaf area of cultivar under standard growth conditions (cm^2/g)
SIZLF	Maximum size of full leaf (three leaflets) (cm^2)
CSDL	Critical Short Day Length below which reproductive development progresses with no daylength effect (for shortday plants) (hour)
XFRT	Maximum fraction of daily growth that is partitioned to seed + shell
WTPSD	Maximum weight per seed (g)
SFDUR	Seed filling duration for pod cohort at standard growth conditions (photothermal days)
SDPDV	Average seed per pod under standard growing conditions (#/pod)
PODUR	Time required for cultivar to reach final pod load under optimal

	conditions (photothermal days)
THRSH	Threshing percentage. The maximum ratio of (seed/(seed+shell)) at maturity.
SDPRO	Fraction protein in seeds (g(protein)/g(seed))
SDLIP	Fraction oil in seeds (g(oil)/g(seed))

Table 4-2. Bell pepper ecotype coefficients in CropGro-pepper.

Index	Description (unit)
MG	Maturity group number for this ecotype, such as maturity group
TM	Indicator of temperature adaptation
THVAR	Minimum rate of reproductive development under short days and optimal temperature
PL-EM	Time between planting and emergence (V0) (thermal days)
EM-V1	Time required from emergence to first true leaf (V1), thermal days
V1-JU	Time required from first true leaf to end of juvenile phase, thermal days
JU-R0	Time required for floral induction, equal to the minimum number of days for floral induction under optimal temperature and daylengths, photothermal days
PM06	Proportion of time between first flower and first pod for first peg
PM09	Proportion of time between first seed and physiological maturity that the last seed can be formed
LNGSH	Time required for growth of individual shells (photothermal days)
R7-R8	Time between physiological (R7) and harvest maturity (R8) (days)
FL-VS	Time from first flower to last leaf on main stem (photothermal days)
TRIFOL	Rate of appearance of leaves on the mainstem (leaves per thermal day)
RWIDTH	Relative width of this ecotype in comparison to the standard width per node
RHGHT	Relative height of this ecotype in comparison to the standard height per node

R1PPO	Increase in daylength sensitivity after R1 (h)
OPTBI	Minimum daily temperature above which there is no effect on slowing normal development toward flowering (^{o}C)
SLOBI	Slope of relationship reducing progress toward flowering if TMIN for the day is less than OPTBI

Table 4-3. Calibration of bell pepper genotype coefficients in CropGro-pepper.

Index	Value	Index	Value
PPSEN	0	CSDL	12.33
EM-FL	40	XFRT	0.6
FL-SH	10	WTPSD	0.007
FL-SD	15	SFDUR	40
SD-PM	330	SDPDV	150
FL-LF	200	PODUR	42
LFMAX	0.98	THRSH	6.5
SLAVR	275	SDPRO	0.3
SIZLF	350	SDLIP	0.05

Table 4-4. Calibration of bell pepper ecotype coefficients in CropGro-pepper.

Index	Value	Index	Value
MG	1	LNGSH	35
TM	1	R7-R8	0
THVAR	0	FL-VS	330
PL-EM	5	TRIFOL	0.35
EM-V1	10	RWIDTH	1
V1-JU	24	RHGHT	1
JU-R0	5	R1PPO	0
PM06	0	OPTBI	0
PM09	0	SLOBI	0

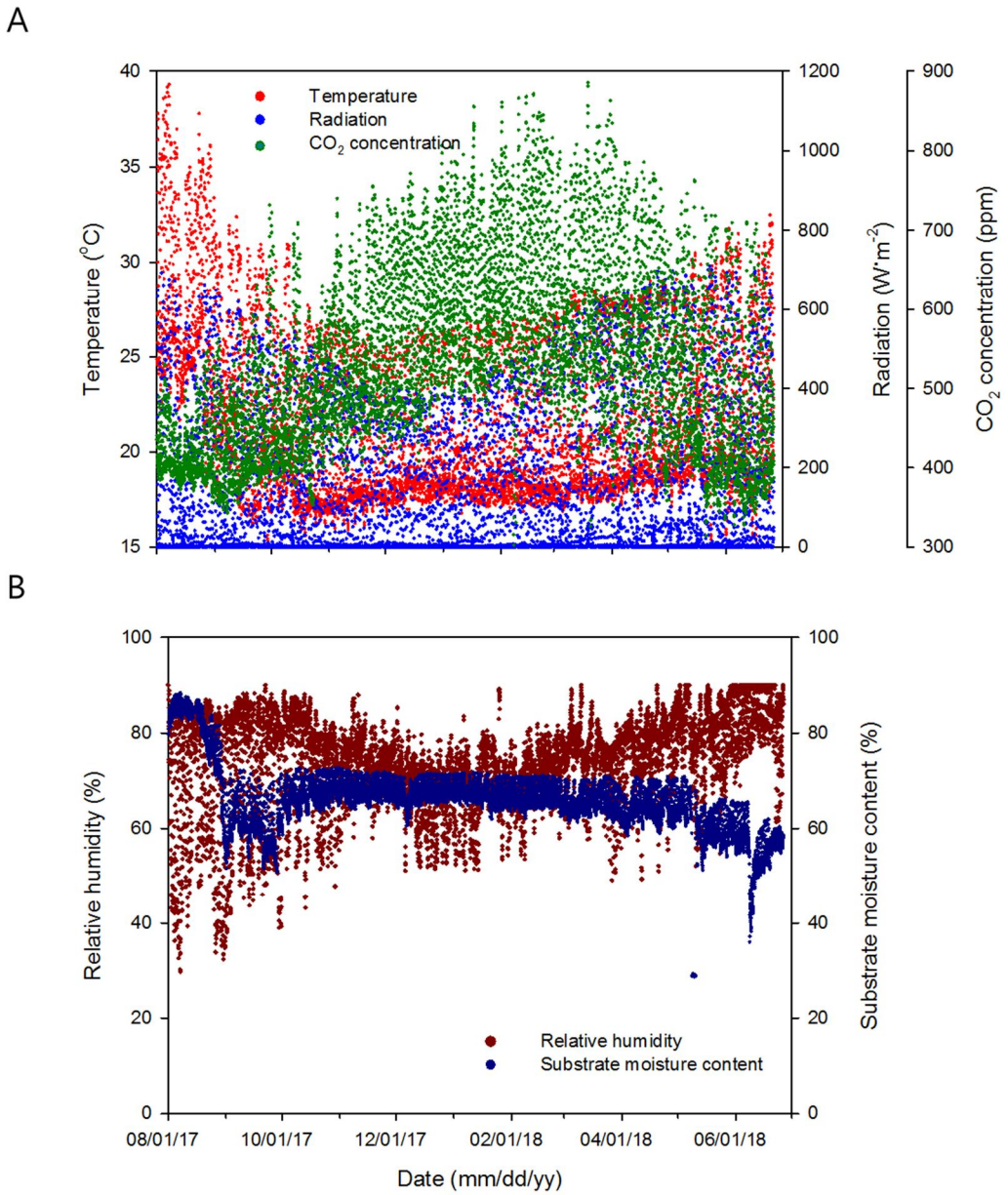

Fig. 4-1. Environmental conditions such as temperature, solar radiation, CO2 concentration (A) and relative humidity and substrate moisture content (B) in the greenhouse during growth period from Aug 01, 2017 to June 01, 2018 used for growth validation.

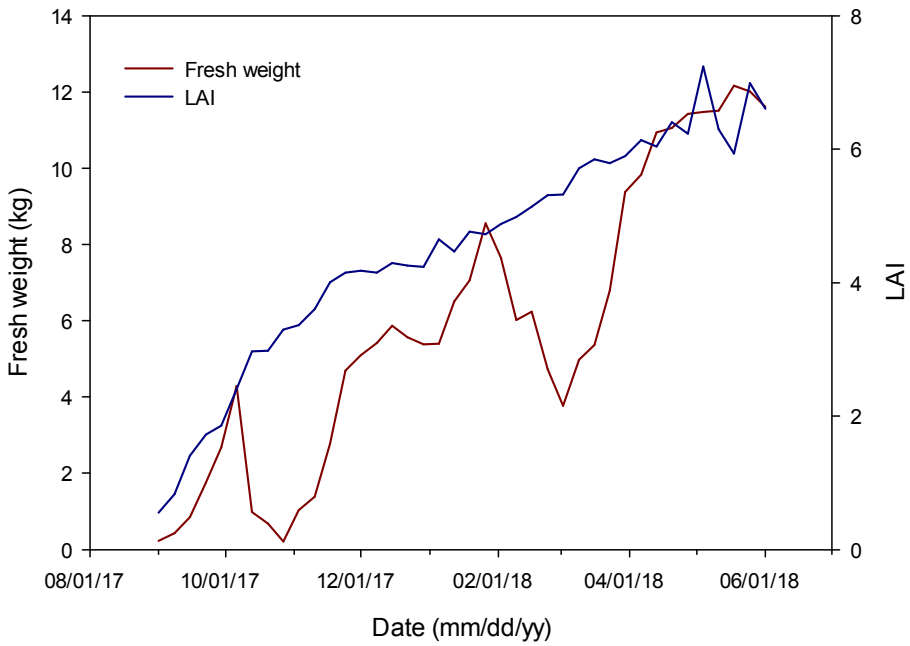

Fig. 4-2. Changes in fresh weight and leaf area index (LAI) during growth period from Aug 01, 2017 to June 01, 2018 used for growth validation.

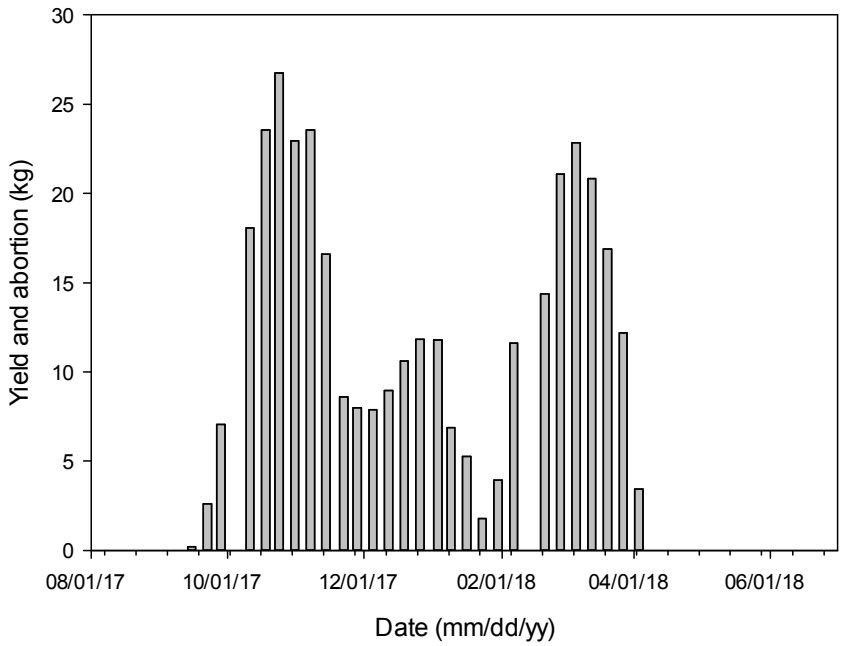

Fig. 4-3. The weights of yield and abortion during growth period Aug 01, 2017 to June 01, 2018 used for growth validation.

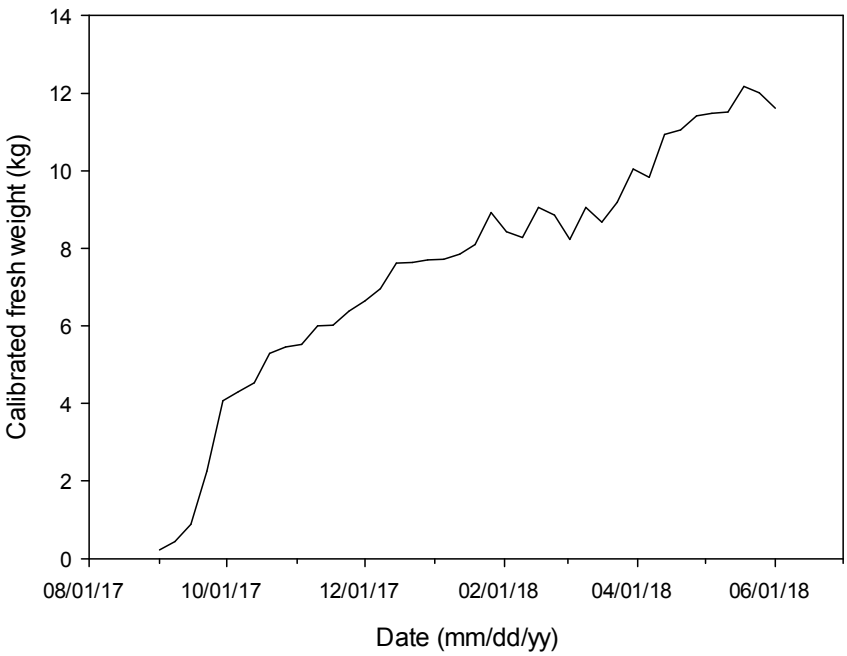

Fig. 4-4. Calibrated fresh weights considering yield and fruit abortions during growth period from Aug 01, 2017 to June 01, 2018 used for growth validation.

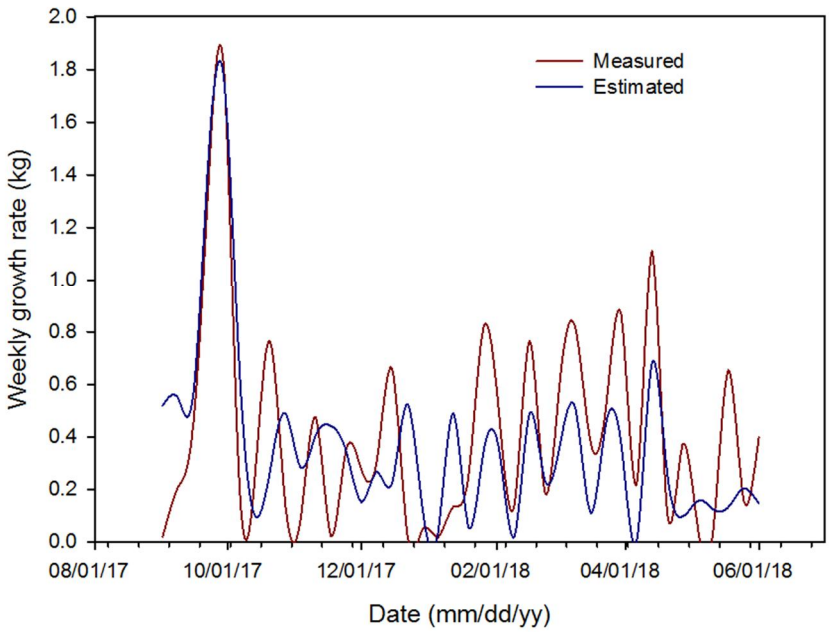

Fig. 4-5. Weekly crop growth rates measured by the system and estimated by the algorithm during growth period from Aug 01, 2017 to June 01, 2018 used for growth validation.

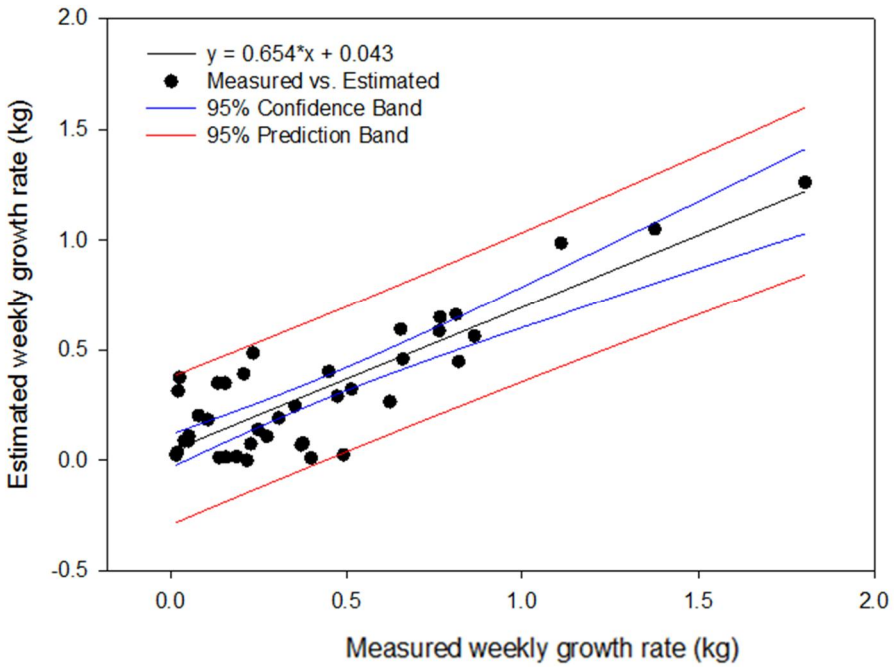

Fig. 4-6. Comparison of crop growth rates measured by the system and estimated by the algorithm during growth period from Aug 01, 2017 to June 01, 2018 used for growth validation

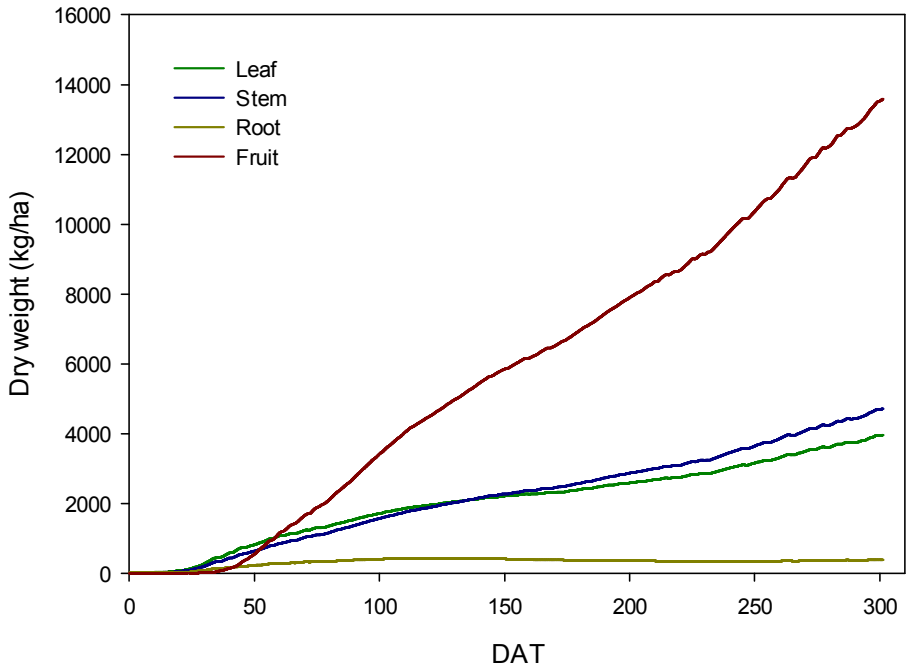

Fig. 4-7. Dry weight of each organ estimated by the process-based model with days after transplanting (DAT).

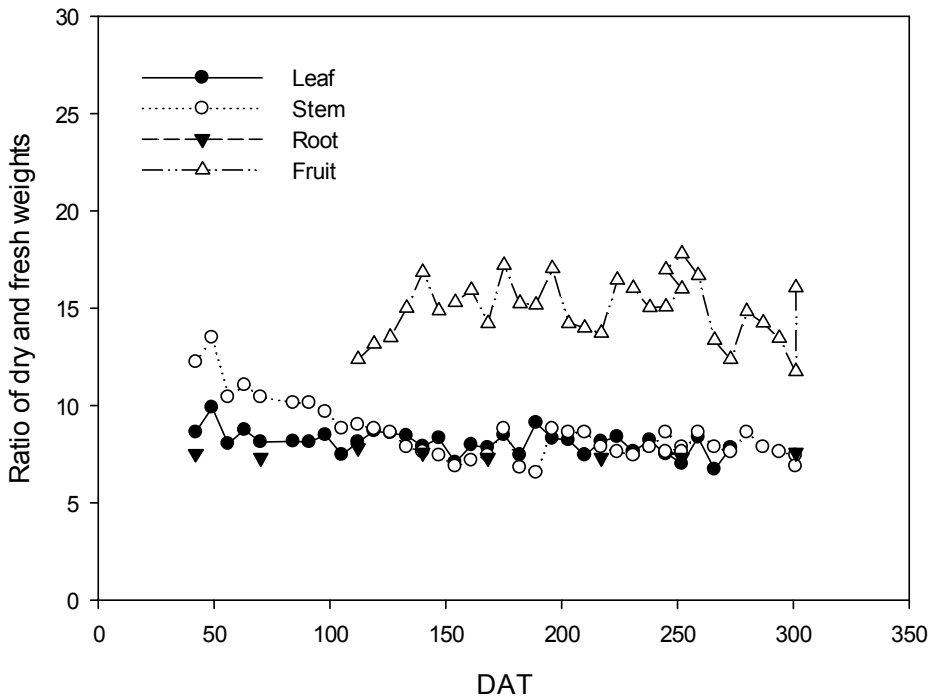

Fig. 4-8. The ratio of dry and fresh weights of each organ with days after transplanting (DAT).

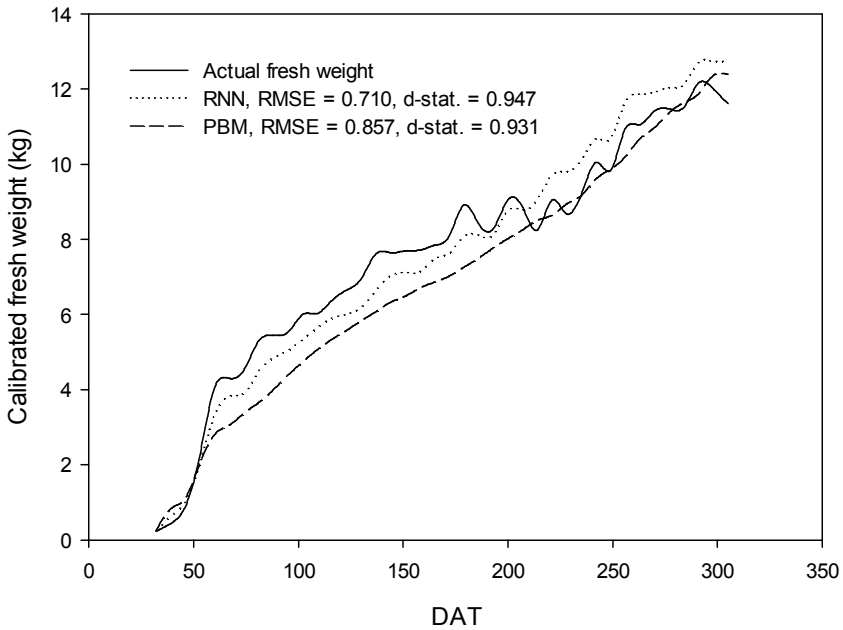

Fig. 4-9. Comparison of calibrated fresh weights estimated by the recurrent neural network (RNN) algorithm and the process-based model (PBM) with after days from transplanting (DAT) in growth validation periods.

CONCLUSIONS

In this study, growth of hydroponically-grown bell peppers (Capsicum annuum L.) were estimated using recurrent neural network through nondestructive measurement of leaf area index and fresh weight. First, an automatic and continuous measurement system for LAI was developed using relationship between light interception of crop canopy and LAI. Ray tracing simulation and machine learning were used. The developed system showed high accuracy with d-stat. = 0.808. Second, an automatic and continuous measurement system for fresh weight was developed using load cells and FDR sensors. Estimated fresh weight showed good agreements with measured ones with a high accuracy of R^2 = 0.935. Third, for estimating the crop growth, a RNN algorithm was designed, which consists of eight environmental variables and three growth characteristics as inputs, and the weekly crop growth rate as an output. Long short term memory (LSTM) algorithm was selected as an optimal algorithm. The machine learning was conducted using the data collected from two crop growth periods in the same greenhouse. The algorithm showed a test accuracy with R^2 = 0.754. Finally, validation of the RNN-based crop growth prediction algorithm was carried out using the data collected from large commercial greenhouse. The parameters of the PBM were calibrated using the growth survey data collected during the growth period for algorithm training. The developed prediction algorithms showed similar accuracies to those of the PBMs in both sides of research and commercial greenhouses. For the results, it was confirmed that the developed measurement systems could nondestructively and continuously collect the

growth information, and the RNN-based crop growth estimation algorithms well estimated the crop growth.

ABSTRACT IN KOREAN

ICT 기술이 기존의 농업 기술에 적용되면서 스마트 팜이 대두되고 있다. 스마트 팜의 완성을 위해서는 작물과 환경 사이의 복잡하고 다양하고 예측 불가능한 관계에 대한 정량적인 분석이 가능해야 한다. 이를 위해 환경에 대한 작물의 반응을 연속적, 자동적, 비파괴적으로 모니터링할 수 있는 시스템과 농업 빅데이터를 해석할 수 있는 새로운 알고리즘 개발이 요구된다. 본 연구에서는 파프리카 수경 재배 조건에서 다양한 환경 요인에 의한 작물의 생육의 변화를 예측하는 순환 신경 회로망 기반 알고리즘을 개발하였다. 파프리카의 생육 예측 알고리즘 개발에 앞서 주요한 생육 변수인 엽면적 지수(LAI)와 작물의 생체중 정보를 자동적, 연속적으로 수집할 수 있는 시스템 개발을 선행하였다. 본 연구에서는 기존의 LAI 비파괴적 측정 방법론에서 고려하지 않았던 요인들(기상 조건, 측정 시간)에 대한 정량적인 분석을 추가하였다. 이러한 요인들을 분석하기 위해 광추적 시뮬레이션과 인공신경회로망 기계 학습을 활용하였다. 개발된 LAI 측정 시스템은 높은 정확도로 실제 LAI 를 추정하는 것이 가능하였다. 작물의 생체중 정보 수집 시스템은 파프리카의 생리적, 재배적 특성을 반영하여 재배 시스템 전체의 무게를 측정할 수 있는 형태로 설계하였다. 또한 배지의 내 수분의 무게를 배지 내 함수율을 통해 보정하여 작물의 생체중을 계산하였다. 개발된 생체중 측정 시스템은 높은 정확도로 실제 생체중을 추정하는 것이 가능하였다.

개발된 작물 특성 측정 시스템을 이용하여 수집된 작물 생육 정보와 센서를 이용하여 수집된 환경 변수를 이용하여 작물 생육 예측 알고리즘을 기계 학습하였다. 작물의 생육은 과거로부터 누적된 환경 요인에 의해 결정되기 때문에 시계열 데이터 분석에 특화되어 있는 순환신경회로망 알고리즘을 활용하였다. 알고리즘의 학습 정확도를 이용하여 주요한 환경 요인을 선정하고 최적의 알고리즘을 개발하였다. 개발된 알고리즘의 학습 정확도를 검증하기 위해 알고리즘 학습 조건과 독립된 실험 조건에서 추가 자료를 수집하였다. 개발된 알고리즘의 정확도를 평가하기 위해 기존의 수식 기반 작물 생육 모델의 정확도와 비교 분석하였다. 검증 결과 개발된 생육 예측 알고리즘은 작물 생육 모델보다 더 높거나 비슷한 수준의 정확도를 나타내었다. 결과적으로 본 연구를 통해 개발된 작물 생육 특성 측정 시스템과 작물 생육 추정 알고리즘은 작물의 생육 정보를 연속적으로 수집하거나 작물 생육과 환경 사이의 관계를 정량적으로 분석하는 데 유용한 도구로 활용 가능할 것으로 판단하였다.

추가 주요어: 자동 측정. 작물 생육 모델, 엽면적 지수, 기계학습 광추적 시뮬레이션

학번 : 2014-30378

감사의 글

2008 년 서울대학교 식물생산과학부 학부 신입생으로 입학하여, 2019 년 가을 박사학위를 받게 되었습니다. 지난 날을 돌이켜 보면 늘 부족함이 많았던 제가 지금의 길을 걷게 되기까지 많은 분들의 도움을 받았습니다.

항상 옳은 길만 걷던 100 점짜리 누나와는 달리, 늘 걱정만 끼쳐드린 제가 공부를 더 하겠다고 하였을 때, 믿어주시고 지금까지 물심양면으로 지원해주신 부모님께 감사드립니다. 먼저 살갑게 대한 적 없는 동생을 이해해주고 항상 뒤에서 남몰래 챙겨주었던 누나에게도 고마움을 전합니다. 어렸을 때 키워주시고 항상 저를 어여삐 여기시던 할머님 생전에 손주가 박사 학위 받는 걸 보여드리지 못해 죄송합니다. 사위로 대하시는 것 이상으로 연구자 선배로써 올바른 연구와 삶의 길을 제시해주시는 장인 어른, 친자식 못지 않게 항상 걱정해주시고 응원해주시는 장모님께도 감사드립니다. 그 외에 모든 가족 분들의 응원과 지원 모두 감사드리며 그 은혜를 잊지 않겠습니다.

학부와 대학원 과정 동안 여러 방면에서 가르침을 주신 아홉 분 교수님들 모두 감사드립니다. 부족함이 많은 논문임에도 불구하고 세심한 지도와 조언을 주신 심사위원들, 전창후 교수님, 김일섭 교수님, 김종윤 교수님, 신종화 교수님께 감사드립니다. 심사위원이 아님에도 제 논문을 한 글자 한 글자 세심하게 지도해주신 이희재 교수님에게도 감사드립니다. 제 연구에 자신감 없는 저보다도 더 제 연구의 가치를 높게 생각하시며 늘 응원을 복돋워 주시고 지지해주신 손정익 교수님께 감사와 존경의 마음을 전합니다.

제게 연구의 걸음마 단계부터 가르쳐 주신 종화형, 한 가정의 가장과 대학원생의 삶 사이의 균형을 함께 고민해준 태인이형, 앞에서 뒤에서 늘 챙겨준 우현이형, 늦은 시간에도 항상 친절하게 설명해주던 태원이, 40 도가 넘는 온실에서 장치 제작과 생육조사를 함께한 두성이, 함께 졸업 준비하면서 많은 밤을 지새운 대호, 힘들게 작업한 스캔 모델을 아무 조건 없이 제공해준 인하, 동필이에게 감사 드립니다. 연구실에서 함께 시간을 보내며 많은 조언과 도움을 주신 시설방 모든 선후배님들과 연구실 모임이면 멀리서도 항상 참석하여 아낌 없는 조언을 해주신 시설방 선배님들께 감사의 마음을 전합니다.

제가 힘들거나 즐거울 때 함께 술을 마시며 시간을 보내준 친구들, 형님들, 동생들 모두 고맙습니다. 아무 조건없이 작물 모델을 설명해준 김연욱 박사에게 감사 드립니다. 다른 관점에서 제 연구를 조언해준 다른 연구실 분들과 학회에서 만나 연구를 논했던 젊은 연구자 분들도 모두 감사합니다. 또한 제 연구에 도움을 주신 여러 기관의 여러 연구원 분들 덕분에 학위 논문을 무사히 마칠 수 있었습니다.

그리고 마지막으로 누구보다도 가장 사랑하는 아내 지수에게 감사의 마음을 전합니다. 그 무엇보다 지수의 무한한 사랑과 지원 덕분에 제가 무사히 박사 학위를 받을 수 있었습니다. 모든 것이 부족했던 학생 신분의 남편을 만나 고생한 시간을 앞으로 더 많은 사랑으로 채울 수 있도록 노력하겠습니다. 또한 삶의 새로운 모티브가 된 내 아들 지산이에게도 고마움과 사랑을 전달합니다. 앞으로 제가 선택하는 모든 길이 지수와 지산이와 함께하는 길이 될 수 있도록 하겠습니다.

제가 받는 농학 박사 학위가 제가 농업 연구의 한 부분을 완성시켰기 때문에 받은 것이라고 생각하지 않습니다. 그동안 훈련 받은 연구를 진행할 수 있는 자격증이라고 생각하고 앞으로 끊임없이 공부하고 연구하겠습니다.